The Dissertation Committee for Sepideh Khoshnevis Certifies that this is the approved version of the following dissertation:

Characterization of Tissue Response to Localized Cooling and Design of a Safer Cryotherapy Device

Committee:

Kenneth R. Diller, Supervisor

Aaron B. Baker

R. Matthew Brothers

Brant Mittler

Laura J. Suggs

Characterization of Tissue Response to Localized Cooling and Design of a Safer Cryotherapy Device

by

Sepideh Khoshnevis, M.D.

Dissertation

Presented to the Faculty of the Graduate School of

The University of Texas at Austin

in Partial Fulfillment

of the Requirements

for the Degree of

Doctor of Philosophy

The University of Texas at Austin

August 2014

Dedication

To my husband, Ramin for his loving support and friendship

To my daughters, Kiana and Parisa for their love

Acknowledgements

First and foremost, I would like to express my gratitude for my advisor, Dr. Kenneth Diller, and for his mentorship, help and support throughout the years. He has been tremendously generous with his time and has provided me with priceless guidance regarding my research, as well as my writing style. He has never failed to return my written work with many edits, so much so that not much remained from the original sentence structure. I should also thank Microsoft Word for providing me with the "Track Changes" option which makes it possible to find traces of my original words embedded within the resulting document.

I would like to thank my committee members, Dr. Aaron Baker, Dr. Matthew Brothers, Dr. Laura Suggs and Dr. Brant Mittler for their time and support. I would like to specially thank Dr. Brothers for all the discussions we have had and for his feedbacks on my writing.

I would like to express my appreciation to Dr. Michael Mahometa for his guidance on statistical analysis of my work.

I would also like to acknowledge my past and present labmates Laura Hemmen, Andrew Mark and Daniel Hensley for their help in my research and many interesting conversations.

Additionally, I'd like to acknowledge the help and support of undergraduate students Natalie Craik and Jennifer Nordhauser for their help in myriad aspects of my project, Natalia Mejia and Rebecca Chen for their assistance with performing human experiments and data extraction, and Karla Sanchez and Charles Davis Wang for their help with conducting the experiments.

Many thanks to my Friend Samira Moorjani, whose thoughtfulness and stimulating talks made years of graduate studies more pleasant.

I would also like to thank my parents, Rezvan Nazeri and Dr. Manoochehr Khoshnevis, for their support and the nurturing environment they created for me while I was growing up.

Last but not least, a special thanks to my daughters, Kiana and Parisa Poorfard, for their understanding and support, and to my husband, Ramin Poorfard, for all the love, help and intellectual support that he has offered me. This would not have been possible without them.

Characterization of Tissue Response to Localized Cooling and Design of a Safer Cryotherapy Device

Sepideh Khoshnevis, PhD

The University of Texas at Austin, 2014

Supervisor: Kenneth R. Diller

Localized cooling is often used to manage both acute and chronic phases of soft tissue injuries by reducing pain, swelling, and inflammation. Cold application would result in a decline in skin temperature and reduction of blood perfusion at the treatment site. In some instances, the use of cryotherapy has been associated with tissue necrosis and nerve damage. Tissue damage was shown to be due to both the direct effect of cooling as well as tissue ischemia resulting from the reduced blood perfusion. The purpose of this research was to examine the effect of localized cooling on skin temperature and blood perfusion and to develop a method to stimulate blood perfusion in tissue following development of cold-induced vasoconstriction. Out of various methods used, thermal stimulation was shown to successfully increase tissue perfusion during cryotherapy experiments.

As a part of this research, tissue response to localized cooling was quantified for each of a variety of cryotherapy units (CTU). Moreover, diverse methods were implemented to investigate and quantify the non-uniformity of surface temperature for multiple cooling pads in combinations with their brand-specific CTUs. It was demonstrated through further studies and tissue blood perfusion comparisons (caused by using different CTUs) that there were no significant differences between studied units. Additionally, no significant difference was observed between knee and ankle/foot in their vasocosnstrictive response to cooling. Using multiple statistical methods, it was illustrated that a significant degree of vasoconstriciton

occurred that lasted well beyond the active cooling period while skin temperature had increased significantly. Furthermore, a hysteresis effect was observed between skin perfusion and temperature during cooling and rewarming periods. In addition, a dose-dependent response in skin perfusion in relation to applied temperature was reported. A hysteresis effect between the skin temperature and perfusion was observed for both cooling and warming experiments and the area of the hysteresis plot was shown to be linearly dependent on applied temperature. Moreover, non-uniformity of skin temperature during cryotherapy was noted, which was independent of pad temperature distribution.

Table of Contents

List of Tables

List of Figures

Chapter 1: Introduction

Cryotherapy is the application of cold for therapeutic purposes. Anything from holding a burnt body part under the cold running water to direct application of ice to injured tissue and the thermal ablation of tissue by applying below freezing temperatures is considered cryotherapy. Localized cooling for clinical applications dates back to ancient times. Cryotherapy was used by ancient Egyptians to treat injuries and inflammation [1]. In 19^{th} century localized cooling was used for pain management and as a skin anesthetics [1,2]. In late 19^{th} century, cryotherapy was used in conjunction with surgical procedures. But it was not until mid 20^{th} century that the effect of cooling on different tissue responses; like, bleeding, inflammation, and swelling, was studied. Around this time cryokinetics was introduced. Cryokinetics combines active exercises with localized cooling. It takes advantage of numbing effect of cooling and increase in tissue perfusion and lymph removal due to active movements [3].

Cooling has an analgesic effect by slowing the nerve conduction velocity [4,5], and relieve of muscle spasm. It might also function by affecting the nerve endings directly [6] and by increasing the pain threshold [5]. The vascular disturbances caused by original injury impose further trauma on tissue by reducing the availability of O_2 and nutrients. By lowering the metabolic need of tissue, cooling counteracts this effect and therefore reduces the occurrence of secondary hypoxic injury [3]. Cooling is commonly used in soft tissue injury in combination with rest, compression and elevation to minimize inflammation. Its anti-inflammatory action might be due to reduction of secondary hypoxic injury and resulted release of inflammatory agents from the cells [7]. The reduction of swelling can be due to reduced vascular permeability. This effect will be canceled out by increase in permeability of lymphatics when tissue temperatures reaches

about 15˚C [8]. The bleeding decreases by application of cold due to induction of vasoconstriction [9].Cryotherapy is used by athletic trainers and physical therapists in both acute and chronic phase of injury. In the acute phase possibly its most important functionality is to reduce secondary hypoxic injury, pain and swelling; in the chronic phase it helps with reducing the sensation of pain so that the early mobilization would be possible. Cryotherapy is commonly used in conjunction with surgical procedures, specially, orthopedics surgeries. However, in contrast to its therapeutic benefits, cryotherapy also presents a risk factor for causing ischemic-induced injuries such as nerve palsy [10–12] and tissue necrosis [13,14].

Since the cryotherapy complications are related to the tissue temperature as well as the reduction in tissue perfusion, understanding the physiological response in the form of skin temperature and perfusion are essential to better apprehend the possible effects of cryotherapy in tissue. This improved knowledge of cryotherapy effect in tissue could result in modifying the cryotherapy practices and modalities such that the healing is accelerated and the chance of complications is reduced. I begin this review by introducing the common modes of cryotherapy application and recommendations for duration of applications and desired thermal condition. Next I will briefly discuss the current understanding of vascular response to localized cooling and the possible modes of injury in tissue following cold application. Then I will continue by introducing possible modalities to stimulate tissue blood flow in the vasoconstricted region following the cold application.

1.1 MODES OF CRYOTHERAPY

There are many alternative schemes for effecting cold therapy to soft tissue, such as crushed ice [15], ice bags [7], cold gel packs [16], and, in particular, cryotherapy units

(CTU) that can provide a continuous or intermittent circulation of ice water from an insulated container to a pliable cooling pad placed onto the treatment area [13,15,17–21]. Local cooling is sometimes combined with complementary therapeutic modalities such as transient tissue compression [17,22]. Powered CTUs that feature the capability for continuous circulation of cold water have facilitated the ability to sustain extended periods of cold therapy measured in hours and days.

The components of a CTU system typically consist of an insulated chest that is filled with ice and water, a submersible pump, a cooling pad that is applied to the treatment area, and insulated tubing that connects the pump to the pad in a closed ice water circulation loop. The cooling pad generally embodies a flexible polymeric bladder with molded conduits through which water is pumped via inlet and outlet ports. An example of such devices is presented in Figure 1.1. The user is instructed to fill the ice chest with water and ice according to the manufacturer's recommendations and apply the bladder on the surface of interest over some form of insulating layers and holds it in place using Ace bandage or a similar product. These devices do not provide any form of feedback to the user and for the most part they re-circulate ice-cold water through the system.

Figure 1.1 A sample cryotherapy device

1.2 CRYOTHERAPY PRACTICES

No single thermal application cryotherapy protocol has been identified that provides an optimum risk/benefit ratio, resulting in a broad spectrum of cryotherapy practices reported in the literature [23,24]. Cryotherapy protocols are generally defined in terms of temperature and duration of application and may be run either continuously or with temporal modulation. Recommendations for the duration of application vary from minutes [7,8] to days [9,19,25]. It is claimed that skin temperature must drop below 13.6°C (56.5°F) to realize the analgesic effect of cryotherapy and that a 50% reduction in tissue metabolism requires tissue temperatures in the range of 10-11°C (50-51.8°F) [26]. Moreover, the ability of hemoglobin to release bound oxygen strongly relates to temperature, and below about 12°C (53.6°F) the residence time of blood flowing through capillaries is shorter than the time constant for oxygen dissociation [27,28]. This condition could result in the creation of tissue hypoxia that may also be exacerbated by

ischemia. In summary, the level of temperature produced by cryotherapy may affect multiple aspects of the procedure outcome.

1.3 MANUFACTURER'S RECOMMENDATIONS

CTU Manufacturers provide user instructions that commonly relate to a target operating temperature but include a paucity of specific implementation guidelines. Alternatively, the responsibility for defining a thermal treatment protocol may be assigned to health care providers. The following are examples of temperature-related instructions provided with CTUs. DeRoyal recommends a target temperature for water flowing to the pad within the range of 7.2-15.6°C (45-60°F) [29], with specific operating temperatures of 7.2±2.8°C (45±5°F) and 6.1-18.3°C (43-65°F) for models T505 and T600 [30], respectively. Game Ready [31] claims that the greatest benefit from cryotherapy takes place at 4.5-15.5°C (40-60°F). Bledsoe [32,33] states that their devices are designed for the temperature of water circulating within the pad to remain at or above 4.4°C (40°F) with other specific recommendations for particular treatment sites, the highest being 10-15°C (50-59°F) for the ankle and the lowest 7-12°C (44.6-53.6°F) for the back, knee and shoulder [33]. DonJoy warns against using their CTU with a water temperature lower than 5°C (40°F) [34]. Breg specifies different temperature ranges depending on the protocol. The temperature range of cooling water for continuous long term operation is 7.2°C – 12.8°C (45°F - 55°F), and the temperature may be below 7.2°C (45°F) for intermittent exposures of 20 minutes or less [35]. EBIce only stipulates that a licensed health care practitioner must prescribe the appropriate treatment details [36] while warning that cooling pads may have wide temperature variation and that cold spots create the potential for tissue damage, and nerve palsy while hot spots may create areas of lessened therapeutic effectiveness.

1.4 MODES OF INJURY

Localized cooling in non-glabrous skin results in on site vasoconstriction through different mechanisms such as activation of Rho-Rho kinase pathway in early stages of cold exposure and the inhibitions of nitric oxide system in its later stages [37–41]. Extended exposure to cold-induced vasoconstriction could lead to state of ischemia with tissue deprivation of oxygen and nutrients supply required to sustain cell metabolism and accumulation of toxic byproducts that may cause injuries which typically fall within the domain termed nonfreezing cold injury (NFCI) manifested by necrosis and nerves damage [42–46]. In addition, a prolonged state of vasoconstriction can lead to the occurrence of reperfusion injury when blood flow is reestablished to the affected tissue [47].

Tissue ischemia is expected to play a major role in tissue necrosis caused by cryotherapy [46]. Nerve damage seems to be ischemia related although low temperatures also play a role. Localized cooling of nerves has been associated with the following changes in endoneurial and epineurial capillaries: increased blood viscosity, plasma skimming, cellular aggregation, damage to endothelial cells and resulted endoneurial and epineurial edema[47,48]. Additionally, some degree of constriction is reported in arterioles, and venules. Jia, et al. [47] also report a no reflow situation in these vessels where the flow does not reestablish in vessels after few hours of rewarming. There are also some reports of thrombotic events taking place. The hypoxia could be followed with a hyperemia phase when the flow returns and might be associated with reperfusion injury [44,48].

Therefore, it is desirable to be able to characterize the mechanistic relationship between the application of therapeutic cooling to skin and the reduction of blood flow in affected tissue structures.

1.5 INJURY PREVENTION

The primary mechanism of NFCI is based on ischemic driven events, one approach to avoiding that injury is to interrupt the ischemic state in a way that it still allows the benefits of cryotherapy to be realized. We have performed many experiments that evaluate various mechanisms to interrupt ischemia. The results of some of these studies which were deemed less desirable are reported in the appendix B. these studies indicate that brief intermittent episodes of rewarming the tissue presents the best approach to regulating ischemia.

Localized heating can be used to increase blood perfusion in tissue in a three-phase vasodilatory response. First, there is a transient increase in perfusion followed by a prolonged plateau response and a die away phase. The early, transient increase in perfusion seems to be caused by axonal reflex and is mainly mediated via warm receptors or heat-sensitive nociceptors. It is suggested that sympathetic function, though not required for the axonal reflex, poses a supporting role. Nitric oxide (NO) system is the main reason for the sustained vasodilation during the plateau phase. The endothelial NO (eNO) is reported to be responsible for 50% of heat-induced vasodilation during the plateau phase with no role in the early transient increase in perfusion. It is suggested that the vasodilatory effect of eNO might be more complex than the NO synthase (NOS) kinetics and other thermally sensitive enzymes which eNO is a substrate to might be involved. NO results in vasodilation through its sympathoinhibitory role as well as its direct effect on smooth muscle cells. The die-away phase is observed when the heating lasts for more than 60 min and it is indicated by a significant reduction in cutaneous vasodilation and is suggested to be under adrenergic control [38].

Thermal blood flow stimulation as well as other possible methods to increase tissue perfusion as described in literature [49–51] were tested and are discussed in more details in Appendix B.

1.6 RESEARCH MOTIVATION AND OUTLINE

My analysis of the state of the art cryotherapy indicates that the control of blood flow by adjusting tissue temperature relating to both the therapeutic advantage of technology and to its potential for causing injury therefore for my PhD research I have undertaken a rigorous experimental analysis of the coupling of tissue blood flow to temperature. I have conducted an aggregate of 230 human subject experiments and based on this work to date, we have submitted 4 archival papers, one book chapter and five peer reviewed conference proceedings.

In the work described here, I have attempted to expand upon the understanding of and to improve cryotherapy practices. Even though, cryotherapy is widely practiced in clinical fields and by athletic trainers many aspects of it remains anecdotal. The applied temperature and the duration of application vary widely between recommendations. The boundary condition applied at skin level is ignored and the understanding of skin temperature and vascular response to localized cooling needs improvement. In the following chapters I have endeavored to address some of these issues. Chapters 2-5 are free standing papers that are either accepted for publication or were just submitted. Chapter 6 presents additional research that I have accomplished but is not yet embodied in a manuscript that has already been submitted but it will be in the future.

In Chapter 2 I have offered a phenomenological description of skin temperature and perfusion response to localized cooling. This chapter provides temperature and perfusion data from multiple cryotherapy experiments using CTUs. These experiments

are chosen from more than 100 cryotherapy experiments performed on 27 subjects. The length and applied temperature of the cooling portion of the experiments vary from 1 to 80 min and 7 to 25ºC, respectively. I also touch on the concept of dose-dependent response of perfusion to duration of application. I demonstrate that increasing the duration of application further reduces tissue perfusion up to cooling duration of 30-40 min beyond which no further reduction if perfusion is observed.

I investigated the temperature profile on cooling pad using IR imaging in Chapter 3. Total of 13 CTUs were investigated with 1-3 device-specific pad types/CTU. To analyze IR images, different statistical approaches were used to define temperature uniformity of pad surface including, min, max and temperature range. I also expressed the temperature range for the middle 90%, 86.5% and 63.2% of occupying the pad surface.

Chapter 4 is based on a selection of 17 experiments using 4 CTUs. In this chapter I showed a significant reduction in tissue perfusion after 60 min of active cooling and that the result was not different between different device types or the two body parts under the study (knee and foot/ankle). I also demonstrated the persistence of vasoconstriction during the recovery period after cessation of active cooling using different statistical method such as a case-control study, pair-wise comparison and mixed model regression analysis.

In chapter 5 I revisited the concept of persistence of vasoconstriction during the rewarming period. The data presented in this chapter was based on 6 cryotherapy experiments using a CTU. I showed that perfusion did not increase significantly for at least the first 90 min of the rewarming period using multiple statistical tests. Additionally, I introduced and discussed the hysteresis effect between skin temperature and perfusion during cooling and rewarming. I postulated that this hysteresis affect was

possibly due to release of a humoral agent that prevents vasodilation during the passive rewarming even though the skin temperature is returning to its original values. Another contributing factor could be the biophysical effect of cold that lasted beyond the cooling period.

We have studied cryotherapy with more complete instrumentation and analysis that we believe has been done in the past. Our research has led to discovery of several physiological phenomena that have not been identified previously. These new insights have led to the design and development of improved devices and methods for performing cryotherapy more safely and effectively.

Chapter 2: Experimental Characterization of the Domains of Coupling and Uncoupling Between Surface Temperature and Skin Blood Flow[1]

ABSTRACT

Purpose: Local therapeutic cooling to soft tissue is known to sometimes cause necrosis and neuropathy via cold-induced ischemia. The purpose of this study is to quantify the occurrence and persistence of cold-induced ischemia associated with cryotherapy.

Methods: FDA approved or exempt cryotherapy devices were applied for localized cooling on human subjects via recommended user protocols. Subjects were instrumented on the cooling site with thermocouples and laser Doppler blood flow probes.

Results: Local cutaneous blood perfusion was depressed to as little as 15% to 20% of baseline and remained depressed for hours following the cessation of active cooling. Induction of vasoconstriction was coupled to active surface cooling, and persistence of vasoconstriction was decoupled from subsequent passive surface rewarming.

Conclusions: Skin blood flow drops progressively during active cooling of skin, but during subsequent passive rewarming the flow may remain deeply depressed and decoupled from the increasing skin temperature. There is a large hysteresis between skin temperature and blood flow during the tissue cooling and warming cycle, having important implications for therapeutic efficacy and safety.

Keywords: bioheat transfer, cryotherapy, hysteresis, ischemia, skin blood perfusion, tissue cooling

[1] This chapter is based on the manuscript accepted for publication by The International Journal of Transport Phenomena coauthored by Sepideh Khoshnevis, Natalie K. Craik and Dr. Kenneth R. Diller [52].

INTRODUCTION

Localized cooling is commonly used following orthopedic surgery and in sports medicine to reduce swelling, pain, inflammation, metabolism, muscle spasm, and bleeding [53,54]. Cryotherapy protocols are typically carried out in conjunction with post orthopedic surgical rehabilitation via a device called a cryotherapy unit (CTU). In contrast with acute cooling treatments used for sports injuries by application of a flexible bag of ice or a gel pack for a relatively short time, cryotherapy as an adjuvant to a surgical procedure is often maintained continuously for days up to a week [9,25,55] based on the extended operating capabilities of a CTU. Most CTUs consist of an insulated container that can be filled with an ice and water mixture and into which an immersion pump is placed to produce a circulation of ice water through a flexible polymeric bladder placed onto the treatment site over a thermal barrier. In general the quantitative insulating properties of the barrier are not specified or enforced integrally to the CTU with the result that a very wide range of temperatures may be created on the skin surface. Our studies show that the temperature of water flowing through the bladder may be as low as 2°C, with the temperature on the bladder surface on the order of 5°C and the skin surface ranging variously over the range from less than 10°C to 25°C or higher. For reference, the temperature of the skin surface when exposed to a thermoneutral environment generally falls within the range of 30°C to 34°C. The variation in temperatures over the surface of a bladder may be 10°C or greater in the absence of a thermal load, with attendant larger thermal gradients on the skin in the treatment area.

CTUs often have no thermal controller, or have one that is not based on a feedback signal from the skin temperature, although regulation of the skin surface temperature is the operational target for the therapeutic procedure. As a consequence,

there can be a large variation in the thermal performance of CTUs, some resulting in limited ability to regulate and execute thermal therapeutic procedures. In this context, a primary physiological response to the imposition of a reduced skin surface temperature is modulation of red blood cell flux through tissue in the treatment area. If one is to design a CTU to embody thermal operating characteristics to achieve a desired physiological outcome, it is necessary to have a quantitative description for the extent of the coupling behavior between skin blood flow and applied surface temperature.

Although therapeutic cooling is tolerated by many patients, there are instances in which application of a CTU for an extended time has led to extensive tissue necrosis and/or nerve injury in the treatment area, sometimes with dire medical consequences [13,56–58]. These events are thought to be a result of the application of cold to the skin surface causing a major loss of blood perfusion in the underlying tissues, resulting in a state of ischemia (low blood flow) that deprives tissue of the supply of oxygen and nutrients required to sustain cell metabolism [45]. Further, the diminution of blood perfusion will allow an accumulation of toxic metabolic byproducts that would normally be carried away from tissues by blood. The consequence is a state in the tissue conducive to the occurrence of nonfreezing cold injury (NFCI) that may be manifested in the death of cells (necrosis) and nerves (neuropathy) [43]. Therefore, it is desirable to be able to characterize the mechanistic relationship between the application of therapeutic cooling to skin and the reduction of blood flow in affected tissue structures.

To this end, we have conducted more than 200 human tests on many different commercially marketed CTUs on four specific areas of the body while measuring the transient temperature and blood perfusion responses of the skin. The protocols embodied an initial period of benchmark data with the bladder applied but no water flow, followed by active cooling with the CTU pumping cold water through the bladder, and finally a

period of passive rewarming with the water flow terminated, but the bladder still remaining in place at the treatment site. The protocols were approved by the University of Texas Institutional Review Board (IRB) and were designed and implemented to mimic typical prescribed uses of the devices.

METHODS

Data presented in this paper is based on experiments run on FDA approved or exempt, commercially available cryotherapy devices, including: Breg Polar Care 300, 500, and 500 Lite (Breg, Carlsbad, CA), DeRoyal T505 and T600 (DeRoyal Industries, Powell, TN), Game Ready (Game Ready, Concord, CA), Artic Ice System (Pain Management Technologies, Akron, OH), and DonJoy Ice man 1100 and Aircast Cryo/Cuff (DonJoy Global, Vista, CA). The data reported herein were recorded for cooling at one of the following sites: the knee, the shoulder, the ankle, or the straight length of the lower leg between the knee and the ankle (calf and shin area).

Blood perfusion was measured using Moor VMS-LDF2 and VMS-LDF1-HP laser Doppler flow probes (Moor Instruments, Millwey, Axminster, Devon, UK), thin ribbon and small bead thermocouples (Omega Engineering, Stamford, CT), and a heat flux gauge (Omega Engineering, Stamford, CT), all mounted directly onto the skin at the site of active cooling. The laser Doppler probes have different focal depths of sensing blood flow, the LDF2 at about 0.5mm and the LDF1-HP at about 2mm [59]. These are denoted as superficial and deep measurements, respectively. The superficial probes incorporate a thermistor on the surface of the fiber optic window to monitor the local skin temperature. Blood pressure was monitored intermittently on the upper arm with a sphygmomanometer, and the values were applied to normalize the blood perfusion

measurements to calculate the cutaneous vascular conductance (CVC), where the CVC is defined in arbitrary units as:

CVC = laser Doppler flux /mean arterial pressure.

National Instruments data acquisition modules NI 9201, 9205, 9211, and 9213 and NI DAQ chassis 9172 and 9174 (National Instruments, Austin, TX) were used to collect blood perfusion and temperature data and as an interface for computer logging, respectively. Temperatures were measured with a tolerance of ±0.5°C. All data was collected with a sampling rate of 12 HZ, and temperature data was subsequently down sampled to 4 Hz.

The area on the skin to which the cooling bladder was applied was covered with a thermal insulation barrier consisting of either a single loose layer of elastic bandage (ACE) or a therapeutic stocking (TED). The barrier also covered all thermal instrumentation placed directly onto the skin under the bladder, but only surrounded the laser Doppler probes because they have a sensor elevation of about 1 cm above the skin surface. A thermocouple was also placed on the surface of the cooling bladder directly overlaying one of the skin temperature measurement thermocouples. In some instances tee connectors with a thermocouple positioned in the side branch were inserted into inlet and outlet water lines adjacent to the bladder to monitor the water temperatures at those points.

The subjects were either seated with their back at a 45º angle from horizontal and the legs extended on the same plane as the hips or reclining in a supine position for the duration of each experiment. Physical movements of the limb being tested were kept to a minimum to avoid introducing blood flow measurement artifacts. All experiments were performed at a constant ambient temperature and relative humidity of approximately 23°C and 50%. A light blanket was placed over the subject, at his/her request, to diminish

any vasoactive response driven by whole body thermoregulation inputs, especially to avoid any reaction to a possible general cooling of the overall skin surface that might induce vasoconstriction.

The sequence by which instrumentation and a cooling bladder were applied to a subject at a test site is illustrated in Figure 2.1.

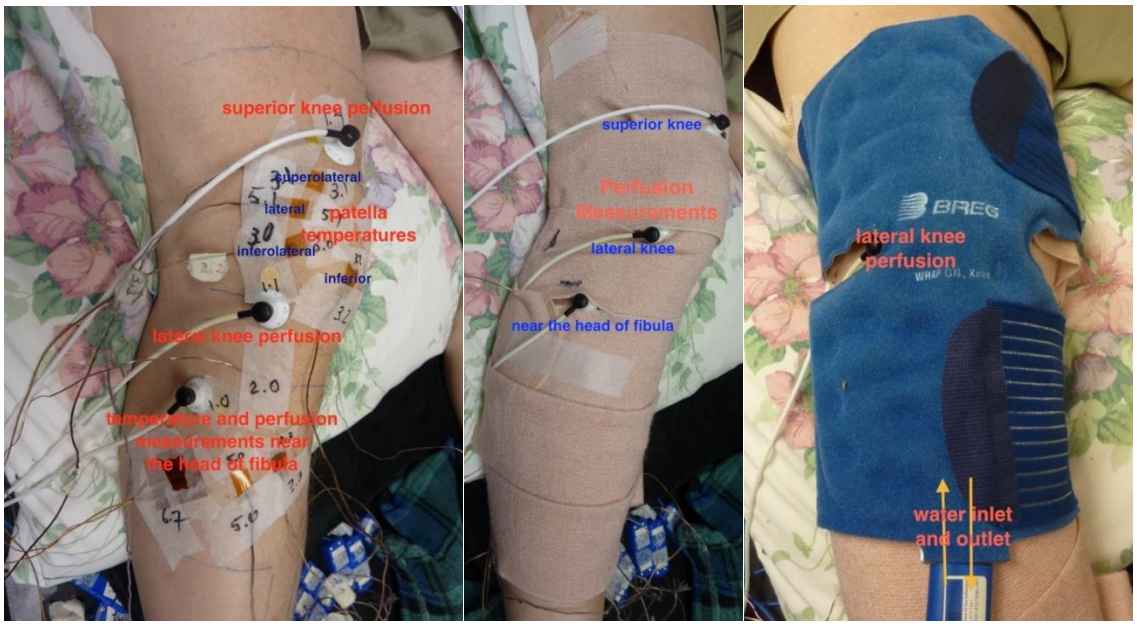

Figure 2.1. Instrumentation of a subject for a CTU tested on the right knee. The view is from the ventral aspect. (a) Sensors applied to the skin, including six smaller rectangular thermocouples, one larger square heat flux gauge, and three fiber optic probes for laser Doppler measurements. Numbers written on mounting tape indicate connection junctions of lead wires to the DAQ. (b) The same area after a thermal insulation barrier consisting of a single layer of ACE bandage wrap has been applied with no elastic stretching. (c) A Breg Polar Care cooling bladder positioned over the thermal barrier.

Approximately one hour was required to apply and connect all of the instrumentation onto the subject at the beginning of an experimental session and to confirm its function. This process allowed the subject to become acclimated to the experimental environment. Extant room temperature water remained captured within the

bladder until the cooling process was commenced by the circulation of ice water. After all of the instrumentation was in place and its function verified and a layer of insulating material was applied to the testing area, the cooling bladder was placed onto the treatment site, after which the bladder surface temperature rapidly approached that of the skin. Each protocol was initiated with a 10 to 45 minute period of baseline data acquisition before ice water flow into the bladder was initiated. The purpose of this period was to obtain values for perfusion and temperature to which subsequent changes elicited by the cryotherapy procedure could be normalized. Although the values of temperature and especially of blood perfusion were never perfectly static, baseline variations were small in comparison with those caused by the cooling procedures.

The cooling process was initiated at the end of baseline data collection by turning on the CTU pump to produce a steady flow of ice water through the bladder (or by increasing the elevation of the ice water container for gravity feed devices.) The duration of the cooling period was a primary control parameter evaluated in this study. Ice water flow through the bladder was maintained continuously for a wide range of times, including approximately 1, 2, 3, 5, 10, 30, 40, 60, and 80 minutes, as well as others, and in some trials the protocol was repeated one or more times.

The cooling process was terminated by turning off the ice water pump, following which both the bladder and the underlying tissues began to warm via a combination of parasitic heat gain from the environment and active warming from within the tissues by metabolism and convection of blood. Both of the latter physiological effects were depressed at the lower local tissue temperatures. The period of time over which the rewarming process was monitored also was varied for a wide range of values from 30 to 240 minutes. In some trials cooling was reinitiated following a defined period of rewarming to establish a cooling and rewarming cycle that could be reiterated. Table 2.1

presents a summary of the value ranges that were measured for key parameters for the aggregate of the CTU trials conducted.

Parameter	*Measured Range*		*Units*
	Minimum	*maximum*	
Baseline period	15	39	min
Cooling temperature	7	25	°C
Cooling period	1	80	min
Warming period	30	240	min
Maximum drop in perfusion from baseline	-31	-85	% change

Table 2.1. Summary of measured ranges of temperatures, cooling rates, cooling duration, and blood flow depression for the CTUs tested.

RESULTS

The reported experiments were conducted on healthy adult subjects covering the age range of 20 – 70 years. In total more than 110 CTU trials have been conducted on 27 subjects, approximately evenly divided between males and females. The selected results reported herein are representative of and consistent with the physiological response to the application of cryotherapy observed and measured in all trials. They are chosen to illustrate the phenomenological domains of coupling between skin temperature and skin blood perfusion encountered during CTU protocols, including active cooling and passive rewarming.

The data are presented primarily in terms of plots of the concurrent time variation in temperature and blood perfusion at specific sites under the cooling bladder. For trials lasting as long as six hours and involving data acquired in parallel from 10 or more sensors, the amount of information generated is large. Only certain transducer outputs are

displayed for each experiment so as to not obscure individual sensor behaviors by crowding and overlapping of plot lines. As would be anticipated, data are not replicated exactly among the various trials or even among various sensor locations for an individual trial, but a number of very important consistent behaviors have been identified. The results are presented in a format to emphasize the primary and most significant phenomena that have been measured and characterized. Perfusion data plots are the result of time averaging over a 3 minute moving window unless otherwise specified. The data from individual CTU trials follow.

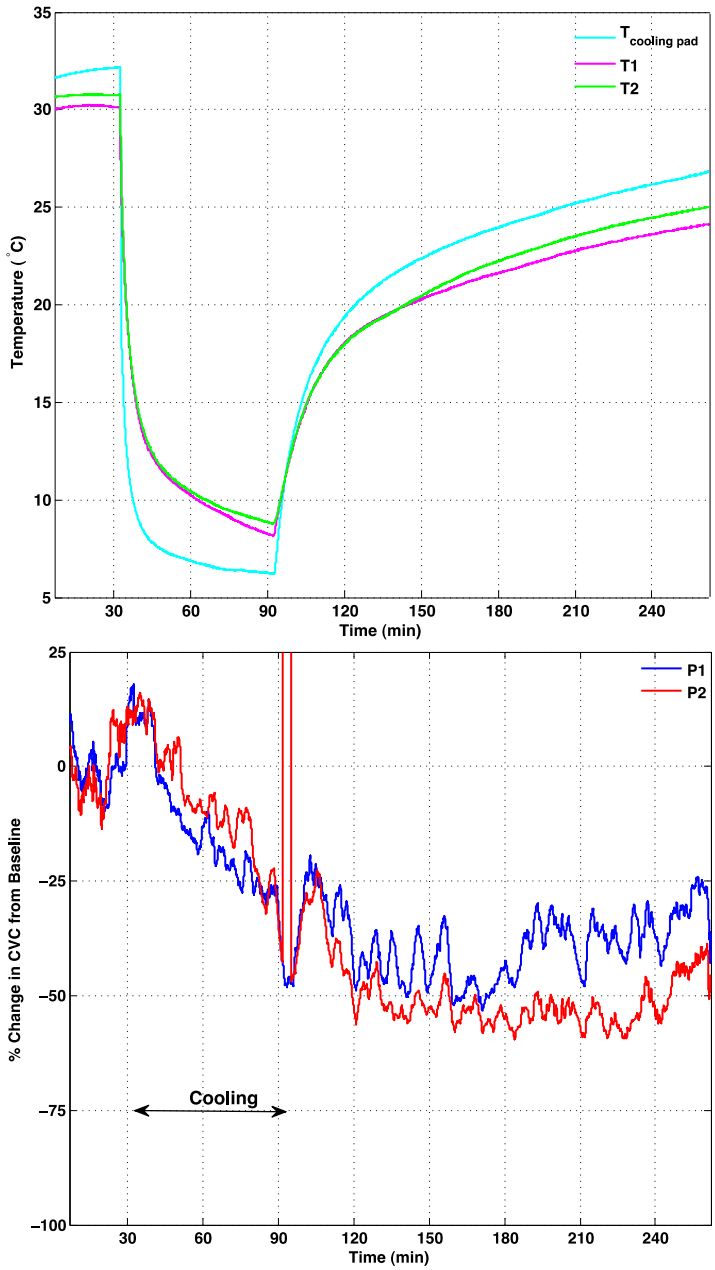

Figure 2.2. Data for a cryotherapy trial with a DonJoy Iceman 1100 system applied to the calf and shin consisting of 30 minutes of baseline data, followed by active cooling for 60 minutes and passive rewarming for 150 minutes. (a) Temperature histories measured at two locations on the skin under the water perfusion bladder (red and green) and on the surface of the bladder (cyan). (b) P1 and P2 represent perfusion histories under the cooling bladder.

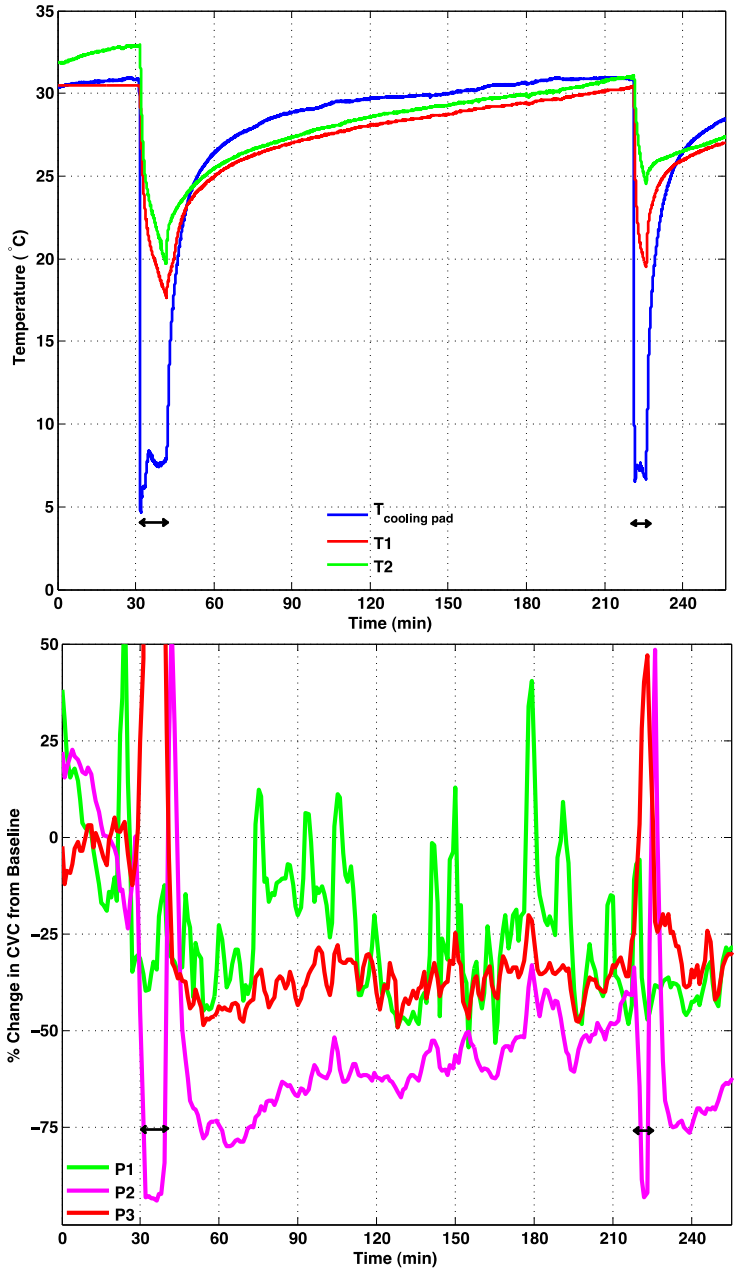

Figure 2.3. Data for a cryotherapy trial with a Breg Polar Care 500 Lite system applied to the knee consisting of 30 minutes of baseline data, followed by active cooling for 10 minutes, and passive rewarming for 180 minutes, resumption of active cooling for 5 minutes, and passive rewarming for 20 minutes. Double arrows mark the duration of each cooling cycle. (a) Temperature histories measured at two locations on the skin under the water perfusion bladder (red and green) and on the surface of the bladder (blue). (b) Two superficial (magenta and green) and one deep (red) perfusion histories under the cooling bladder.

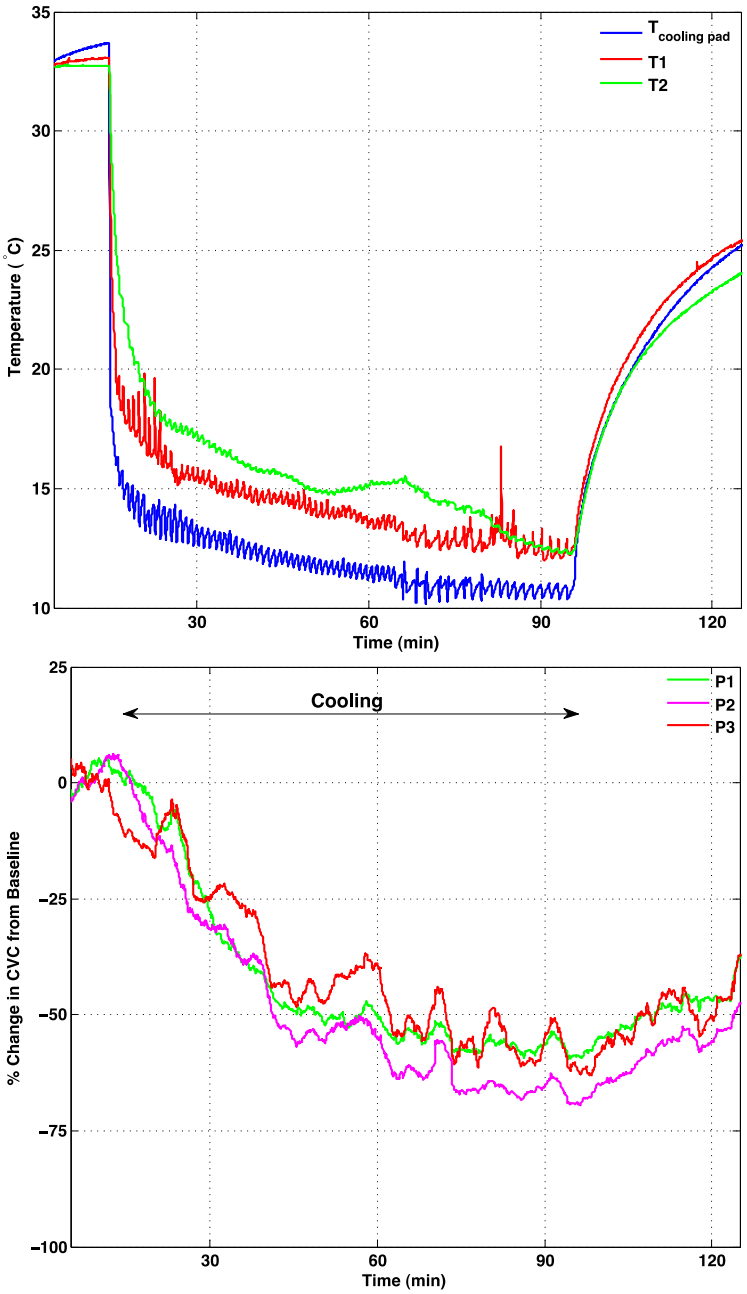

Figure 2.4. Data for a cryotherapy trial with a DeRoyal T600 applied to the shoulder consisting of 15 minutes of baseline data, followed by active cooling for 80 minutes, and passive rewarming for 30 minutes. (a) Temperature histories measured at two locations on the skin under the water perfusion bladder (red and green) and on the surface of the bladder (blue). (b) Two superficial (magenta and green) and one deep (red) perfusion histories under the cooling bladder.

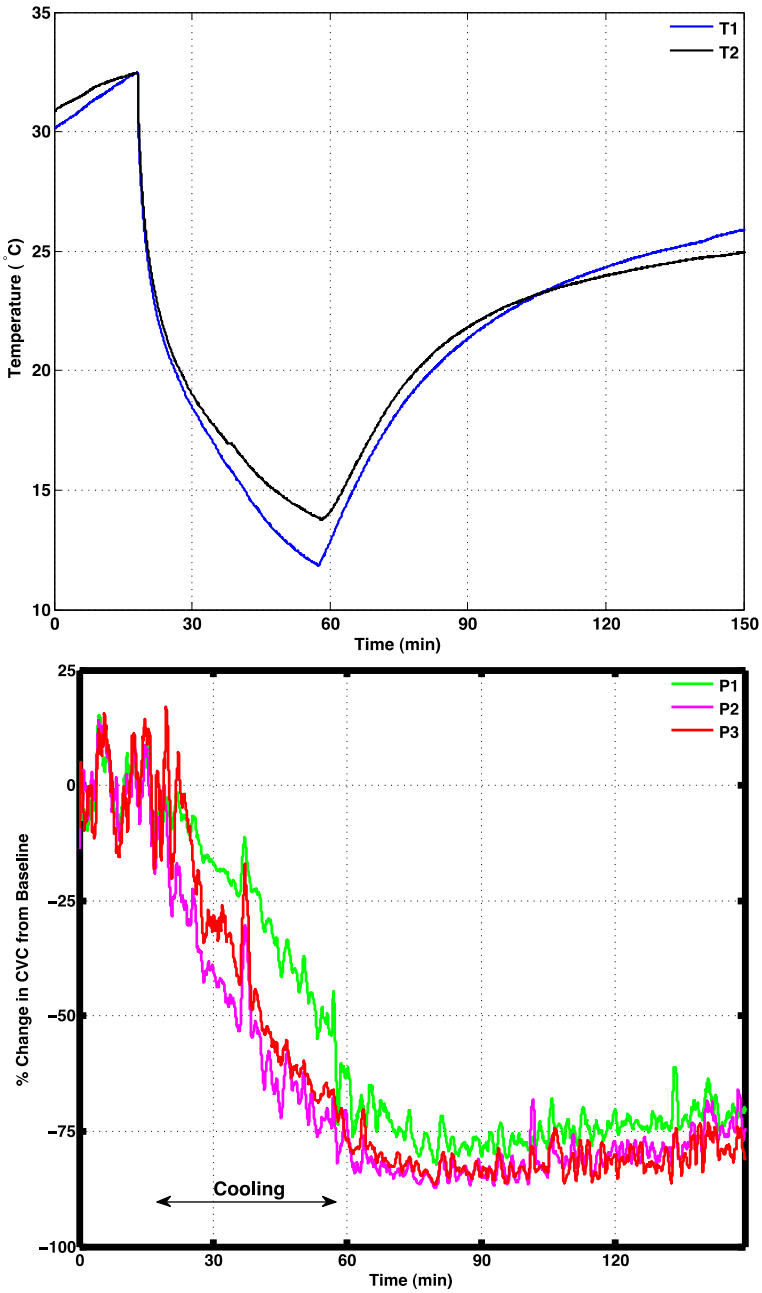

Figure 2.5. Data for a cryotherapy trial with an Arctic Ice System applied to the calf and shin area of the lower leg, consisting of 15 minutes of baseline data, followed by active cooling for 40 minutes and passive rewarming for 90 minutes. (a) Temperature histories measured at two locations on the skin surface under the cooling bladder (black and blue). (b) Superficial (green and magenta) and deep (red) perfusion histories at three sites in the skin under the cooling bladder. Perfusion data was time averaged over a 1 minute moving window as distinguished from a 3 minute window for the other trials.

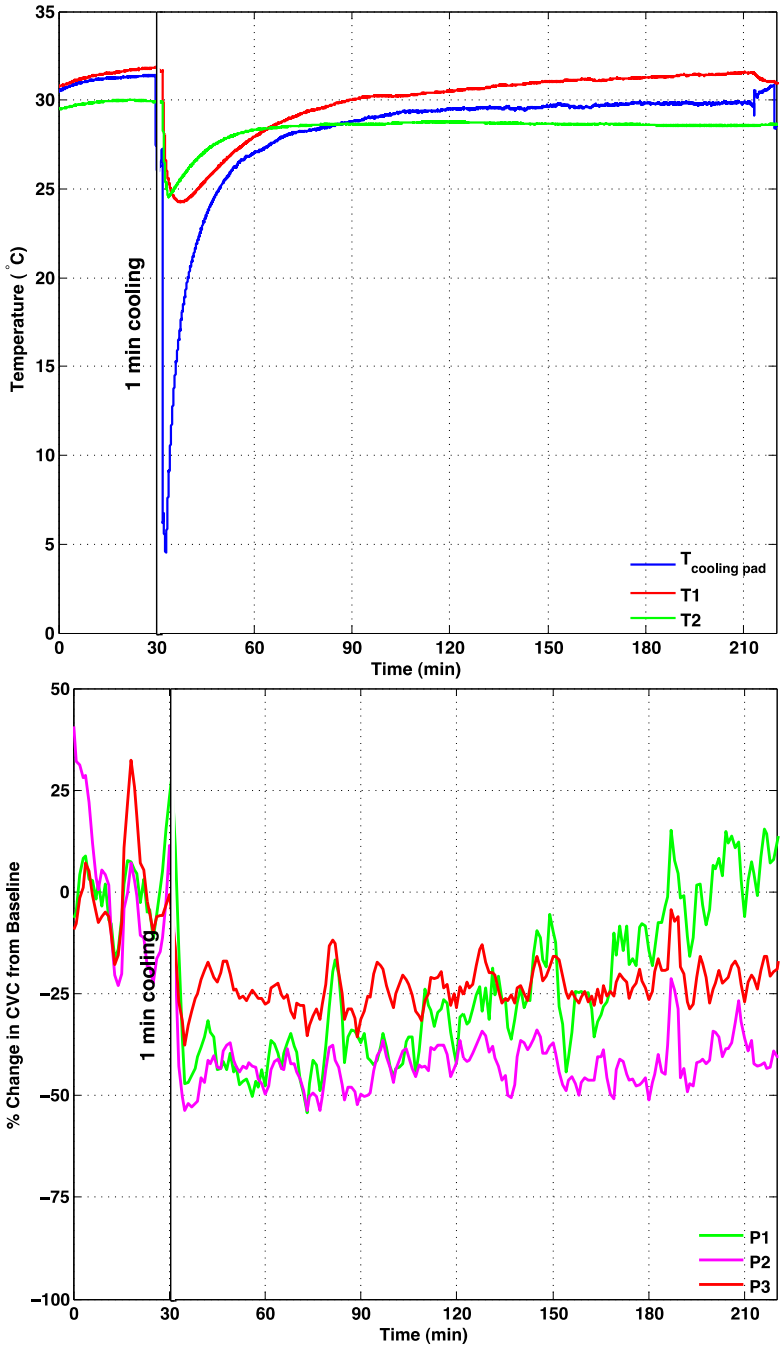

Figure 2.6. Data for a cryotherapy trial with an Arctic Ice System applied to the calf and shin area of the lower leg, consisting of 30 minutes of baseline data, followed by active cooling for 1 minute and passive rewarming for 195 minutes. (a) Temperature histories measured at two locations on the skin surface under the cooling bladder (red and green) and on the surface of the bladder (blue). (b) Superficial (green and magenta) and deep (red) perfusion histories at three sites in the skin under the cooling bladder.

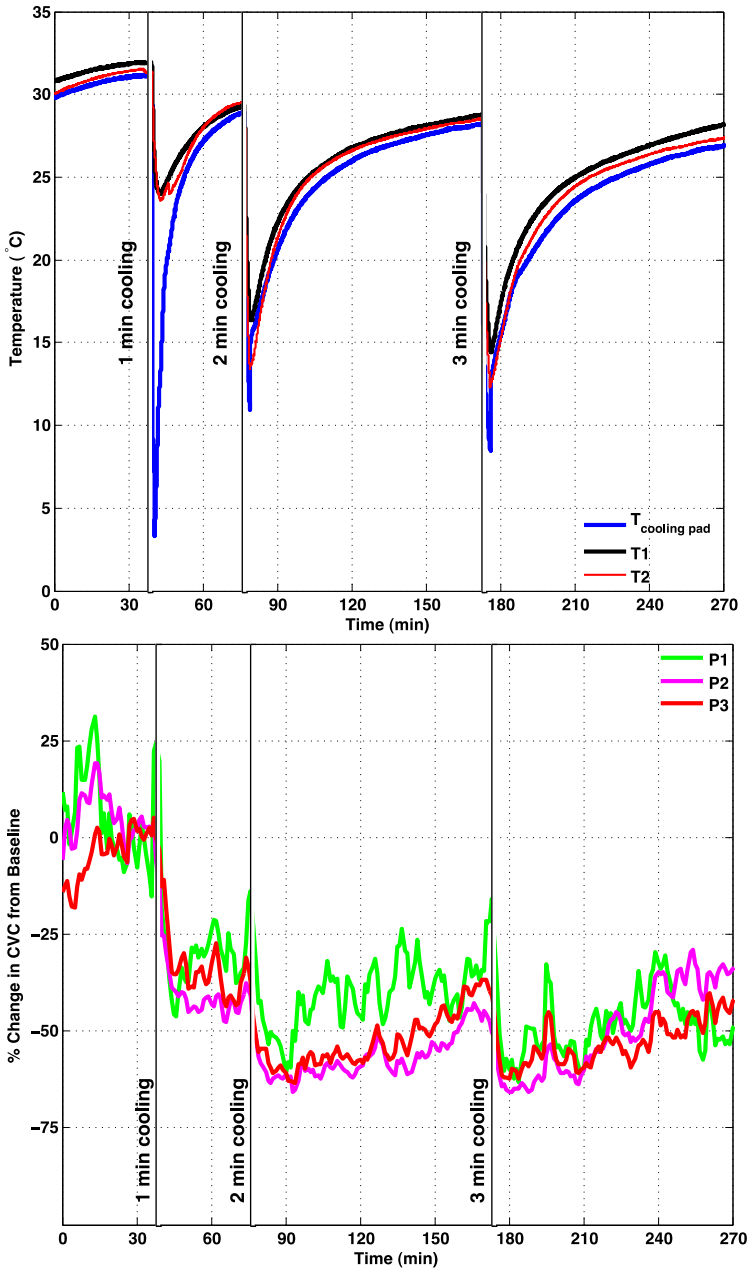

Figure 2.7. Data for a cryotherapy trial with an Arctic Ice System applied to the calf area of the lower leg, consisting of 39 minutes of baseline data, followed in sequence by active cooling for 1 minute and passive rewarming for 37 minutes, 2 minutes of active cooling and 96 minutes of passive rewarming, and 3 minutes of active cooling and 122 minutes of passive rewarming. (a) Temperature histories measured at two locations on the skin surface under the cooling bladder (red and black) and on the surface of the bladder (blue). (b) Superficial (green and magenta) and deep (red) perfusion histories at three sites in the skin under the cooling bladder.

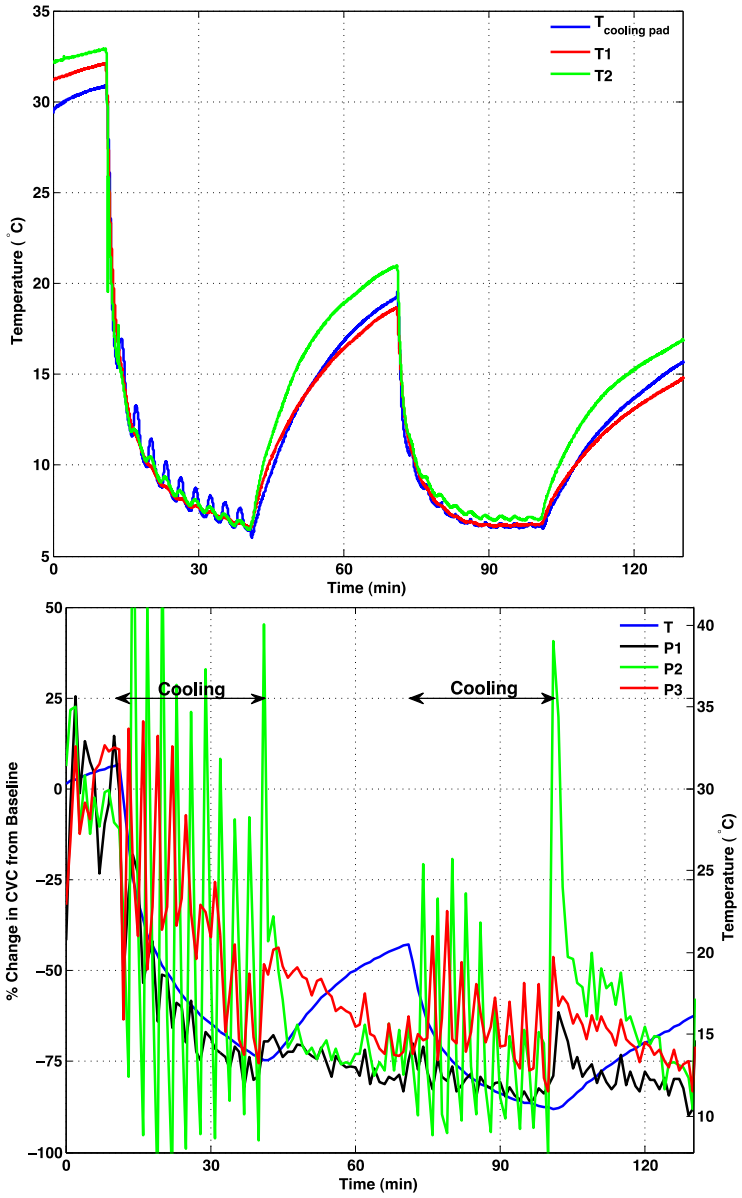

Figure 2.8. Data for a trial with a Game Ready CTU applied to the knee, consisting of 10 minutes of baseline data, followed sequentially by active cooling for 30 minutes and passive rewarming for 30 minutes, then a second identical episode of active cooling for 30 minutes and passive rewarming for 30 minutes. (a) Temperature histories measured at two locations on the skin surface under the cooling bladder (red and green) and on the surface of the bladder (blue). (b) Superficial (green and black) and deep (red) perfusion histories at three sites in the skin under the cooling bladder. The blue plot shows the temperature history measured via one laser Doppler probe. Note that the intermittent pressurization feature was operative during this trial in which an outer air bladder was periodically inflated and deflated for 90 seconds sequentially.

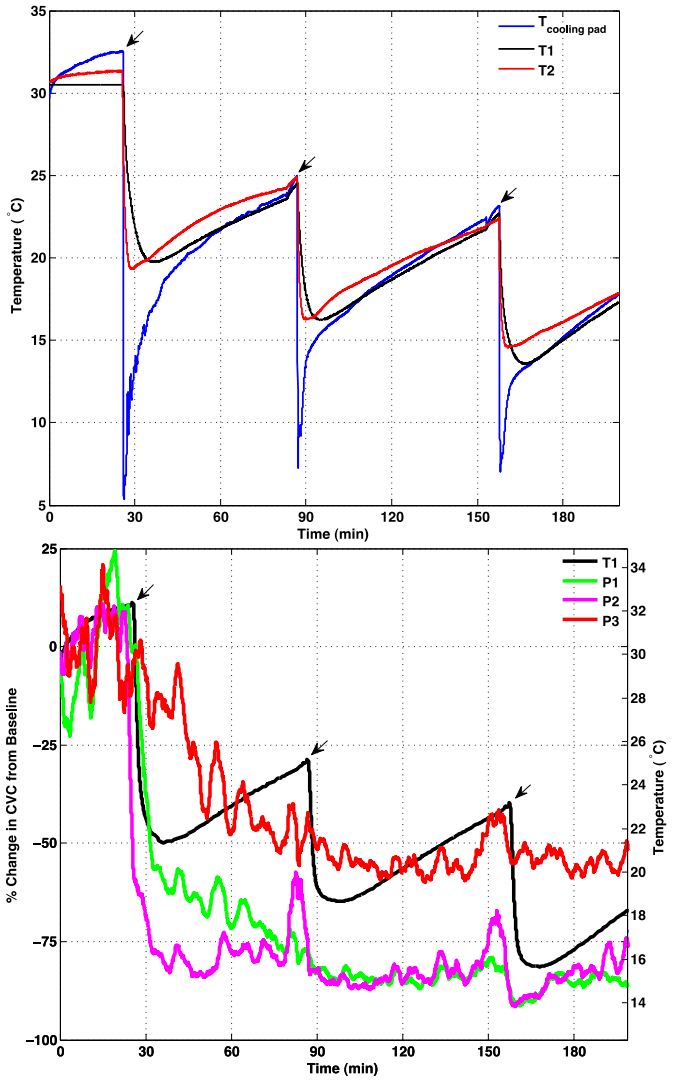

Figure 2.9. Data for a trial with an Aircast Cryo/Cuff CTU applied to the knee, consisting of 26 minutes of baseline data, followed which the cooling bladder was filled with ice water by gravity feed with the source container elevated approximately 0.3 m above the bladder and kept in position with the air vent opened for approximately 56 minutes. The source container was then lowered below the bladder to allow the water to drain from the bladder, and at 60 elapsed minutes after the first cooling episode it was again raised 0.3 m above the bladder to provide a second cooling cycle. A third cooling episode was initiated after an additional 72 elapsed minutes. A slight perturbation to the slope of the temperature plots can be observed during the lowering of the source container just prior to the start of subsequent cooling episodes. (a) Temperature histories measured at two locations on the skin surface under the cooling bladder (red and black) and on the surface of the bladder (blue). (b) Superficial (green and magenta) and deep (red) perfusion histories at three sites in the skin under the cooling bladder. The black plot shows the temperature histories measured via the thermistor on one of the two low power laser Doppler probes. Black arrows point to the start of each cooling period.

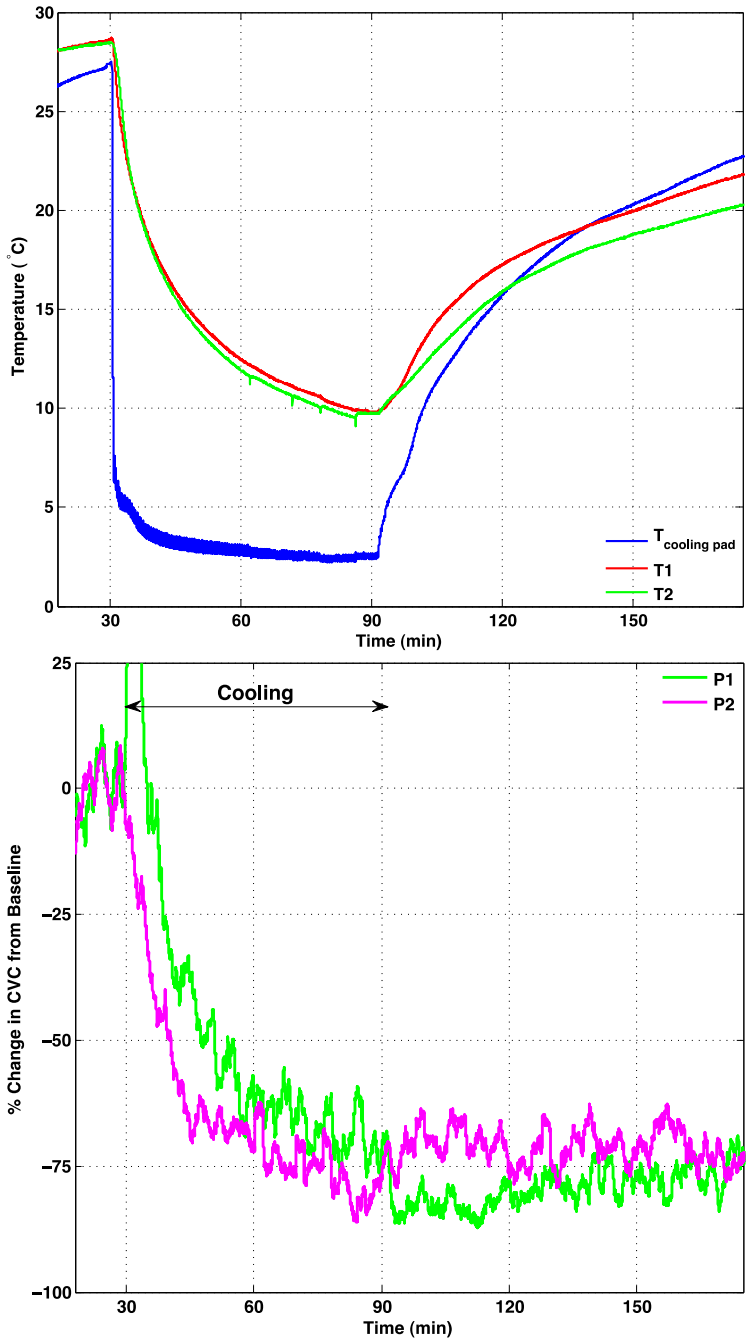

Figure 2.10. Data for a trial with a Breg Polar Care 300 cryotherapy unit applied to the knee, consisting of 30 minutes of baseline data, followed by active cooling for 60 minutes and passive rewarming for 84 minutes. (a) Temperature histories measured at two locations on the skin surface under the cooling bladder (red and green) and on the surface of the bladder (blue). (b) Superficial (green and magenta) perfusion histories at two sites in the skin under the cooling bladder.

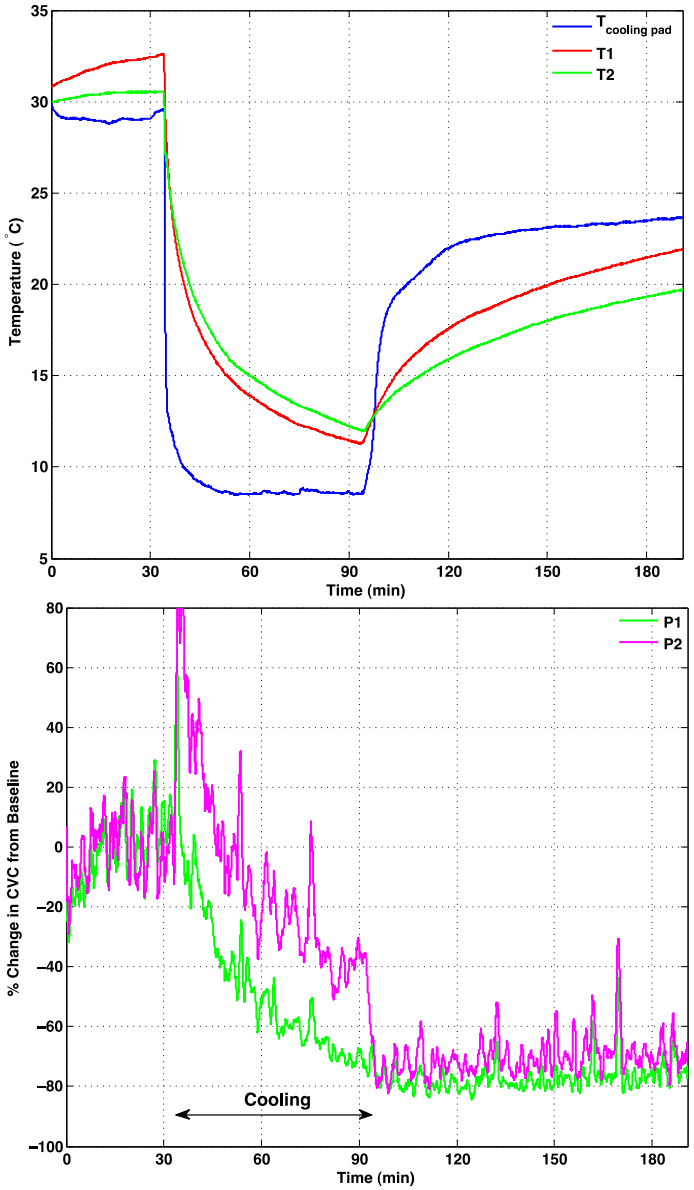

Figure 2.11. Data for a trial with a DonJoy Iceman 1100 unit applied to the ankle, including 34 minutes of baseline data, followed by active cooling for 60 minutes and passive rewarming for 86 minutes. Temperature histories were measured at two locations on the skin surface under the cooling bladder (red and green) and on the surface of the bladder (blue). (b) Skin blood perfusion measured at two locations under the cooling bladder. The magenta perfusion plot shows a sudden increase and decrease with the initiation and termination of water flow through the cooling bladder, respectively, due to sudden change in applied mechanical pressure. This effect is not seen in the green perfusion plot. This variation in response is likely due to differences in the anatomical locations of the probes relative to the water flow pattern within the bladder and alteration of the probe/tissue orientation with the start and stop of pressurized water flow through the bladder. Double arrows mark the duration of cooling which lasted for 60 minutes.

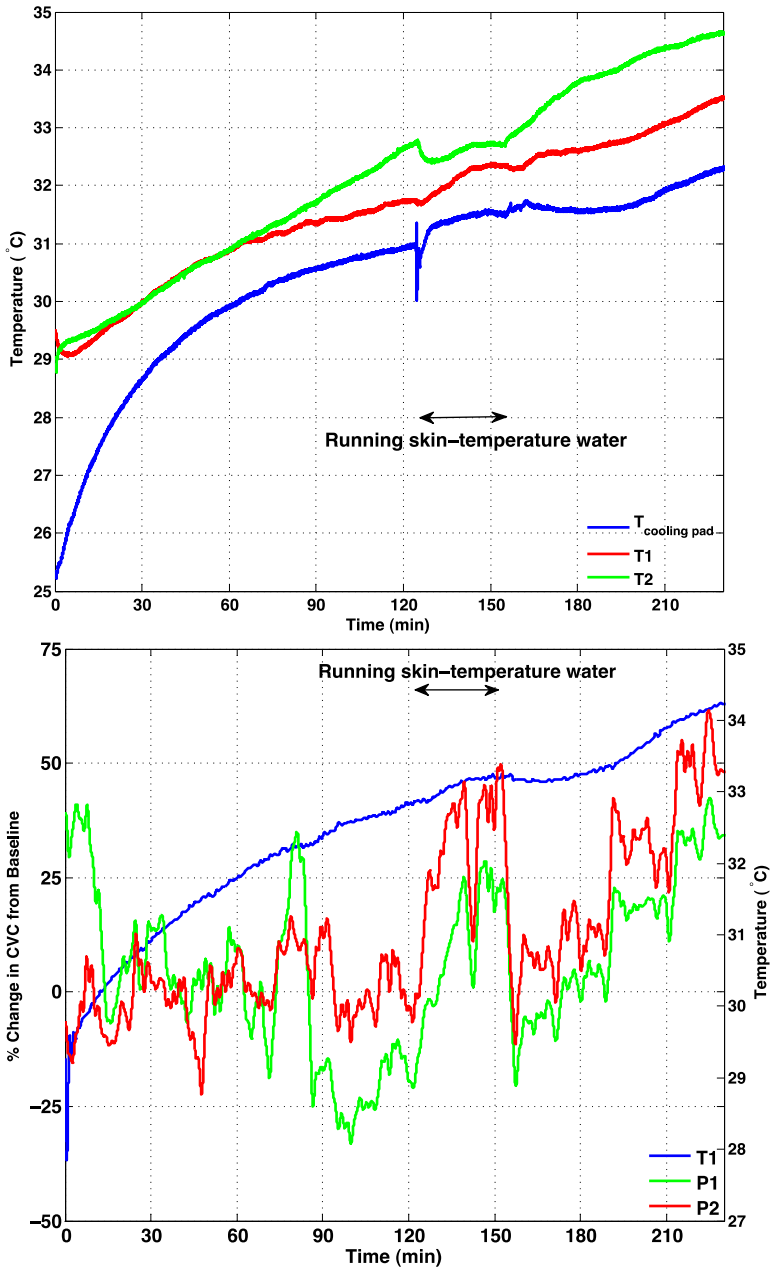

Figure 2.12. A control experiment with full instrumentation and a Breg Polar Care 500 Lite cooling bladder applied to the knee. Thermally neutral skin temperature water at about 32°C was pumped through the bladder from 125 to 155 minutes. There was no water flow through the bladder at other times. (a) Temperature histories measured at two sites on the skin under the cooling bladder (red and green) and on the surface of the bladder (blue). (b) Skin blood perfusion measured in the skin at two locations under the cooling bladder. P1 (green) and P2 (red) represent superficial and deep perfusion measurements, respectively. Also, the temperature measured via the thermistor on the laser Doppler probe at the superficial perfusion site is plotted (blue).

The foregoing figures illustrate the existence of a profound and persistent state of ischemia following the cessation of active cooling when the cooling bladder and underlying tissues are allowed to passively rewarm via natural convection with ambient air. This general behavior has been observed for the entire spectrum of standard cryotherapy protocols we have investigated. In this context, we undertook a nonstandard protocol in which an active rewarming process was imposed following a period of usual passive rewarming by circulating heated water through the cooling bladder. The prime objective of this study was to see if active heating could be used to break the state of post-cooling ischemia. Following active rewarming, a second cycle of active cooling and passive rewarming was applied to determine whether the state of persistent post cooling ischemia would be reestablished. The transient temperature and perfusion plots for this study are shown in Figure 2.13.

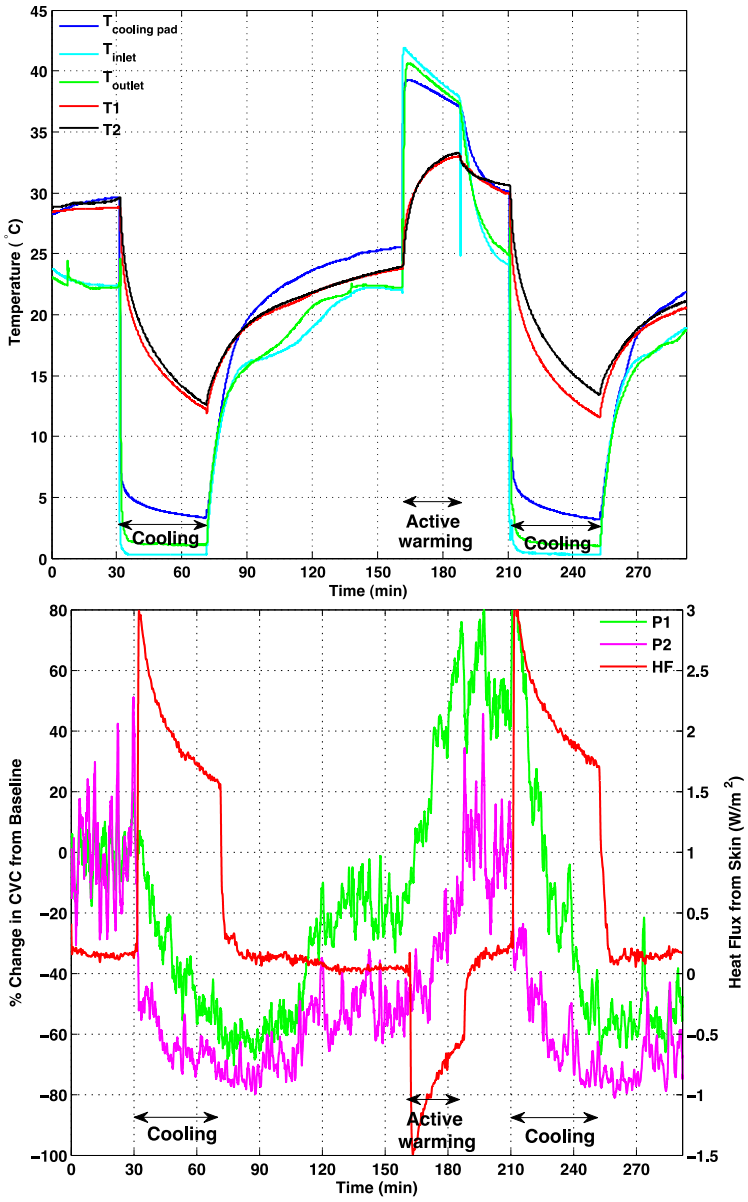

Figure 2.13. Data for a trial with a Breg Polar Care 500 cryotherapy unit applied to the knee, consisting of 30 minutes of baseline data, followed by active cooling for 40 minutes and passive rewarming for 90 minutes, then active rewarming for 27 minutes, passive heat transfer for 22 minutes, then active cooling for 42 minutes and passive rewarming for 40 minutes. (a) Temperature histories measured at two locations on the skin surface under the cooling bladder (red and black), on the surface of the bladder (blue), and in the water flow lines at the bladder inlet (cyan) and outlet (green). (b) Superficial (green and magenta) perfusion histories at two sites in the skin under the cooling bladder. Output from a heat flux gauge on the skin (red). The temperatures measured via the thermistors on both laser Doppler probes are plotted to show the correlation between perfusion and temperature.

Inspection of the thermal data presented in the foregoing figures shows that there is variation in the temperatures measured at different skin sites under a cooling bladder during individual trials. One possible source of these variations may be due to thermal gradients on the surface of the cooling bladder. Therefore, we acquired thermal images of the surface of a cooling bladder through which water was circulating to quantify the spatial disparities in the temperature pattern. For this purpose we placed a bladder in an unfolded configuration onto a flat surface with the cooling surface oriented upwards. We positioned a thermal camera (FLIR Systems, Boston, MA) directly above the bladder to record the two dimensional pattern of temperature on the surface. An example image for a Breg Polar Care 300 knee pad is shown in Figure 2.14. A more comprehensive analysis of this phenomenon will be reported in another companion paper.

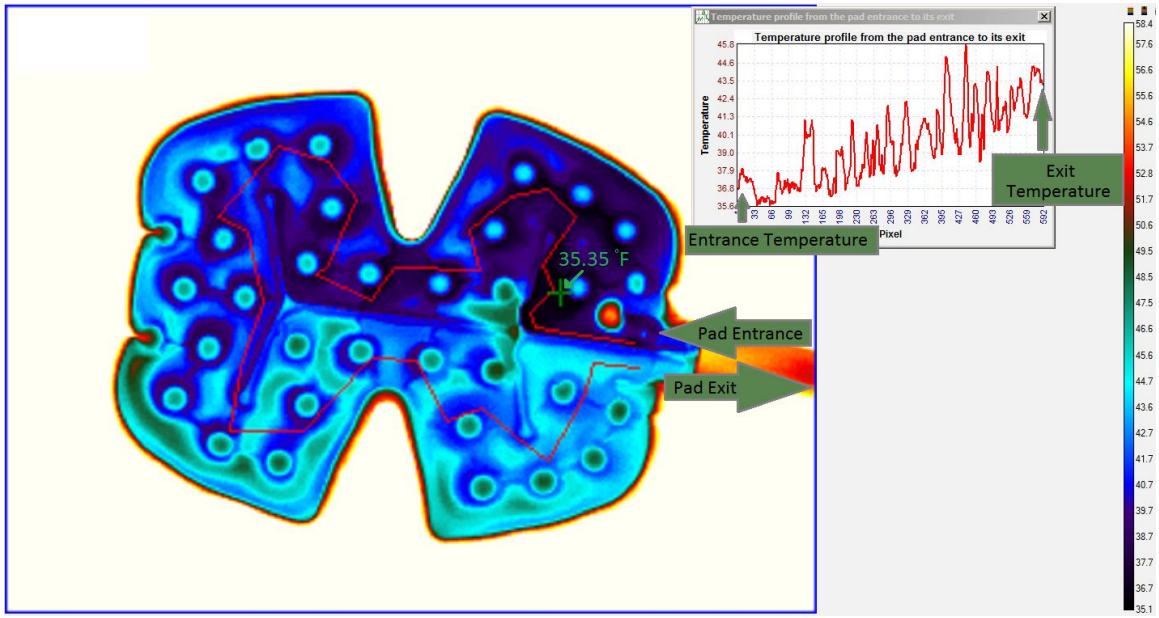

Figure 2.14. Infrared thermograph of the temperature distribution on the surface of a Breg Polar Care 300 knee bladder during perfusion with ice water. The surface was exposed to room air at 23°C.

There was no water condensation on the bladder surface that could corrupt the IR image. Temperatures are indicated on a pseudocolor scale. An exemplar flow pathway was manually traced between the inlet and outlet as indicated by the red line, with the temperatures of individual image pixels along the path plotted to the upper right. The warming differential on the bladder surface between inlet and outlet is about 4.5°C. Areas near the periphery of the water flow path and where the upper and lower surfaces of the bladder are welded together are substantially warmer. Temperature differences over the bladder surface are as large as 8°C.

A striking feature that is common to all of the CTU experiments we have conducted is that there is a profound hysteresis effect between the temperature applied during cryotherapy and the responsive skin blood flow as illustrated by the two exemplar data sets in Figure 2.15. During cooling the skin blood flow follows the falling skin temperature to values that are a small fraction of the precooling baseline value. When the skin temperature rises after cessation of active ice water flow, the rate of blood flow remains nearly static, in the absence of external stimulation, for periods that can extend for hours. The direct coupling, or lack thereof, between skin perfusion and temperature are illustrated by the hysteresis loop that develops through a cooling and heating cycle and is a primary feature of the physiological response to cryotherapy.

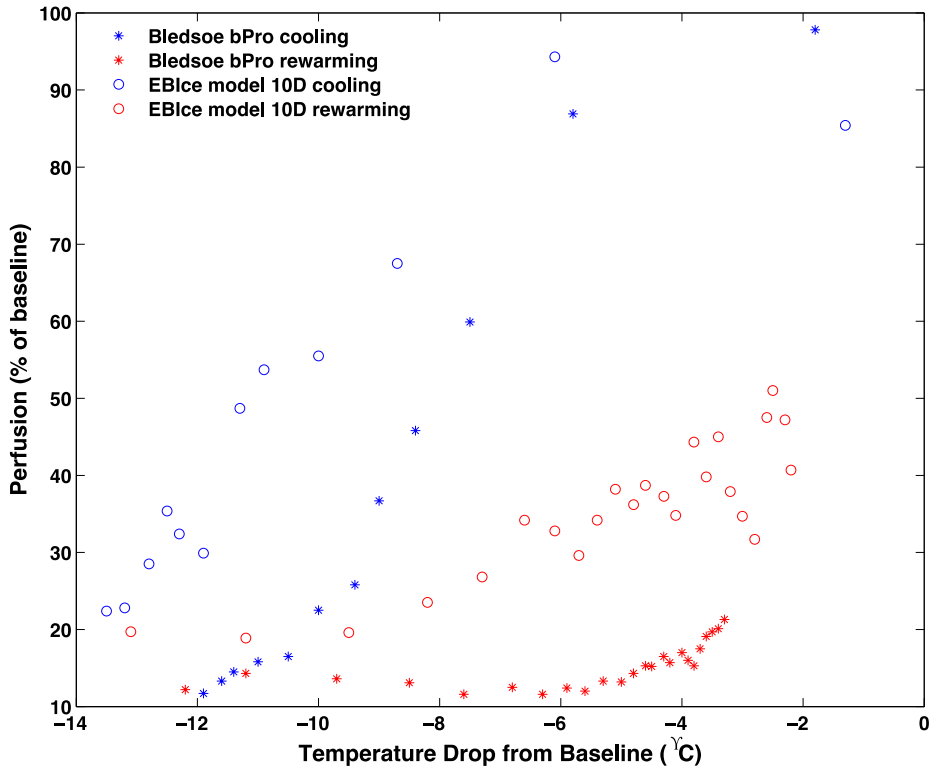

Figure 2.15. Hysteresis in local skin blood flow responding to falling and rising skin temperatures during cryotherapy for two different devices and subjects. Owing to experimental time limitations the cryotherapy cooling and heating cycle did not accommodate a complete return of perfusion to its baseline value.

DISCUSSION

The data plots, as an aggregate, document temperature and blood perfusion characteristics that are common across all of the trials we have conducted with various devices on different areas of the body and that provide broad insights into the physiological response to cryotherapy. Perhaps the most significant outcome of this study is that the application of a CTU procedure initiates a state of persistent ischemia at the treatment site. In the absence of an independent stimulation of blood flow, the ischemic state may extend long after the circulation of ice water is terminated. The impact of this outcome is the fact that exposure to ischemia over an extended period of time may

contribute to the development of tissue necrosis and neuropathy, as has been recognized widely in prior literature. There are also differences among the measured temperatures and blood perfusions among and within the various trials that are important to recognize and understand. These are discussed as follows.

Temperature Effects

As would be anticipated, during cooling the temperature on the bladder surface drops ahead of the skin temperature, creating a gradient in which heat flows from tissue to the bladder and the cold water circulating through it. For trials in which active cooling lasted long enough for the bladder surface temperature to reach a steady state value (Figs 2.4(a), 2.10(a), 2.11(a), 2.13(a)), the skin continued to cool long after the bladder was at steady state. This behavior is due in large part to the much larger thermal mass of the tissue being cooled in comparison with the bladder and to the fact that the bladder is located more proximally to the heat sink provided by the circulating ice water. In like manner, in Figure 2.13(a) the temperature of the water circulating in the bladder precedes the bladder surface temperature in decreasing during cooling starting at 30 and 210 minutes and in increasing during warming starting at 160 minutes. The difference between the inlet and outlet temperatures is less than 1°C. This temperature difference, multiplied by the specific heat of water and the mass flow rate through the bladder, can provide an indication of the rate of heat transfer between the bladder and the skin.

Another feature of the temperature data is that the rates of temperature drop during active cooling with forced convection are always much larger than the rates of temperature rise during passive rewarming via natural convection. The differential in heat transfer rates during active and passive rewarming processes is illustrated dramatically in Figure 2.13(a) in which the slopes of the tissue temperature curves increased abruptly

when warm water was perfused through the cryotherapy bladder. At 187 minutes when the water perfusion through the bladder was ceased, converting the environment for the skin from forced to free convection, albeit with the same water temperature in the bladder, there is an immediate change from an increasing to a decreasing slope of the transient temperature gradient. This inversion of the slopes of the skin temperature curves illustrates clearly the strong effect imposed on the underlying tissue by switching from a forced to a free convection boundary condition. Operation of the bladder with a forced convection flow of water is an important component of the functionality of cryotherapy units. Another example of this phenomenon is seen by comparing the cooling curves for the Aircast Cryo/Cuff device in Figure 2.9(a) with those of the forced convection devices in all other cryotherapy trial figures. The Cryo/Cuff device operates via a single admission of ice water into the bladder where it remains static for the duration of the cooling cycle in the absence of a forced convection source that is able to sustain a continuous high rate of heat removal from the tissue. Therefore, following an initial drop in temperature on the surface of the bladder, there is a continuous rise in temperature as the bladder absorbs heat from the underlying tissue. The rate of heat transfer decreases continuously as the temperature differential between the bladder and the skin diminishes.

In all of the trials the temperatures of the skin and the bladder were rising during the initial baseline period during which there is no active temperature control imposed. This trend occurs because metabolism and blood flow in the tissue provide an inner source of heat, and the outer bladder layer provides insulation of underlying structures. The result is that energy is generated and transported within the tissue at a rate larger than it can be lost via passive heat transfer to the environment, resulting in a net accumulation of energy that drives the temperatures upward prior to starting the circulation of ice water through the bladder.

The data in all of the trials also show that there were always positional differences in temperature histories. For example, there may be points on the skin surface with temperatures as low as 8 – 9°C, whereas on occasions during a single trial there may be other locations that simultaneously are 20°C or higher. For clarity in viewing and interpreting the temperature data we have presented plots for only a minimal number of measurement sites, but much more data was gathered that supports this behavior. There are multiple potential contributing causes for spatial variations in temperature. (i) There may be differences in the local thicknesses of the thermal barrier. Typically a thermal barrier is placed between the bladder surface and the skin, although in general the device manufacturers do not define or specify specific standards for the thermal properties of barriers to be applied by end users. This effect is most probable when the barrier is applied as a wrap that may have a nonuniform pattern of application causing uneven thermal resistance. (ii) The temperature distribution on the surface of the cooling bladder is known to have spatial variations, as shown in Figure 2.14. These variations will translate to gradients on the skin surface. (iii) The bladder may not fit uniformly against the thermal barrier and the underlying tissue, resulting in creation of insulating air gaps that will act as a thermal contact resistance, depending on the relative geometries of the bladder and the anatomy, causing a larger temperature drop between the skin and bladder. This effect is difficult to quantify and predict, but it is very real. We have observed at sites of poor fit a skin to bladder temperature differential that can be 15 – 20°C larger than at locations where there is an intimate fit. The local physiological response will be modulated if the conformation of the cooling bladder to the body surface is poor. (iv) There may be areas of higher contact pressure between the bladder and the thermal barrier and underlying tissue. Greater pressure will reduce contact thermal resistance and may also compress the barrier material, lowering its resistance. The thermal effect of

increased applied pressure on reducing the heat flow resistance is seen clearly in Figure 2.8(a) for operation of the Game Ready device with cyclic pressure applied to the pneumatic cuff. Increased pressure reduces the temperature drop between the bladder and skin surface. Increased mechanical or pneumatic pressure will also further depress blood flow through the tissue, rendering it more susceptible to being cooled.

The cryotherapy trials all involve the circulation of water from an ice bath through a bladder placed on the subject at a simulated treatment site. The water flow tubes are all insulated with a light foam material to minimize heat gain from the surrounding air. Some cryotherapy systems offer a control of the water temperature as it is supplied to the cooling bladder. For systems in which ice water is pumped directly to the bladder, in line measurements of water temperature as it enters the bladder show values as low as 0.5°C. As steady operating conditions are approached, the temperature of the outer cooling surface of the bladder may be as low as 3 – 6°C, depending on the thermal resistance of the bladder material and the effectiveness of convection heat transfer with the water as it flows through the bladder.

The therapeutic (and possibly injurious) response elicited in tissue occurs as a function of the applied temperature and duration on the skin surface. Thus, variations in the temperature pattern imposed onto the surface of tissue may compromise the execution of cryotherapy, resulting in an unintended or unwanted response. Accurately producing a targeted temperature field onto a treatment area remains a fundamental challenge in perfecting cryotherapy devices.

Blood Perfusion Effects

As noted earlier, we have now conducted more than 200 instrumented cryotherapy trials, all on healthy adult subjects, and every trial demonstrated a sharp

decrease in blood flow to the affected area that persisted subsequent to cooling unless there was an intervention to restimulate the flow. In the absence of instrumentation to monitor blood perfusion, as is commonly the case for the clinical use of cryotherapy devices, this phenomenon is not likely to be detected or to be perceived. Nonetheless, the affected tissue area will be deprived of a normal supply of oxygenated blood with nutrients, and toxic metabolic byproducts will accumulate locally. The result is a condition that can lead to cell injury and death which, if enabled to accrue on a large scale, may be manifested as clinically observed necrosis and/or neuropathy, with the more general descriptor of nonfreezing cold injury [46]. As noted in the background section, the literature of cryotherapy has many citations of these types of outcomes.

There are a number of specific features of the blood perfusion response to cryotherapy in addition to persistent ischemia that should be highlighted. It is readily apparent that the blood perfusion curves are not as smooth as are the temperature curves, which is due to the difference in the nature of the control mechanisms. Regulation of the human cardiovascular system has been studied and written about extensively for many years. One of the more comprehensive and elegant reviews is found in the book of Rowell [60] to which readers are referred for details. As Rowell notes, “The primary function of the cardiovascular system is to deliver oxygen and nutrients to the tissues and to remove their waste products….Other important functions of the peripheral circulation are the regulation of blood pressure, body temperature, and distribution of blood volume, and the performance of the heart.” Simply stated, humans may experience variations in local blood flow in conjunction with changes in the driving pressure from the pumping heart and in the continuous redistribution of blood volume around the body via exquisite adjustments in vasomotor function that cause modulations in the local flow resistance. The latter factor is undoubtedly the primary source of the relatively rapid small scale

fluctuations in local blood flow rates observed in all of the data reported herein. These fluctuations occur in the normal functioning of the cardiovascular system and are not a consequence of the application of cryotherapy, as evidenced by data acquired during the baseline periods.

The laser Doppler flow measurements may be subject to artifact generation owing to changes in the relative geometry between the probe and the skin surface. Such changes can occur if the subject moves or even flexes a muscle in the measurement area. Therefore, the subjects were cognizant to remain passively still throughout experimental trials to the greatest extent possible. Another source of movement artifact is the application or removal of a force that presses the probe normally or obliquely against the skin surface, as may occur when a CTU pump establishes or discontinues the flow of ice water through a cooling bladder that covers a probe. This effect can be observed in some, but not all, of the blood flow plots in conjunction with the start and end of the ice water pumping that defines active cooling periods. The control study of Figure 2.12 demonstrates the pressure induced perturbation in flow measurement in the absence of a thermal influence on blood perfusion. A similar effect is observed in the data presented in Figure 2.11(b). In this experiment, two blood perfusion probes were applied to the skin under the cooling bladder. There are sudden changes in flow measurements with the start and stop of water flow in P2 (magenta line), whereas P1 (green line) only experiences a transient increase in flow with the start of the cooling and without any similar response with the stop of the water flow. As long as water flow was maintained through the cooling bladder, there was a constant upward offset in the value for P2 that disappeared when the flow stopped. The magnitude of the offset was approximately equal at the beginning and the end of the flow period. The difference in response between the two

probes is likely due to their relative positioning with respect to the bladder that could influence the degree of pressure loading they experienced during the flow of water.

A pressure effect on blood perfusion measurements is also quite apparent in Figure 2.8(b) for operation of the Game Ready cryotherapy unit with its external pneumatic pressurization cuff activated periodically during cooling. Three probes were positioned on the skin beneath the cooling bladder during this trial, one deep and two superficial. Although all three probes had flow measurements altered by the application and release of pressure, there are marked differences among the magnitudes of these responses. These differences may be attributed to unique aspects of the relative positioning of the probes on the skin and under the bladder, causing differential sensitivities to the application of flow pressure within the bladder. In general, the application of pressure produces a reduction in measured blood flow in the underlying tissue, and release of pressure likewise produces an increase in flow.

Another feature of the response of blood perfusion to the application of cryotherapy is the relative rate at which the local flow drops as the temperature is initially reduced. At the risk of oversimplification, the rates of perfusion drop can be grouped into two general classes: relatively slow and relatively rapid. Slow rates of decrease are seen in Figures 2.2(b) and 2.4(b), whereas rapid rates are seen in Figures 2.3(b), 2.5(b), 2.6(b), 2.7(b), 2.10(b) and 2.13(b). Interestingly, Figures 2.8(b) and 2.9(b) show both slow and rapid rates of drop in blood perfusion among the different probes on the same subject during the same trial. These individual probes are located at different sites where there may be differentials in the applied thermal histories and in the local control of vasomotor regulation.

A major question concerning the cryotherapy induction of ischemia is whether there is a dose response effect, where the dose is characterized in terms of both time and

temperature of exposure on the skin surface. As with most elicited biological responses to thermal stress, the application time and temperature during cryotherapy are not independent in their causative potentials for producing kinetic physiological reactions [61,62]. A full answer to this question would require a broad matrix of experimental studies that are beyond the scope of the current investigation, although we are currently engaged in experimental evaluation of the combined time and temperature dosage in causing vasoconstriction. Johnson [37,38,63,64], Thompson [41,65] and others [66] have studied in depth the effect of local cooling on cutaneous vasoconstriction, showing that temperature reductions to the range of 24°C consistently can produce major vasoconstrictive responses to decrease cutaneous vascular conductance by as much as 80% of baseline values. It is thought that inhibition of the NO vasodilator system may play an important role in this behavior [37,38]. Preliminary experiments by our research team using the microdialysis technique [67,68] are confirming to this mechanism for the cryotherapy induced vasoconstriction that persists following the completion of the active cooling portion of a protocol.

The control data in Figure 2.12 for perfusion with water at a baseline skin temperature of 32°C show no indication of a thermally induced vasoconstriction. During the last approximate 90 minutes of this trial the thermal insulating effect of the bladder and thermal barrier caused skin temperatures to rise continuously with a concomitant increase in blood flow to 50% above the baseline value. This effect is in accordance with data in the literature for the effect of heating skin on inducing vasodilation [38,69,70].

Figure 2.13(b) presents the response of blood flow to active local heating via passage of warm water through the bladder that was started during the period of post cooling vasoconstriction. There was an immediate and continuous increase in the rate of skin blood flow throughout the time of active heating, resulting in blood perfusion values

that at one measurement site were well in excess of baseline. When the active heating was stopped, the blood perfusions leveled off at their peak values and were maintained until active cooling was resumed, at which time the cycle of deep vasoconstriction was again initiated, continuing into the post cooling period as occurred during the initial cycle. An interpretation of this data is that induction of a large positive heat flux into the skin offsets the action of the factor(s) that cause persistent vasoconstriction during and following active cryotherapy cooling, and that these factors are reestablished with subsequent cryotherapy application.

We studied cryotherapy protocols in which the initial period of applied cooling lasted over a range of times from 1 minute (Figures 2.6(a) and 2.7(a)) to 80 minutes (Figure 2.4(a)) to determine the exposure time effect on the dose response of blood perfusion to cryotherapy. It is well understood from the principles of heat transfer that during the surface cooling of a semi-infinite medium such as the skin and underlying tissues, the cold front will penetrate inwardly as a wave [71]. Thus, the surface temperature will reduce progressively over time, and the extent of cumulative surface cooling will be much less for short periods of exposure than for longer periods. This effect is illustrated in Figure 2.16 which plots the minimum skin temperature reached during the initial cooling period as a function of the duration of exposure to a cooling bladder with continuously circulating ice water.

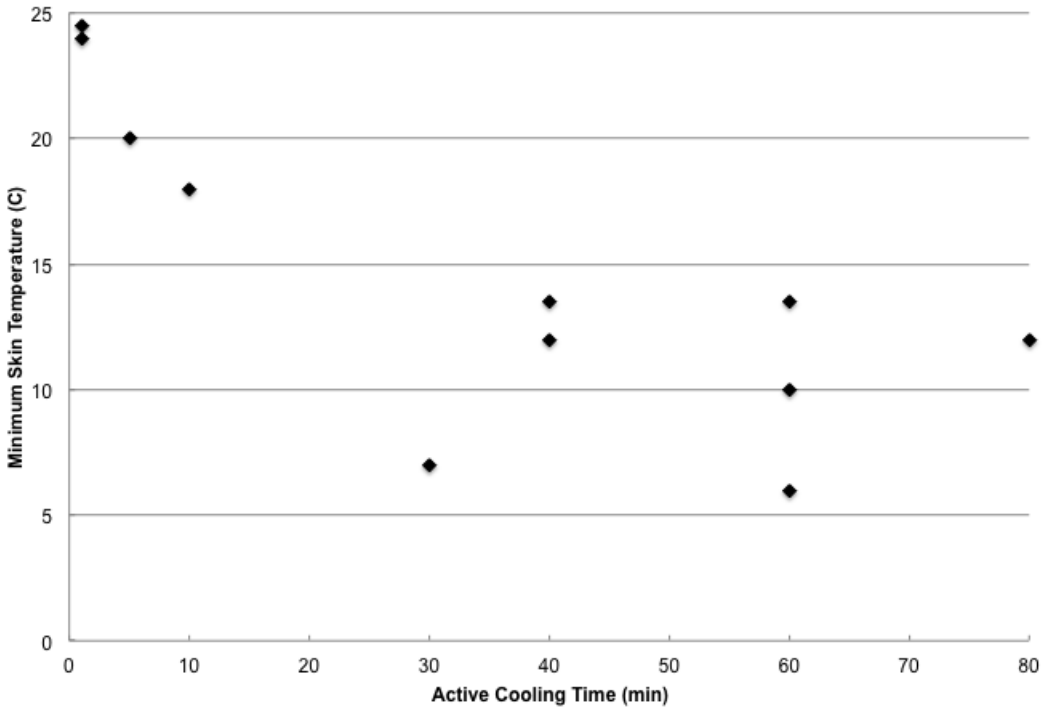

Figure 2.16. Scatter plot of minimum temperature achieved on the skin surface as a function of the duration of the initial episode of cooling applied with a cryotherapy cooling bladder with continuously circulating ice water. Cumulative data from multiple trials previously reported individually.

The data in Figure 2.16 are from Figures 2.2-2.8, 2.10-2.11 and 2.13, excluding Figure 2.9 which is for the Cryo/Cuff that does not provide a continuous circulation of ice water through the bladder and therefore produces a very different type of thermal boundary condition for the cooling process. Although this data is from four different device manufactures with their own cooling bladders and applied to three different areas of the body, there is clearly a common behavior to be observed. The surface temperatures reached after 30 minutes of cooling tend to fall into a group with a range of about 10 ± 4°C, although the skin temperatures were continuing to fall asymptotically after even 60 and 80 minutes of cooling. For shorter cooling periods, the drop in temperature was directly proportional to the duration of applied cooling (Figure 2.16). Importantly, for

even 1 minute of active cooling, the skin surface reached 24°C, which corresponds to the value used by physiologists to study the effect of local cooling in causing vasoconstriction [37,38,63,64,66]. The effect of cryotherapy that carries the greatest potential impact on the risk of causing injury is the depression of blood flow. Figure 2.17 presents aggregate data of the percentage depression of skin blood perfusion for all of the continuous flow cryotherapy trials (excluding the Cryo/Cuff).

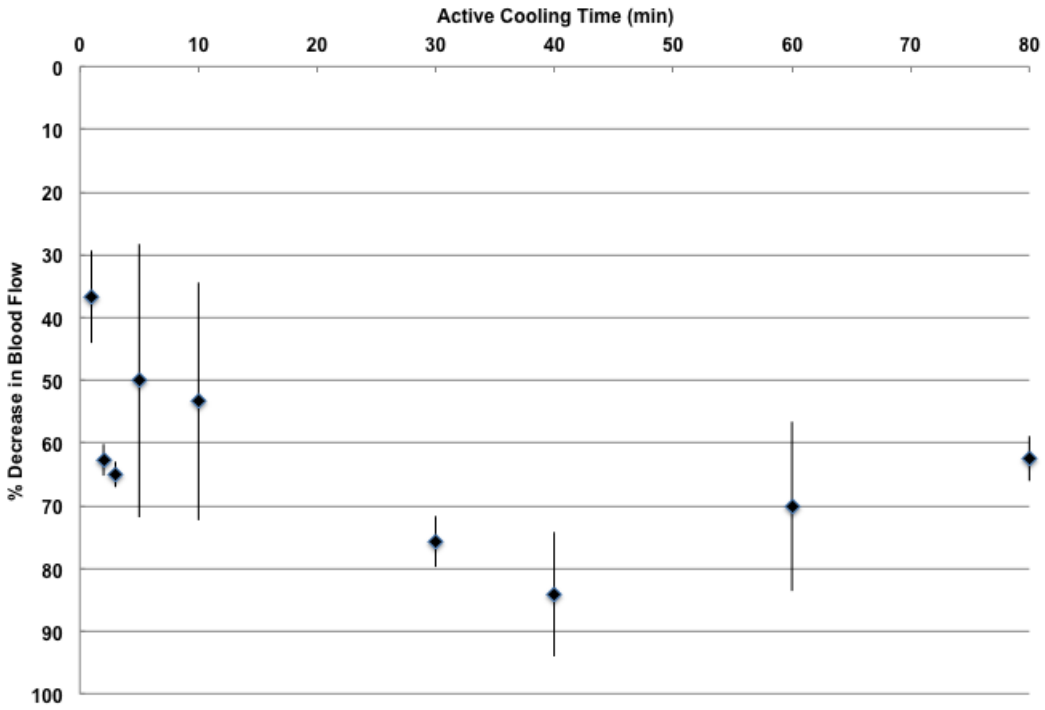

Figure 2.17. Decrease in cutaneous blood perfusion as a function of the period of application of continuous flow ice water cryotherapy. Average and standard deviation values are based on data from each individual perfusion measurement from all trials. *n* varies between 2 and 6 as can be observed from Figures 2.2-2.8, 2.10-2.11, and 2.12.

The data shows that even very brief periods of cryotherapy are sufficient to lower the skin to a temperature wherein significant vasoconstriction occurs. Figure 2.6(b) shows that for only 1 minute of cooling there can be a 25% to 50% depression of the

local blood flow that lasts for more than three hours, at which point in time this particular experiment was terminated. Figure 2.7(b) shows sequential cooling periods of 1, 2, and 3 minutes for which there is an accumulative temperature effect that precipitates a compounded long term diminution in the cutaneous blood flow. Recent experiments in our laboratory have documented that reduction in skin temperature to values as high as 27.5°C may result in a significant loss in skin blood flow.

The most important result of the current study is that a reduction in local tissue temperature produces a depression in blood perfusion and that it may persist long after the tissue is rewarmed from the cooling episode. It is anticipated that continuous cryotherapy protocols will hold the state of vasoconstriction as long as cooling is applied, with the potential for subsequent persistence. The implications for development of ischemia and potential causation of tissue necrosis and neuropathy are serious and, we believe, warrant further investigation and a plan for remediation.

In support of the title of this paper, it is unequivocally clear that the depression of skin blood flow that occurs during cryotherapy is tightly coupled with the reduction of local skin temperature. In simple terms, the change in blood flow follows the change in temperature. However, subsequent to the cessation of active CTU cooling, skin blood flow is decoupled from the rising skin temperature and may remain depressed for hours under the action of as yet unidentified vasoactive mediators. This condition during which the skin blood flow and skin temperature are essentially decoupled becomes progressively dangerous during rewarming since as the temperature increases the metabolic needs for oxygen and nutrients likewise are greater, but the supply via blood flow remains diminished, enhancing the potential for ischemic tissue injury.

CONCLUSIONS

The focal message delivered by this study is that virtually all cryotherapy devices that are available commercially have inherent operating conditions that produce a vasoconstrictive state having the potential for causing ischemia resulting in injuries such as tissue necrosis and neuropathy. The results demonstrate that even short episodes of cryotherapy can produce a prolonged vasoconstriction in the local area of treatment. The state of vasoconstriction endures long after local temperatures have rewarmed toward the normal range, indicating that the existence of vasoconstriction is not associated with maintenance of a cold state in the tissue. Following exposure to low temperatures, the level of blood perfusion in tissue becomes decoupled from the thermal state. Complementary experiments in our laboratory indicate it is likely that a long acting humoral agent is released locally with a continuing vasoconstrictive effect long after tissue temperatures have rewarmed toward their baseline values. We anticipate that further research to confirm, identify and characterize the action of local vasomotive agents will aid in understanding and controlling the phenomenon of cold-induced vasoconstriction. It would appear that there is a significant opportunity to improve the practice of cryotherapy by reducing or eliminating the risk of the provoked persistent, possible long term ischemia without compromising the therapeutic efficacy of the technique.

AUTHOR DISCLOSURE STATEMENT

A patent application has been submitted by Dr. Khoshnevis and Dr. Diller to the United States Patent and Trademark Office under the title *Improved Cryotherapy Devices and Methods to Limit Ischemic Injury Side Effects*. Ownership rights to this patent have been assigned by The University of Texas at Austin to a corporation jointly owned by the inventors, Bioheat Transfer, LLC, according to an agreement that includes royalty rights

for the University. The authors have received no compensation from Bioheat Transfer, LLC, and Bioheat Transfer, LLC provided no financial support for this research. Initial analysis of the data was performed by colleagues having no connection with Bioheat Transfer, LLC. Dr. Diller has served as an expert witness for both plaintiff and defendant counsel since 2000 in numerous legal cases regarding the safety and design of existing cryotherapy devices.

ACKNOWLEDGEMENTS

This research was sponsored by National Science Foundation Grants CBET 0828131, CBET 096998, CBET 1250659, National Institutes of Health Grant R01 EB015522, and the Robert and Prudie Leibrock Professorship in Engineering at the University of Texas at Austin.

Chapter 3: Quantitative Evaluation of the Thermal Heterogeneity on the Surface of Cryotherapy Cooling Pads[2]

ABSTRACT

We have investigated thermal operating characteristics of 13 commercially available cryotherapy units (CTUs) and their associated cooling pads using IR imaging. Quantitative examination of the temperature profiles from pad IR images shows diverse, non-uniform temperature distribution patterns. The extent of heterogeneity of the temperature fields was quantified via standard image analysis methods, including thresholding, spatial gradient diagrams, and frequency histogram distributions. A primary conclusion of this study is that it is a misnomer to characterize the thermal performance of a CTU and cooling pad combination in terms of a single therapeutic temperature.

MATERIALS & METHODS

Thirteen commercially marketed CTUs were evaluated as follows: Breg Polar Care 300, 500, and 500 Lite (Breg, Carlsbad, CA); DeRoyal T505 and T600 (DeRoyal Industries, Powell, TN); Game Ready (Game Ready, Concord, CA); Artic Ice System (Pain Management Technologies, Akron, OH); DonJoy Ice man (DonJoy Global, Vista, CA); EBIce model 10D (EBI, LLC., Parsippany, NJ); Össur Cold Rush (Össur Americas, Foothill Ranch, CA); and Bledsoe bMini, Cold Control, and bPro (Bledsoe Brace Systems, Grand Prairie, TX). Associated CTU brand-specific pads commonly used for the knee were tested. Pads were assigned unique identifier codes based on their manufacturer, intended application site, and/or geometric shapes. Four-letter identifier acronyms applied for reporting results in this study are: knee pads for Polar Care 300,

[2] This chapter is based on the manuscript accepted for publication by the Journal of Biomechanical Engineering coauthored by Sepideh Khoshnevis, Jennifer E. Nordhauser, Natalie K. Craik, and Dr. Kenneth R. Diller [72].

500, and 500 Lite; Game Ready; Arctic Ice; Össur; and Bledsoe Cold Control, bMini, and bPro; DeRoyal T505 and T600 U-shaped pad and universal pad; DonJoy McGuire pad and universal pad; and EBIce model 10D U-shaped pad, square pad, and two-winged "butterfly" pad. Table 3.1 presents a listing of identifier codes for the pad/CTU combinations.

Each CTU and cooling pad combination was evaluated in a dedicated trial using a common protocol that followed the manufacturer's instructions. The cooling pad was connected to the CTU, purged of air, laid flat on a carpeted substrate with the therapeutic surface designed to face the skin oriented upward, and ice water circulation through the pad acitvated. An infrared camera was mounted on a tripod directly above the pad at a distance adjusted to ensure the field of view encompassed the full pad area. The trials were conducted in a 35 m^2 laboratory room with air temperature and relative humidity at approximately 23°C and 50%, respectively. Care was taken to ensure that no ambient water vapor condensation collected on the surface of the cooling pad during IR temperature measurements that would confound its thermal emissivity properties.

Device	Pad Type	Code	Flow Rate ± 12.5 (cc/min)	Water Flow Function	Feed Back Control	Compre-ssion
Arctic Ice	Universal	AION	1200	Continuous	None	None
EBIce Model 10d	Butterfly	EBOB	1050	Duty cycle is controlled with an analog dial	None	None
	Square	EBOS	1050			
	U-Shape	EBOU	1125			
Bledsoe Cold Control	Universal	BLCN	1300	Analog control of flow rate	None	None
			1425			
			1400			
Bledsoe Mini	Universal	BLMN	1300	Continuous	None	None
Bledsoe Pro	Universal	BLPN		Analog control of flow rate	None	None
DeRoyal T505	Universal	DRFN	225-400 (5.1-6.1 °C)	Duty cycle depends on temperature of water returning to CTU	Yes	None
	U-Shape	DRFU				
DeRoyal T600	Universal	DRSN	675-825 (7.2-8.3 °C)	Similar to DeRoyal T505	Yes	None
	U-Shape	DRSU				
Össur Cold Rush	Universal	OSON	400	Analog control of flow rate	None	None
			650			
			775			
Game Ready	Universal	GRON	425	Analog control of flow rate	None	Yes
			450			
			425			
Polar Care 500	Universal	PCFN		Analog control of flow rate	None	None
Polar Care 500 Lite	Universal	PCLN		Continuous	None	None
Polar Care 300	Universal	PCTN		Continuous	None	None
DonJoy Iceman	Universal	DJON	550	Continuous with analog dial	None	None
	Maguire	DJOM				

Table 3.1. Cooling pad/CTU combinations tested, the unique identifier codes, and unique operational characteristics. The last letter of the acronym defines the pad type. (N=universal, B=butterfly, U=U-shaped, S=square, and M=McGuire)

Infrared temperature images of subject pad surfaces were obtained with either a FLIR A325sc thermal camera with 320 x 240 pixel resolution and ± 2°C thermal accuracy (FLIR Systems Inc., Boston, MA) or a FLIR T650sc with 640 x 480 pixel resolution and ±1°C thermal accuracy (FLIR Systems Inc., Boston, MA) that could capture simultaneous infrared and optical images of pad surfaces (the latter system was acquired partway through the study). FLIR ExaminIR software (FLIR Systems Inc., Boston, MA) was used for initial image processing and analysis of infrared data. The thermal radiation emissivity of the pad material was measured using the calculator function in ExaminIR for multiple isothermal regions on the surface at room temperature. The emissivity was applied in the software to extract temperature values from the thermal images. Further image analysis calculations were performed with MATLAB (Mathworks Inc., Natick, MA).

24 AWG type T thermocouples (Omega Engineering, Stamford, CT) were applied to monitor and record ambient air and pad surface temperatures in conjunction with National Instruments (NI) input modules NI 9211 and 9213 and NI DAQ 9172 and 9174 and LabView SignalExpress software (National Instruments Corp., Austin, TX). A handheld IR thermometer (Fluke 62Max, ± 1°C, Fluke Corporation, Everett, WA) was used for further confirmation of pad surface temperatures. The ice water flow rate was measured for each CTU and pad combination via an in-line flow meter (Key Instruments, Trevose, PA) positioned between the outlet from the ice chest and the pad inlet port.

Trials were conducted by activating the CTU to circulate ice water through the cooling pad. Thermal images of the surface were acquired after the pad reached a steady thermal state, which generally required about 10 minutes of operation. Some CTUs provided an option for adjusting the water temperature. For these systems, an initial steady state was produced at the warmest setting, the thermal data was recorded, and this

process was repeated at incrementally lower settings until the lowest temperature was reached. For those devices with intermittent flow, the thermal images were analyzed at the completion of the on-phase of the duty cycle after steady state was achieved.

Thermal images were transferred from the camera to a host computer where they were subjected to various enhancement and analysis algorithms to quantify and characterize the magnitude and distribution of the temperature variation across the cooling pad surface. The first processing step was to establish a threshold temperature value in order to isolate the pad area from the warmer background region of an image. Given that the highest lateral temperature gradient in an image occurred among the pixels at the pad edge, a spatial temperature gradient matrix map was created to identify the boundary of the pad. The gradient matrix was generated in the x, y image plane and was calculated as the root sum square of the difference between adjacent x and y temperature values. The temperature of the pixel with the highest gradient magnitude in the pad edge region was set as the threshold value to isolate pad data and filter out background data from the initial image. This algorithm showed a very close correspondence between the visual and threshold identified boundaries of the pad. The thresholding method always successfully removed the background completely.

A histogram was created to display the pixel occurrence frequencies of specific temperatures on the pad surface along with the mean, median, and standard deviation. A figure of merit was defined to quantify the extent of nonuniformity in pad temperature by removing the outer 10%, $1/e^2$% or 1/e% of the frequency bins from the histogram (defining the middle 90%, 86.5% and 63.2% of occurrence frequencies, respectively). The range of the remaining bins was defined as a measure of the breadth of temperatures occurring on any given pad. Box plots were calculated and drawn for temperature variation statistics, providing the inter quartile range (IQR) as an additional metric for

temperature variations on the pad. Important thermal features of the IR image were visualized by plots of: temperature contours, spatial temperature gradient magnitude maps, and the discrete Laplacian operator (second derivative set to zero, representing an edge detection scheme). However, the Laplacian plots did not add any significant insight into the extent of pad surface temperature nonuniformity beyond that of the first order gradient magnitude and therefore are not included in the analysis presented here.

The various pads have unique shapes and sizes, and there may be a variety of pad configurations for any given CTU. The pads may be matched to the anatomy of the site of therapy and the dimensions of the treatment region. The therapeutically effective surface area of the pad depends on the pad shape as well as the outline of the treatment region. These factors are not constant among different clinical cases, and therefore comparison of pad according to their sizes was not included in this analysis.

RESULTS

Features of the CTU/pad combinations tested are listed in Table 3.1, including the measured water flow rate through the pad, method of control if it existed, and whether the CTU/pad was capable of simultaneous pneumatic compression of tissue in the thermal treatment area. Although most CTUs produce a constant flow rate of water, some provide intermittent flow via an adjustable duty cycle. For example, ice water flow to the cooling pad for the EBIce model 10D is regulated manually, whereas the DeRoyal T505 and T600 have a feedback control mechanism based a comparison of the temperature of water returning from the pad to a set point value.

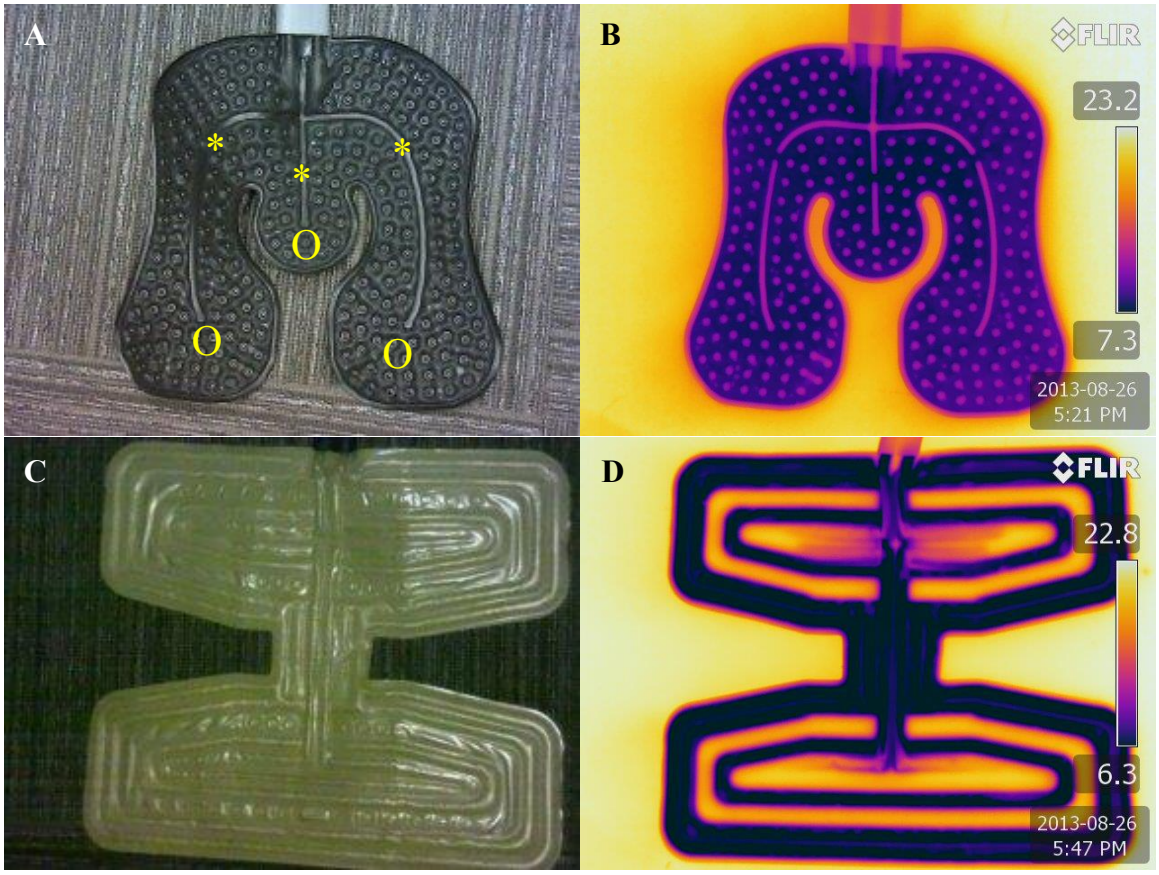

Figure 3.1. Optical (A and C) and IR (B and D) images of Bledsoe Universal (A and B) and EBIce model 10D butterfly pads (C and D). The symbols * and O in (A) demark alternate parallel water flow pathways.

The optical and IR images in Figure 3.1 for a universal cooling pad from Bledsoe (BLMN) and of an EBIce knee cooling pad (EBOB) illustrate contrasting temperature patterns that may be encountered. A pseudocolor bar for the IR images shows the range of temperatures on the subject pad, with the extreme values denoted numerically. By casual visual inspection, the Bledsoe Universal pad appears to be more thermally uniform than the EBIce Butterfly pad. In both IR images there is a thermal halo effect surrounding the pad owing to lateral cooling of the underlying carpet substrate. This phenomenon is

more obvious for the Bledsoe pad than the EBIce pad due to the former's greater thermal homogeneity and, perhaps, a lower level of thermal insulation on the back of the pad.

	Min	Max	Mean
Average Pad Temperature	2.6	10.9	6.8 ± 2.5
Coldest Temperature	0.7	7.9	4.4 ± 2.4
Warmest Temperature	11.1	17	14.5 ± 1.7
Breadth (10% exclusion)	2.0	9.1	5 ± 2.3
Breadth ($1/e^2$% exclusion)	1.7	8.2	4.2 ± 2.0
Breadth (1/e% exclusion)	0.5	5.3	1.8 ± 1.3
IQR	0.8	4.2	1.9 ± 1.2

Table 3.2. Aggregate thermal data of cooling pad surface temperature distributions for all trials

Table 3.2 presents a summary of the ranges of steady state spatial temperature distributions measured on the various subject cooling pads. This data includes the lowest, highest, average and standard deviation of the local temperatures, plus the minimum, maximum, average, standard deviation, and IQR of the temperature ranges. The coldest temperature measured was 0.7°C on the Össur pad, and the mean and standard deviation of all average temperatures was 6.8 ± 2.5°C. Determination of the range of temperatures over the surface by the 10%, $1/e^2$% and 1/e% methods (defining the middle 90%, 86.5% and 63.2% of occurrence frequencies, respectively) provides a more insightful discrimination among pads (described later in the Results section). The highest value for IQR occurred on the EBIce butterfly pad (4.2°C), and the lowest value on the DonJoy universal pad (0.8°C).

Figure 3.2 presents temperature contours and the temperature gradient map for the EBIce butterfly pad. In the IR image, the temperature of the background region was set to the threshold value to increase the visible thermal resolution on the pad. The pad temperature covers the range of 4-14°C, with a significant portion of the surface above 12°C. The temperatures of areas that directly overlay water flow channels are 4-7°C. Regions on the pad having the largest magnitude of lateral spatial temperature gradient are located primarily along the outer margin the edges of water flow pathways.

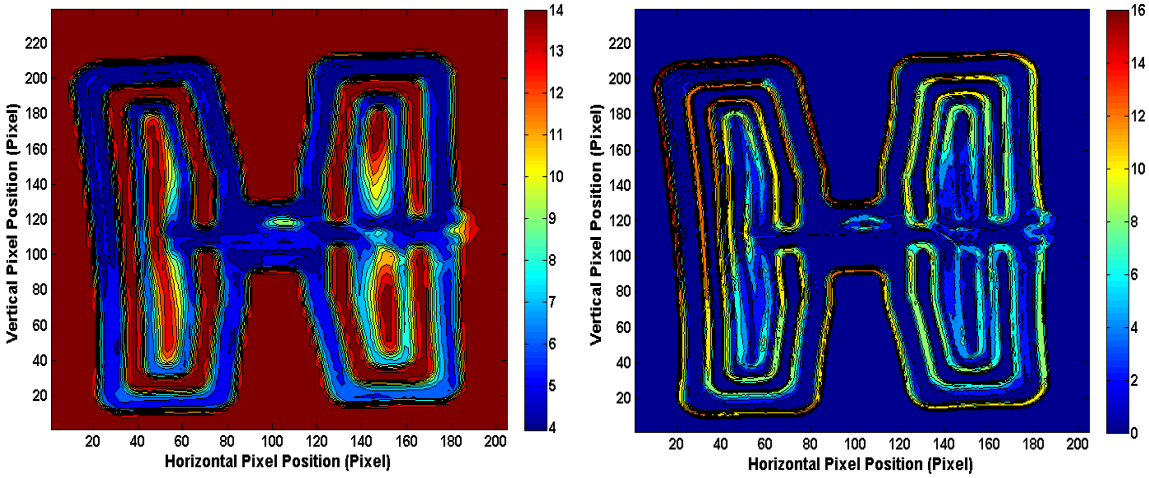

Figure 3.2. IR image of EBIce model 10D butterfly pad (left) and its gradient magnitude map (right). The color bars show temperatures (°C) for the IR image and (°C/pixel) for the gradient map.

Histograms were created to provide a graphical representation of the occurrence frequency of specific temperatures on the surface of each pad tested. Two exemplar histograms are shown in Figure 3.3. The EBIce butterfly pad histogram exhibits a skewed distribution with a relatively large degree of thermal non-uniformity. The Bledsoe Cold Control pad also demonstrates a skewed distribution, but with a significantly more homogeneous pattern. The top, middle and bottom histograms indicate the temperature

ranges for the outer 10%, 1/e% and $1/e^2$% of values. Note that the vertical frequency scales are different for the two systems, reflecting the difference in relative tightness of the two temperature distributions.

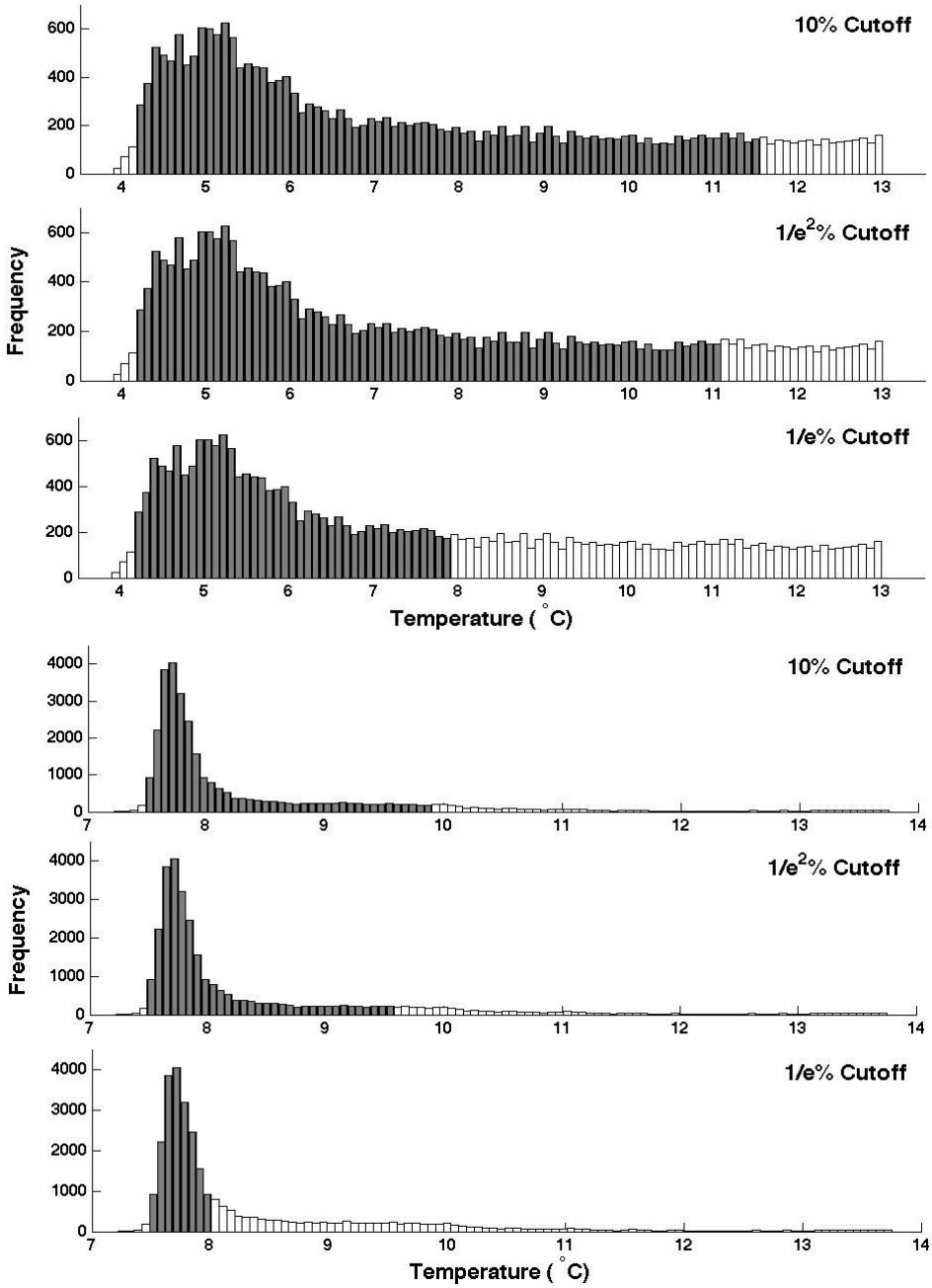

Figure 3.3. Histograms of pad temperature distributions with the outer 10%, $1/e^2$%, and 1/e% of values excluded as indicated by unfilled bars. Upper panels are for EBIce model 10D butterfly pad, and lower panels for Bledsoe Cold Control universal pad.

Figure 3.4 shows an explicit contrast between the relative spread of temperatures for the EBIce butterfly and Bledsoe Cold Control universal pads. The 10% breadth margins for both pads are marked on their corresponding plots. This representation of the data clearly illustrates the very large differential in variance of temperatures that may occur over two different pad surfaces. Data presented in this format enables a graphic assessment of the relative temperature heterogeneity among multiple CTU/pad systems.

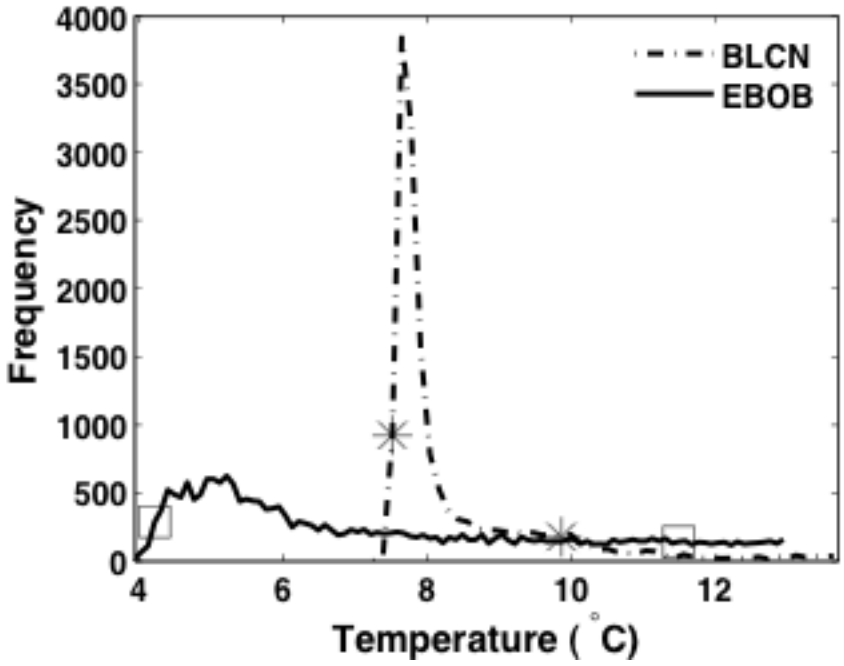

Figure 3.4. Direct comparison of the relative spread of temperature distributions for the Bledsoe Cold Control knee pad and EBIce model 10D butterfly pad. The stars and squares mark the 10% breadth limits for the two pads.

Another differentiating feature among the various CTU/pad combinations is whether the ice water flow is continuous or intermittent, the latter of which will produce oscillating pad temperatures even after a steady operating state is reached. Figure 3.5 presents histograms of EBIce Model 10D butterfly pad (EBOB) temperatures at the

beginning and end of one water flow cycle. The overall temperature drops during active water flow and increases to a bimodal distribution when the water flow is off, reflecting the pattern of passive heat transfer with the environment.

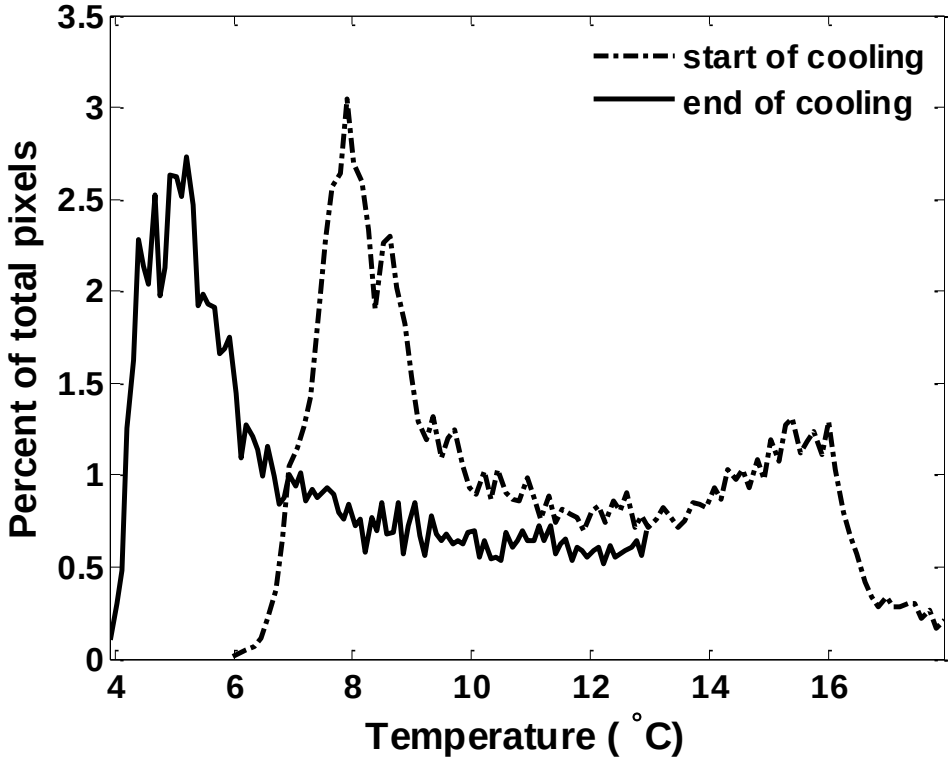

Figure 3.5. Change in the temperature distribution on the EBIce butterfly pad at the beginning and end of the gated-on portion of an intermittent flow duty cycle with the controller adjusted to the coldest setting.

Figure 3.6 presents box plots of the pad temperature statistics for all devices tested (see Table 3.1 for identifier codes). Each box plot displays the maximum, minimum, first and 3rd quartiles, and median of pad temperatures for one CTU/pad operation. This data shows that the EBIce model 10D butterfly pad (EBOB) and DeRoyalT505 universal pad (DRFU) have the most non-uniform temperatures, with

interquartile ranges (IQR) of about 4°C. In contrast, the Bledsoe Cold Control (BLCN) and DonJoy Iceman (DJON) have an IQR of only 0.8°C.

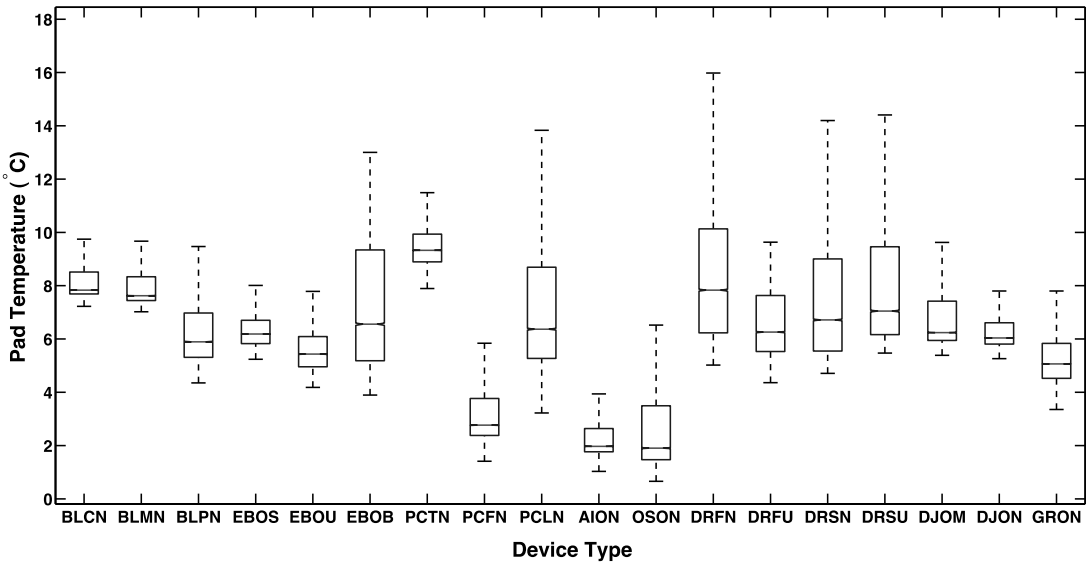

Figure 3.6. Box plots of pad temperature distribution statics for the indicated CTU/pad combinations

Some CTUs offer a feature for the user to adjust the intensity of cooling provided by the system. The mechanism for implementing this feature involves modulation of the water flow through the cooling pad by one of various methods. The question arises as the extent to which adjustment of the CTU control actually changes the temperatures produced on the cooling pad. CTUs having this feature were operated at high, intermediate and low settings, and the resulting temperature distributions were measured on their cooling pads. Data from these trials is presented in Figure 3.7. In general, CTUs with a cooling adjustment at best had a nonlinear relationship between the controller setting and the pad temperature, and in some cases, the controller exerted no perceptible effect on pad temperatures. For example, the Össur Cold Rush (OSON) and Polar Care 500 (PCFN) CTUs manifest no change in pad temperatures for controller adjustments

across their entire range. The Bledsoe Cold Control (BLCN) temperature decreased by more than 5ºC between the warmest and intermediate settings, but there was not significant change in pad temperature for colder settings. The existence of the control adjustment sends an implicit message to the user that altering the setting will produce a significant change in thermal performance, whereas data shows that not to be the case for many systems.

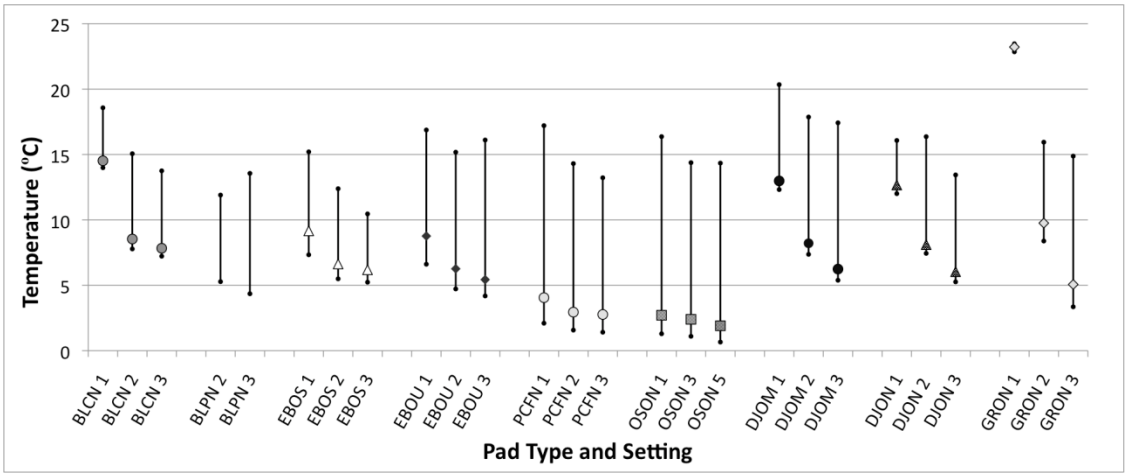

Figure 3.7. The effect of adjusting the user-controlled temperature setting on measured pad temperature ranges. The plots show the low, median and high values. Data are grouped by device type, with right and left plots for the designated coldest and warmest settings, respectively. Central plots denote intermediate control settings.

DISCUSSION

Over the course of our extensive past testing of CTUs we have consistently observed significant lateral temperature variations on the skin underlying a cooling pad. These measurements were obtained from multiple simultaneous thermocouple readouts or by pulling a single thermocouple laterally on the skin under a cooling pad. However, this temperature data was obtained mainly on an anecdotal basis, without the benefit of continuous two dimensional temperature maps afforded by IR imaging. Since

cryotherapy is driven by the temperature applied to the skin surface, the present study was undertaken to measure how large the lateral thermal differences may be on the cooling pad surface of selected CTU systems. The drawback in using IR imaging is that it is not possible to obtain continuous reading of skin temperatures. However, the cooling pad defines the thermal boundary condition applied to the skin during cryotherapy, and consequently the IR images do provide information relevant to understanding the physiological response to application of a cryotherapy system.

We have observed that in addition to the thermal boundary conditions imposed by a cooling pad, local features of anatomical structure and circulatory function may contribute to variations in skin temperature at a cryotherapy site. Therefore, this study was explicitly confined to only measuring the potential effects of the cooling device in defining the thermal boundary conditions that may be applied to the skin surface during cryotherapy.

Eighteen different CTU and cooling pad combinations were evaluated with an infrared camera to determine the extent to which they were able to create a uniform temperature field for cryotherapy. As anticipated, all systems produced thermal profiles that varied by location on the pad surface. Since cooling is caused via the circulation of ice water through channels integral to the pad, an inherent consequence of this style of cooling system is that there will be thermal dead spaces interspersed between the channels. Cooling pads are fabricated from flexible polymeric sheets that have relatively low thermal conductivity. Therefore, the lateral distribution of the cooling effect of ice water flowing through the pads is limited. The thermal images and temperature gradient maps quantify this effect for the various systems.

Thermal distinctions among CTU/pad systems appear to be primarily due to the design of the water flow pathways through individual pads and the method by which a

CTU pumps water through a pad. The temperature variation across a single pad varied greatly from one pad to another. A comparison of the temperature variation magnitude amongst different pads showed a maximum ratio of about 5 to 1.Thus, these unique design features can be quite substantial.

Ultimately, the utility of cryotherapy relates to its ability to improve the healing of soft tissue injuries, and this role has long been acknowledged. There is vast empirical documentation and experience supporting the value of cooling injured tissues, but there is far from a complete quantitative picture of the underlying mechanisms of action. It is recognized that a key action of cryotherapy is to reduce the rate of blood flow to the target tissue as the temperature is lowered. The sensitivity of the physiological response to an applied cooling temperature as portrayed in terms of modulation in skin blood perfusion has been measured in experiments parallel to those described in this paper and is reported in other publications [52,73,74]. The coupling between an applied therapeutic temperature and the changes produced in skin blood flow is a key component dictating the efficacy of cryotherapy regimens. The data presented herein for the thermal qualities of cryotherapy devices is complementary to designing cooling therapies to elicit desired physiological responses to improve tissue healing processes.

CONCLUSIONS

CTUs are widely applied to provide localized therapeutic cooling for soft tissue injuries, and their thermal performance is frequently expressed in terms of a single representative temperature. This study has documented that all CTU cooling pads instead create a finite range of temperatures that will be transmitted to the skin. Furthermore, there are substantial differences in the magnitude, range and distribution of temperatures over the cooling pad surface among the various CTU/pad combinations tested. As a

result, use of a single value to represent the general applied therapeutic temperature is not justified. A more useful characterization of the thermal performance of the CTU/pad combination would be the minimum temperature and the range of temperatures produced on the pad. Although some devices are equipped with a user-controlled adjustment for the pad temperature, often the resulting overall effect on thermal performance of the device is far less than the inherent spatial variations in temperature across the cooling pad surface. In summary, care and insight should be exercised in prescribing the user protocols of CTUs based on nominal thermal performance specifications, based on an awareness of the temperature producing characteristics of a particular device.

ACKNOWLEDGMENT

This research was sponsored by National Science Foundation Grants CBET 0828131, CBET 096998, and CBET 1250659, National Institutes of Health Grant R01 EB015522, and the Robert and Prudie Leibrock Professorship in Engineering at the University of Texas at Austin.

CONFLICT OF INTEREST DISCLOSURE

A patent application has been submitted by Dr. Khoshnevis and Dr. Diller to the United States Patent and Trademark Office under the title *Improved Cryotherapy Devices and Methods to Limit Ischemic Injury Side Effects*. Ownership rights to this patent reside with The University of Texas System. Dr. Diller has served as an expert witness for both plaintiff and defendant counsel since 2000 in numerous legal cases regarding the safety and design of existing cryotherapy devices.

Chapter 4: Cold-Induced Vasoconstriction May Persist Long After Cooling Ends: an Evaluation of Multiple Cryotherapy Units[3]

ABSTRACT

Purpose: Localized cooling is widely used in treating soft tissue injuries by modulating swelling, pain and inflammation. One of the primary outcomes of localized cooling is vasoconstriction within the underlying skin. It is thought that in some instances cryotherapy may be causative of tissue necrosis and neuropathy via cold-induced ischemia leading to nonfreezing cold injury (NFCI). The purpose of this study is to quantify the magnitude and persistence of vasoconstriction associated with cryotherapy.

Methods: Data is presented from testing with four different FDA approved cryotherapy devices. Blood perfusion and skin temperature were measured at multiple anatomic sites during baseline, active cooling, and passive rewarming periods.

Results: Local cutaneous blood perfusion was depressed in response to cooling the skin surface with all devices, including the DonJoy (DJO, $p = 2.6 \times 10^{-8}$), Polar Care 300 (PC300, $p = 1.1 \times 10^{-3}$), Polar Care 500 Lite (PC500L, $p = 0.010$), and DeRoyal T505 (DR505, $p = 0.016$). During the rewarming period, parasitic heat gain from the underlying tissues and the environment resulted in increased temperatures of the skin and pad for all devices, but blood perfusion did not change significantly, DJO (n.s.), PC300 (n.s.), PC500L (n.s.), and DR505 (n.s.).

Conclusions: The results demonstrate that cryotherapy can create a deep state of vasoconstriction in the local area of treatment. In the absence of independent stimulation, the condition of reduced blood flow persists long after cooling is stopped and local temperatures have rewarmed toward the normal range, indicating that the maintenance of

[3] This chapter is based on the manuscript accepted for publication by Knee Surgery, Sports, Traumatology, Arthroscopy coauthored by Sepideh Khoshnevis, Natalie K. Craik and Dr. Kenneth R. Diller [73].

vasoconstriction is not directly dependent on the continuing existence of a cold state. The depressed blood flow may dispose tissue to NFCI.

Keywords: cryotherapy; vasoconstriction; tissue blood perfusion; tissue cooling; nonfreezing cold injury.

MATERIALS AND METHODS

Experiments were conducted on FDA approved, commercially available cryotherapy devices, namely: BREG Polar Care 300 (PC300; BREG, Carlsbad, CA), BREG Polar Care 500 Lite (PC500L; BREG, Carlsbad, CA), DeRoyal T505 (DR505; DeRoyal Industries, Powell, TN), and DonJoy Ice man 1100 (DJO; DonJoy Global, Vista, CA). Similar tests were conducted on other CTUs issuing in consistent results, although not in statistically significant numbers to warrant reporting herein: BREG Polar Care 500 (BREG, Carlsbad, CA), DeRoyal T600 (DeRoyal Industries, Powell, TN), Game Ready (Game Ready, Concord, CA), Artic Ice System (Pain Management Technologies, Akron, OH), Aircast Cryo/Cuff (DonJoy Global, Vista, CA), EBIce Controlled Cold Therapy 10D (EBI, LLC., Parsippany NJ), Bledsoe bMini (BledsoeBrace Systems, Grand Prairie, TX), Bledsoe bPro (BledsoeBrace Systems, Grand Prairie, TX), and Bledsoe Cold Control (BledsoeBrace Systems, Grand Prairie, TX).

The CTUs tested in this study were available only on a temporary basis that we did not control and that therefore dictated the scheduling of specific trials. Subjects were assigned to trials as a function of the CTU time-wise availabilities. Accordingly, the study was conducted in three sequential phases. In the first phase three subjects each underwent three single trials using three different CTUs (DJO, PC300, and PC500L). The resulting data was subjected to repeated measure analysis using the Friedman test.

Nine subjects were recruited for the second phase and randomly assigned to a single trial on one of three different CTUs (DJO, PC300, and DR505) so that each CTU was tested three times. The data was assessed via independent study analysis using the Kruskal-Wallis test. For the third phase seven subjects were assigned to a single trial with a DJO CTU and a test site at either the knee or the foot/ankle. The data from these experiments was analyzed using the independent t-test. Some subjects participated in multiple phases of the study. No more than one trial was conducted per week on any given subject. Individual subjects were included in various specific trials as a function of their shared time-wise availability with the various CTUs to be tested, in combination with the need for distribution of the subjects among different trials to satisfy the requirements for statistical analysis of data.

Subjects were recruited from the University of Texas at Austin faculty and student body and were screened for contraindications of cryotherapy described by Rheinecker [75] and Lee et al.[14], including use of vasoactive medications, pregnancy, or a fresh wound at the site of cooling. The demographic data and assignment of protocols is presented in Table 1.

The basic research protocol consisted of applying CTUs to human subjects and measuring changes in the skin temperature and blood perfusion in a targeted treatment area before, during, and following a period of active cooling. The protocols were designed and implemented to mimic typical prescribed uses of the devices.

Device Type	DonJoy (DJO)	Polar Care 300 (PC300)	DeRoyal T505 (DR505)	Polar Care 500 Lite (PC500L)
Number of Subjects	n=8	n=4	n=3	n=3
Subject IDs	S1,S2,S3,S6,S7,S8,S9,S12	S1,S3,S4,S7	S3,S6,S11	S1, S3, S7
Site of Cooling	Knee (n=3), Foot/Ankle (n=4), Shoulder (n=1)	Knee (n=4)	Knee (n=3)	Knee (n=3)
Cooling Duration (min)	55.3 ± 8.4	59.4 ± 3.0	92.8 ± 24.1	61.0 ± 1.2
Gender	F(3) M (5)	F(2) M (2)	F(2) M (1)	F(2) M(1)
Age (years)	33.0 ±17.4	38.8 ±21.6	36.0 ±14.0	44.3 ± 22.6
BMI (kg/m^2)	22.7 ± 3.3	22.8 ± 4.7	20.8 ± 3.0	22.5 ± 5.7

Table 1 Demographic data and experimental protocols by device type

Instrumentation

The data presented in this paper was collected using MoorVMS-LDF2 laser Doppler blood perfusion and temperature probes (Moor Instruments, Millwey, Axminster, Devon, UK) with a flux accuracy of 10% of magnitude for perfusion and an accuracy of ± 0.3°C for temperature, based on manufacturers' specifications [76]. The Moor probes measure perfusion within the superficial 0.5 mm of tissue [77]. Thin ribbon or small bead thermocouples (Omega Engineering, Stamford, CT) were used to monitor temperature flux (± 0.1°) at multiple sites. Each sensor was mounted directly onto the skin beneath the site of the cooling pad. Blood pressure was monitored intermittently with a sphygmomanometer, and the values were applied to calculate cutaneous vascular conductance (CVC) to represent skin perfusion [59].

National Instruments (NI) input modules 9201, 9205, 9211, and 9213 (National Instruments, Austin, TX) were used to acquire blood perfusion and temperature data from the sensors, and NI DAQ 9172 and 9174 were used as a computer interface. Data was

collected with a sampling rate of 12 Hz. Temperature data was subsequently down sampled to 4 Hz, a rate that prevented aliasing.

Figure 4.1 shows sequential stages of the subject preparation, including placement of sensors, application of an ACE wrap as a thermal barrier, and positioning of the cooling pad. Additional thermocouples measured temperature on the cooling pad surface, ice water bath, and room air. In some instances, temperatures of the ice water flowing at the pad inlet and outlet were monitored with inline thermocouples.

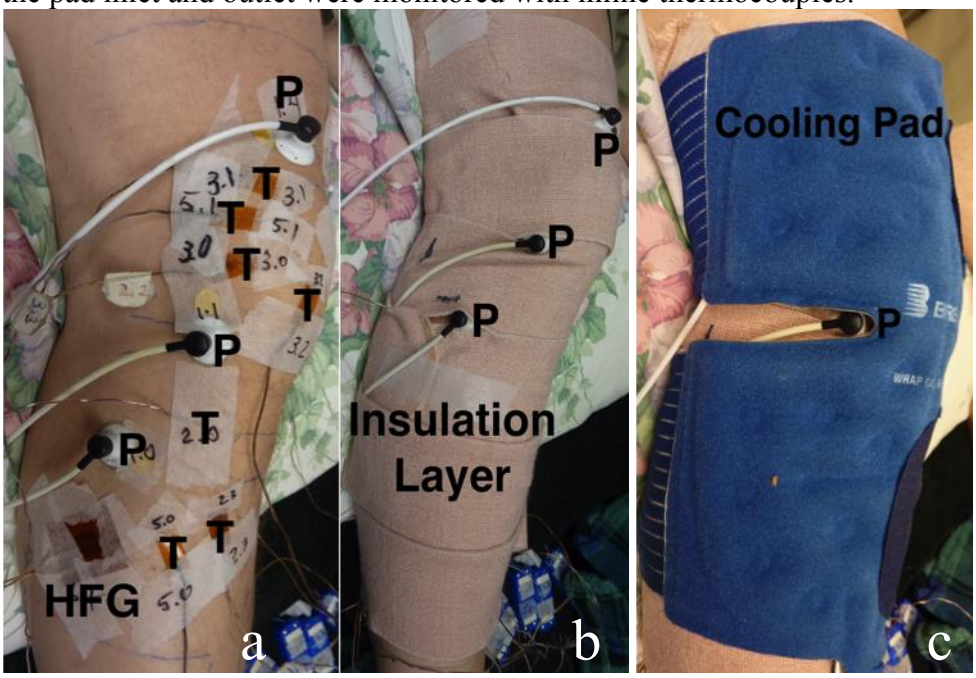

Figure 4.1 Photographs of thermocouples (T), heat flux gauge (HFG), and LDF2 probes (P) applied to the ventral aspect of the right knee (A). Same location after application of a single thermal insulation layer (ACE bandage wrap) with no elastic stretching (B) and after application of a PC300 cooling pad over the insulation layer (C).

Experimental protocol

Each experiment was composed of 3 instrumented sequential segments: 1) baseline, 2) active CTU cooling, and 3) passive rewarming with the CTU pump off. Subjects were in a semi recumbent position during the experiments and were asked to

minimize physical movements of the test site to avoid creating motion artifacts in the laser Doppler perfusion data. All experiments were performed at a fixed room temperature (22±0.5°C) and humidity (50% r.h.) environment. At least 1 hour was provided to acclimate to ambient conditions while being instrumented. A blanket was applied at subject request to prevent global vasoconstriction from ambient air exposure.

Data extraction

Data was grouped into five minute segments beginning with the start of the rewarming period. Perfusion data was represented by the median value for the associated time segment. The baseline value was calculated over the last five minutes of that period. All perfusion values were normalized to the baseline. When data was available, the perfusion measurements at multiple different locations were averaged.

Extraction of data was performed by a single researcher who is not an author using a Matlab (MATLAB7.10, The MathWorks Inc., Natick, MA) program that automatically isolated all necessary data, with the exception of manually marking the start and end points of the cooling period. To independently verify the integrity and accuracy of this process, extraction from the same data sets was repeated by two additional researchers within the lab, one of whom is not an author, and intraclass correlation was used to compare their findings using SPSS (Statistical Package for Social Science, IBM SPSS Version 20.0 for Windows; IBM Corp, Armonk, NY) software.

This study and all related protocols were approved by the University of Texas Institutional Review Board (IRB UT #2011-05-0106).

Statistical Analysis

A major challenge for statistical analysis was the small sample size (n=3) of the data. Among various available tests for normality, the Shapiro-Wilk [78] is the most

suitable for small samples. However, it carries a very low power for small n, such as P<20% for n = 10 [79]. The same limitation is true for the Kolmogorov-Smirnov, Lilliferos and Anderson-Darling tests. Therefore, for data analysis we chose to use nonparametric tests which do not require the assumption of normality. Nonparametric tests, such as Friedman and Kruskal-Wallis, were used whenever possible. Since there is no accepted non-parametric equivalent for a *t*-test, it was used as needed.

The DonJoy cryotherapy experiments consisted of four to the foot and ankle, three to the knee, and one to the shoulder. The minimum perfusions achieved during cooling were compared between the foot/ankle and knee experiments through unpaired *t*-tests (Matlab) to evaluate the effect of these anatomic locations on the vascular response to cold exposure.

Friedman and Kruskal-Wallis tests were performed to evaluate minimum perfusion values for all devices on the knee to determine whether significant differences existed. Pairwise comparison using paired *t*-tests was also performed between the perfusion values for adjacent time points to evaluate transient changes in blood flow.

One-sample *t*-tests were used to quantify the significance of changes in perfusion during cooling relative to baseline. G*Power version 3.1 was used to calculate sample size for a significance of 0.05 and power of 0.95 [80,81], which was n = 3.

Dunnett's test was applied in SPSS to evaluate the extent of perfusion change during rewarming. Values from the first 5 minutes of rewarming for each trial were compared to those at subsequent times in a case-control fashion. This same analysis was also performed to evaluate changes in temperature during rewarming.

Plots of standard error were used to determine the degree of overlap among perfusion values during the rewarming period, and a linear mixed model regression analysis was applied to evaluate the general trends. This type of analysis was used since

the data included measurements involving different rewarming durations for subjects. Unlike general linearized regression analysis, linear mixed model regression does not stipulate independence and allows for missing data at later time points. Time was assigned to be a fixed effect in this analysis to determine whether a perfusion trend occurred. Time was assigned to be a random effect to check for non-independence.

RESULTS

Cooling pad and skin surface temperatures and skin blood flow data for an exemplar protocol are shown in Figure 4.2 to illustrate the temporal characteristics of the data. Notice how the perfusion falls with decreasing temperature but does not follow the subsequent trend of increasing temperature.

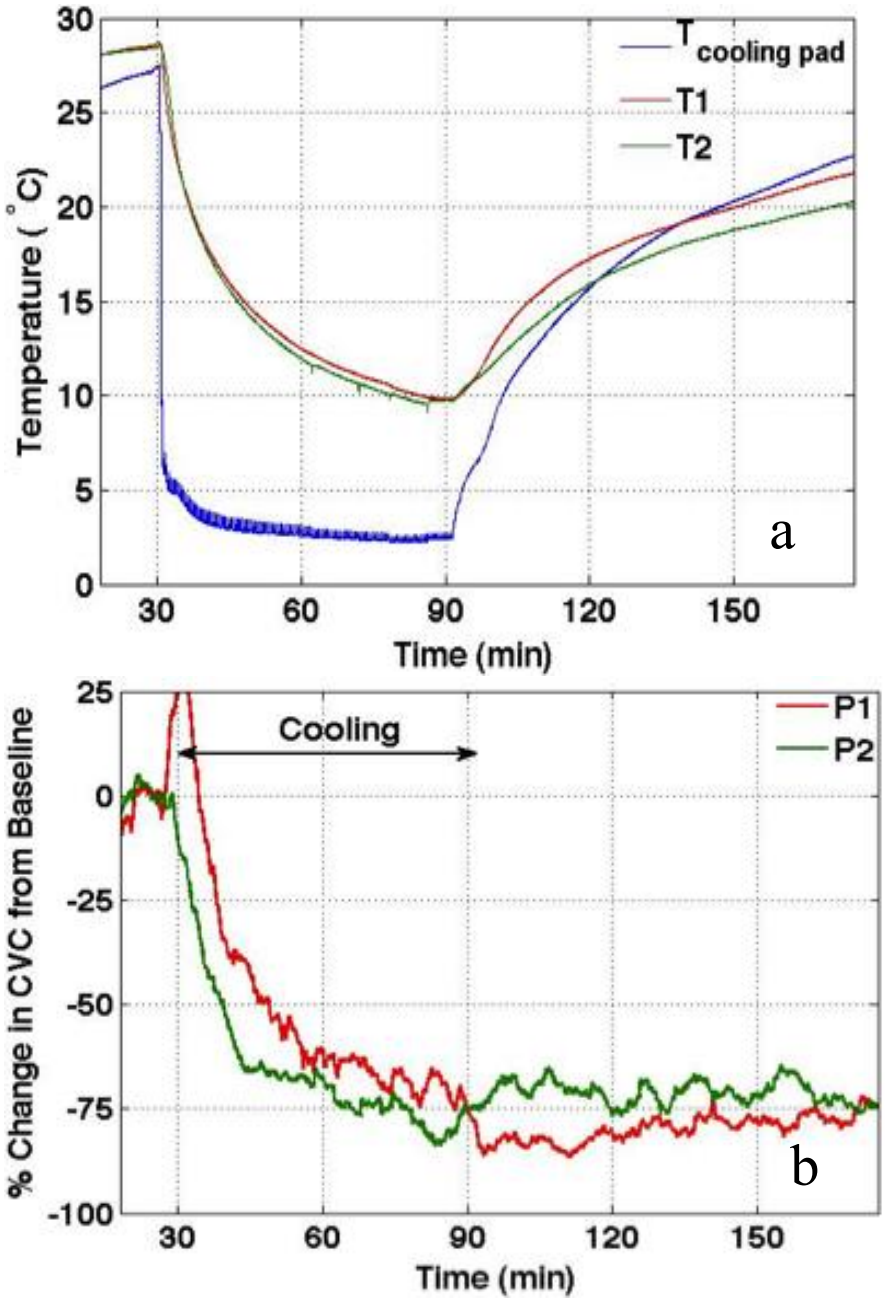

Figure 4.2 Data for a trial with a BREG Polar Care 300 cryotherapy unit applied to the knee, consisting of 30 minutes of baseline data, followed by 60 minutes of active cooling, and 84 minutes of passive rewarming. Temperature histories measured at two locations on the skin surface under the cooling pad (red and green) and on the surface of the pad (blue) (A). Perfusion histories at the two sites in the skin under the cooling pad (B).

Effect of Anatomical Location

An independent *t*-test performed between the DJO data for the knee (n = 3) and foot/ankle (n = 4) revealed no significant difference in the extent of vasoconstriction between these locations (n.s.).

Comparison among CTU Devices

Both dependent and independent statistical analyses were applied to analyze the degree of vasoconstriction induced by different CTU devices. A Friedman test was performed to compare the vasoconstriction in subjects (n = 3) who all used the DJO, PC300, and PC500L. A Kruskal-Wallis test was performed to compare the extent of vasoconstriction among independent groups (n = 3) who used the DJO, PC300, or DR505. No significant differences were found ($\alpha = 0.05$, n.s.). Table 4.2 presents a summary of statistics comparing the various CTU and anatomical combinations.

Phase	Device 1	Device 2	Device 3	Test Type	p Value	Body Part	Subject Assignment
1	DJO	PC300	PC500L	Friedman	1	knee	S1, S3, S7
2	DJO	PC300	DR505	Kruskal-Wallis	0.56	knee	S2, S6, S8 S1, S3, S4, S7 S3, S6, S11
3	DJO	DJO	N/A	Independent *t*-test	0.93	knee foot/ankle	S3, S7, S9 S1, S2, S8, S12

Table 4.2 Summary of experiments and statistical tests used to analyze data. Subject assignments are indicated by common alignment with the test identifier.

Effect of Cooling on Depression of Blood Perfusion

One sample *t*-tests confirmed that a significant difference existed between baseline and minimum perfusion values caused by cooling (Table 4.3).

CTU	p Value	n
DJO	2.6×10^{-8}	8
PC300	0.0011	4
PC500L	0.01	3
DR505	0.016	3

Table 4.3 Results of one sample t-test showing the significant drop in perfusion in response to localized cooling

Transient Gradients in Perfusion during Rewarming

Pairwise comparison for all devices between perfusion at adjacent 5 min periods during rewarming showed that no significant differences ($\alpha = 0.05$) except for single points on DJO for 5 and 10 min ($p = 0.033$) and PC300 for 10 and 15 min ($p = 0.045$).

Persistence of Vasoconstriction during Rewarming

A case control study for all devices used Dunnett's test to compare current and subsequent perfusion values and showed that there was no significant increase in blood perfusion during the observed rewarming period for any of the cryotherapy devices. The mean and standard deviation of perfusion were calculated for the PC300 and DJO data over each 5 minute rewarming interval showing that there was no net accrued increase in perfusion. Figures 4.3 (a) and (b) respectively show the aggregate calculated PC300 and DJO data that document the absence of change in perfusion during rewarming.

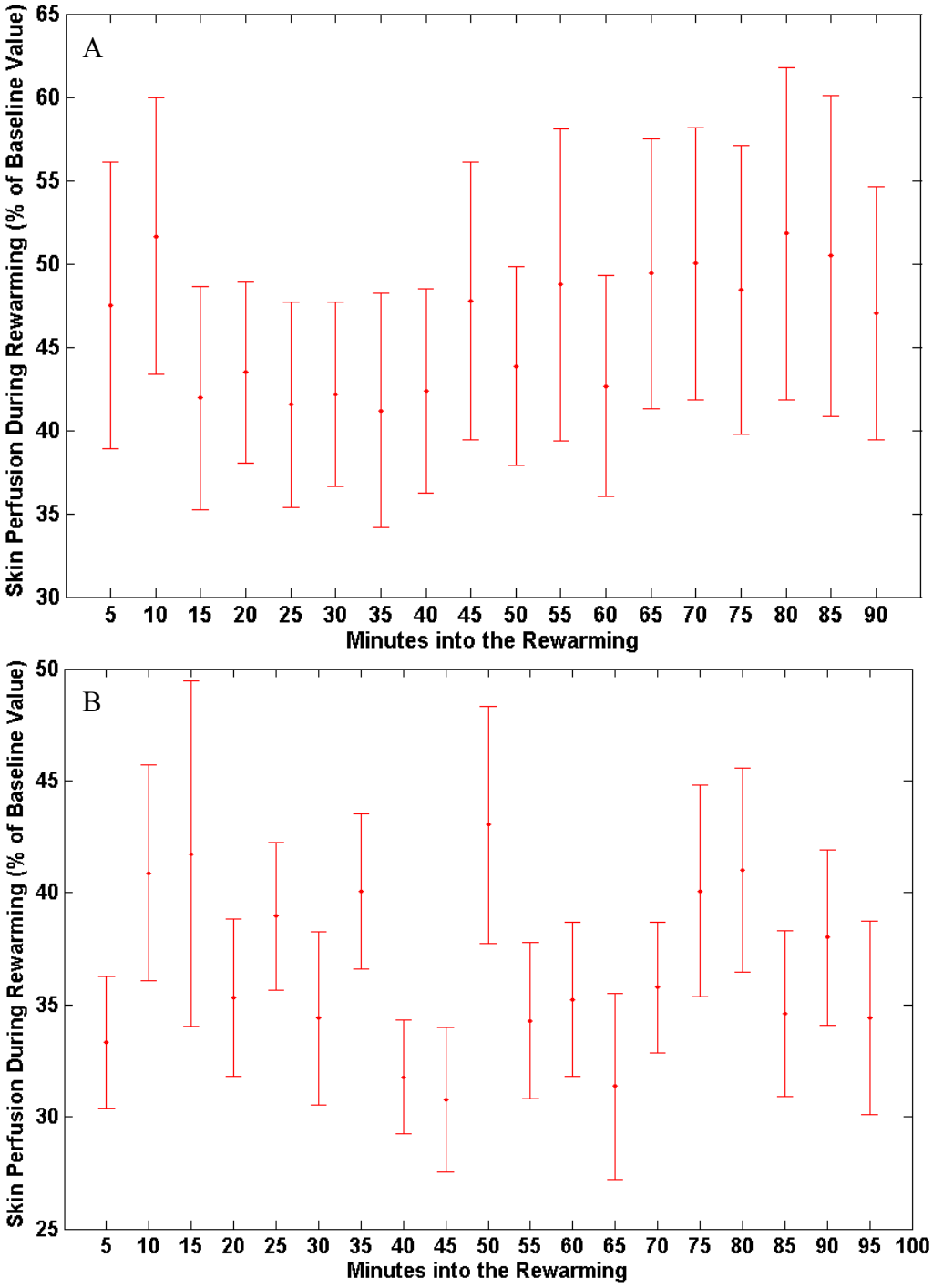

Figure 4.3 Mean and standard errors of perfusion values from the PC300 (A) and DJO (B) cryotherapy devices during 90 and 95 minutes of rewarming, respectively. The overlap among the error bars shows that there is no overall significant change in perfusion during rewarming.

Mixed Model linear regression analysis was performed on this rewarming data to derive the regression equations presented in Table 4.4.

CTU	Regression Equation	p value	Duration (min)
DJO	y = 0.00017x + 37	0.997	95
PC300	y=-0.024x + 50	0.807	90
DR505	y = -0.036x + 44	0.81	20
PC500L	y = -2.6x + 98	0.40	15
PC500L	y = -0.20x + 52	0.70	120

Table 4.4 Linear regression equation describing the change in perfusion during passive rewarming period

Increase in Temperature during Rewarming

A case control analysis via Dunnett's test compared the temperature at the start of rewarming and subsequently. It showed a significant increase after 15 and 30 minutes for DJO and PC300, respectively. Although temperature showed an increasing trend for both DR505 (5.5ºC in 20 minutes) and PC500Lite (3.5ºC in 15 minutes), the increase was not significant by this measure. The results are in Table 4.5.

CTU	Metric	5	10	15	20	25	30	35	40	45	50	55	60	65	70	75	80	85	90	95
DJO	Perfusion																			
	Temperature																			
PC300	Perfusion																			
	Temperature																			
DR505	Perfusion																			
	Temperature																			
PC500L	Perfusion																			
	Temperature																			

Table 4.5 The persistence of vasoconstriction and reduced temperature during rewarming period based on the case control study using the Dunnett's test. The numbers define the time in minutes from the start of rewarming period. The shaded areas show the region where no significant increase in either skin perfusion or temperature takes place. For PC300, DR505 and PC500L the rewarming only lasted for 90, 20 and 15 minutes, respectively.

Data Extraction Reliability

A single rater (who is not an author) performed the extraction for all data reported herein. This work was verified via partial replication by two other raters (one not an author) and compared by Intraclass Correlation (ICC) analysis. The ICC values were 0.97 for the minimum perfusion data, 0.97 at 5 minutes and 0.99 at 30 minutes later. Fleiss ranks ICC values over 0.75 as excellent [82]. Flack et al. and Walter et al. associate our ICC values and number of trials with a power of at least 0.98 [83–85].

DISCUSSION

The most important finding of the present study was that following the large drop in blood perfusion caused by surface cooling of soft tissue, in the absence of an imposed stimulation the perfusion will remain depressed for an extended time even while the tissue temperature is returning toward baseline. To our knowledge, this phenomenon has not been identified in prior studies of the effects of cryotherapy.

No obvious anatomical differentials in the response to cryotherapy were detected. There would appear to be a common local vasomotive control mechanism. The vasoconstriction response to surface cooling appears to be ubiquitous. Thus, the site of cooling application is not considered as a distinguishing factor in this data set.

There was no significant difference in the extent of vasoconstriction induced by the different devices tested: DJO, PC300, PC500L, and DR505. These statistical results suggest that device type does not significantly affect the level of vasoconstriction induced by cryotherapy. The response to other ice water circulating CTUs that we have measured, but not reported herein, is fully consistent with these results.

Primary limiting factors in the present study are that blood perfusion and temperature measurements were performed only at singular locations, inherently missing the two dimensional distributions of these properties across the entire treatment area. We

have casually observed that anatomical structures such as the knee patella may influence both temperature and perfusion, but explicit data that document this effect remain to be acquired owing to limitations of our current instrumentation. We have made two dimensional temperature measurements via IR thermography at a single time point that will be included in subsequent publications. Also, the blood perfusion probes have an approximately 1cm vertical height, meaning that where they are positioned, the cooling pad is locally held away from the skin surface, resulting in a reduced cooling effect. The temperatures measured with the perfusion probe thermal sensor are approximately 2 - 3°C warmer during cooling than sensed by thermocouples at peripheral sites directly below the pad. Thus, the dose response effect of cryotherapy on blood flow is compromised. This phenomenon has been quantified and will be reported in a subsequent publication under preparation.

There are few published studies that have systematically analyzed the microcirculatory modification effects of cryotherapy and still fewer that have been conducted on human subjects. One such human subject study concluded that cryotherapy results in a significant decrease in superficial (2 mm depth) and deep (8 mm depth) microcirculatory blood flow during a 30 minute cooling period [22], consistent with our findings. But, post-cooling perfusion measurements were not recorded.

Another study in rats showed that 20 minutes of cryotherapy caused a significant decrease in perfusion [86]. Contrary to our findings, the blood flow depression did not persist following the cessation of active cooling. However, this study measured perfusion in deeper skeletal muscular and only at relatively infrequent intervals.

The data from this study indicate that it is likely that a long acting humoral agent is released locally with a continuing vasoconstrictive effect that persists while tissue temperatures rewarm toward the baseline values. We are pursuing further research to

confirm, identify, and characterize the action of local vasoactive agents with the objective being to better control cryotherapy-induced tissue ischemia.

A focal message delivered by this study is that many commercially available cryotherapy devices have inherent operating conditions that produce a significant degree of vasoconstriction that may last long after cessation of cryotherapy. The experimental results show an uncoupling between skin perfusion and temperature during the passive rewarming period. The extent of vasoconstriction and its prolongation are sufficient to possibly lead to an equivalent ischemic state and then to NFCI.

CONCLUSION

The results demonstrate that standard cryotherapy methods produce a significant and persistent state of vasoconstriction in the local area of treatment during both active cooling and subsequent passive rewarming. The data presented in this paper that extend the understanding of the response in blood perfusion to cryotherapy may be embodied in improved therapeutic schemes to reduce the risk of ischemic injury.

AUTHOR DISCLOSURE STATEMENT

A patent application has been submitted by Dr. Khoshnevis and Dr. Diller to the United States Patent and Trademark Office under the title *Improved Cryotherapy Devices and Methods to Limit Ischemic Injury Side Effects*. Ownership rights to this patent reside with The University of Texas System. Dr. Diller has served as an expert witness for both plaintiff and defendant counsel since 2000 in numerous legal cases regarding the safety and design of existing cryotherapy devices.

ACKNOWLEDGEMENTS

This research was sponsored by National Science Foundation Grants CBET 0828131, CBET 096998, and CBET 1250659, National Institutes of Health Grant R01

EB015522, and the Robert and Prudie Leibrock Professorship in Engineering at the University of Texas at Austin. We would also like to thank Ms. Natalia Mejia for investing long hours of careful and conscientious work in her critical role in extracting data for this publication, and Dr. Michael Mahometa of the Division of Statistics and Scientific Computation, College of Natural Sciences at the University of Texas at Austin for his help and guidance in statistical analysis of data. Comments by the reviewers have been very helpfu

Chapter 5: Persistent Vasoconstriction After Cutaneous Cooling: Hysteresis Between Skin Temperature and Blood Perfusion[4]

ABSTRACT

Localized cooling is commonly used to manage soft tissue injury by reducing pain, swelling and inflammation and may also result in prolonged skin vasoconstriction at the treatment site.. The goal of this study was to investigate the persistence of cold-induced vasoconstriction following cessation of active surface cooling and the resulting temperature-driven hysteresis in skin perfusion over the cooling and rewarming cycle. An Arctic Ice cryotherapy unit was applied for 60 minutes of active cooling followed by 120 min of passive rewarming to the knee region of 6 healthy subjects. Multiple laser Doppler flowmetry perfusion probes were used to measure skin blood flow (expressed as cutaneous vascular conductance, CVC) during the experiments. Surface cooling produced a significant reduction in CVC ($p < 0.001$). The Dunnett's test, repeated measure ANOVA, Friedman test, and mixed model regression analysis all showed the persistence of vasoconstriction throughout the rewarming period. The occurrence of a hysteresis effect between CVC and skin temperature during cooling and rewarming cycle of the skin was calculated to be significant ($p < 0.005$). Mixed model regression showed a significant difference in the slopes of the CVC-skin temperature curves during cooling and rewarming ($p<0.0005$). Localized cooling causes significant vasoconstriction that continues beyond the active cooling period during a significant subsequent rewarming of the skin.

[4] This chapter is based on the manuscript readied for submission to the Journal of Applied Physiology and is coauthored by Sepideh Khoshnevis, Natalie K. Craik, Dr. R. Matthew Brothers and Dr. Kenneth R. Diller.

INTRODUCTION

Localized cooling (cryotherapy) of soft tissue is commonly applied following orthopedic surgery and sports injuries to reduce pain, swelling, inflammation, bleeding, and secondary hypoxic injury. Cryotherapy may be used in conjunction with cryokinetics by physical therapists to reduce the sensation of pain and to allow early mobilization [3,6]. Although cryotherapy has been adapted widely, protocols largely have been derived empirically, and many diverse operational methods are recommended [24].

Cooling sources requisite for cryotherapy include cubed or crushed ice [15], refrigerated gel packs[16], and commercially available cryotherapy units (CTU) that are distinguished by the ability to provide prolonged cooling episodes [15,20,21]. A CTU generally consists of an insulated chest that is filled with ice and water, a cooling pad, a submersible water pump, and tubing that connects the pad to the pump. A user is instructed to maintain the chest with ice and water per the manufacturer's recommendations. For these CTUs, the cryotherapy temperature is based on the melting state of water (0°C), and the duration prescribed for a single application episode may vary from minutes [7,8,14] to days [9,19,25,87]. A more sophisticated and sensitive, albeit expensive, approach to regulating the temperature of CTU cooling water is via a thermoelectric refrigeration source to replace the ice. A circulating water cooling pad consists of a pair of flexible polymeric sheets having inlet and outlet ports connecting moulded flow channels that direct the movement of cold water over a treatment surface in a specific geometric pattern. Many different pad designs exist, giving rise to unique temperature patterns on the treatment area [72].

Localized cooling of non-glabrous skin results in vasoconstriction through activation of vasoactive pathways [37–41]. Prolonged cold-induced vasoconstriction may result in tissue ischemia leading to non-freezing cold injury (NFCI)

[42,45,46]Furthermore, reestablishing tissue blood flow following a prolonged period of tissue ischemia may result in reperfusion injury [47]. There are sundry reports in the literature of ischemic cryotherapy related injuries ranging from ice burn [88] to full thickness skin necrosis [13,14] and nerve damage [10,89,90].

Despite the widespread use of cryotherapy and the occurrence of related injuries, the relationship between skin temperature and tissue perfusion during the cooling and subsequent rewarming periods remains relatively unknown. Therefore, the goal of this study was to investigate the relationship between skin temperature and CVC during and following localized cooling of non-glabrous skin with a commercially available CTU. We hypothesize that there exists a hysteresis between CVC and skin temperature during the cooling and rewarming phases of cryotherapy in the absence of artificial external stimuli.

METHODS

Ethical Approval and Subjects

This study was approved by the Institutional Review Board of The University of Texas at Austin prior to start of experiments. All subjects provided voluntary written consent to participate after being informed about the nature of the experiments and their possible side effects.

The experiments were performed on 6 healthy non-smokers (3 male) with an average age (± SE) of 22.5 ± 1.4 years and BMI (± SE) of 23.4 ± 1.6 kg/m^2. All subjects were free from any known cardiovascular, metabolic, or neurological disease and were not taking any medication. None of the subjects reported a history of cryotherapy or other form of cold exposure in the lower extremities for at least a year prior to the experiment and had no history of knee injury for at least a few weeks prior to enrolling in the study. Each subject participated in a single identical trial.

Instrumentation and Measurements

All experiments were performed in the right knee region with the subject seated in a semi-recumbent position in the same laboratory environment with room temperature (± SE) of 21.8 ± 0.4˚C and relative humidity of 50%. Prior to the start of data collection, the right knee of each subject was instrumented with three laser Doppler flowmetry probes (two VP1T/7 and one VP1-HP in conjunction with moorVMS-LDF2 and moorVMS-LDF1-HP monitor, respectively; Moor Instruments, Millwey, Axminster, Devon, UK) to provide a continuous index of cutaneous blood flow. The average penetration depth of moorVMS-LDF2 and MoorVMS-LDF1-HP were 0.5 and 2 mm, respectively [59]. Thermocouples (Omega Engineering, Stamford, CT) were placed at multiple areas under the cooling pad to monitor skin temperature. Perfusion measurements were obtained at three different locations: proximolateral, distolateral and proximomedial to the knee joint.

Following instrumentation placement, the measurement area was carefully wrapped with a single layer of loose ACE bandage to provide a thermal barrier between the skin surface and the cooling pad (see below). Then a commercially available cryotherapy cooling pad (Arctic Ice universal pad; Pain Management Technologies, Akron, OH) was applied overlying the instrumented area, and fixed in place using another layer of Ace bandage. Figure 5.1A presents an image of instrumentation prior to application of the thermal barrier wrap. This figure also shows the general location of the various probes in the active treatment area. The Arctic Ice universal cooling pad in place is shown in Figure 5.1B. An Arctic Ice CTU (Pain Management Technologies, Akron, OH) was used to deliver cold water through the cooling pad applied to the subject's right knee following the manufacturer's recommendation (see below for more detail). Intermittent blood pressure measurements and heart rate were obtained every 15 minutes

by auscultation of the brachial artery with an electrosphygomanometer (SunTech, Raleigh, NC), and mean arterial blood pressure (MAP) was calculated as one-third of pulse pressure plus diastolic pressure.

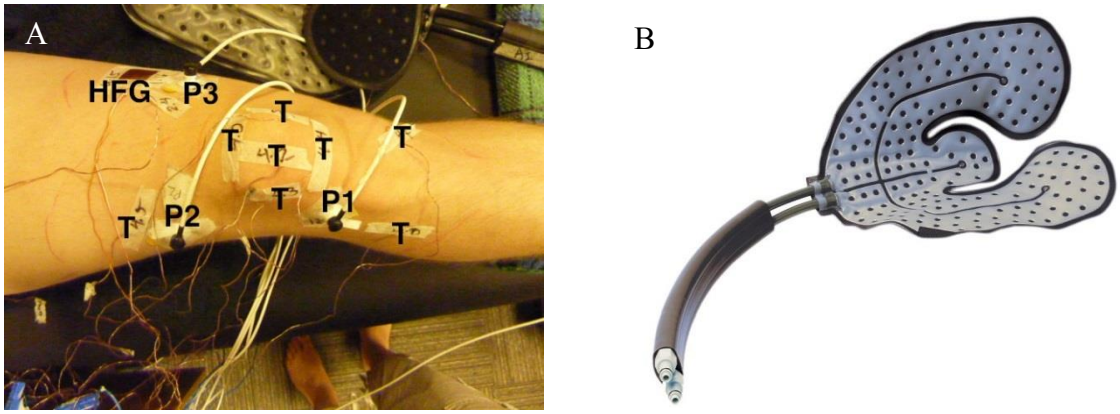

Figure 5.1. A sample instrumentation image (A). P1, P2 and P3 mark the three perfusion probes, HFG is the heat flux gauge and T marks the location of different thermocouples used to measure skin temperature in the knee region. All shown measurements are at location that will be covered with the cooling pad. An image of Arctic Ice cooling pad used in our experiments to deliver cold water to the treatment site (B). The cooling pad is composed of three flaps, two bigger ones on the sides and a smaller one in the middle designed to cover the medial and lateral segment of the joint and patella, respectively.

Additional thermocouples were placed on the anterior surface of the left shin, right thigh, right arm, and chest for monitoring of mean skin temperature using the method of Ramanathan [91]. Core temperature was measured via a type T bead thermocouple embedded in a single use, silicone ear plug placed at the proximity of the tympanic membrane and occluding the ear canal [92–94]. In addition to the laser-Doppler flowmetry probes located at the treatment site, two additional probes were located at control sites not exposed to the cooling; one on the dorsal surface of the right foot distal to the treatment area, and another on the lateral surface of the left knee proximal to the joint.

Experimental procedure

Subjects were in a semi-recumbent position for the duration of the experiment and asked to refrain from moving their lower extremities as much as possible to eliminate causing motion artifacts in the signal. Subjects were allowed to acclimate to room temperature during 1 hour of instrumentation prior to the start of data collection. During this time period a blanket was provided if requested to prevent vasoconstriction due to exposure to room temperature air. Immediately following instrumentation (including placement of the cooling pad) there was a 30 min period of baseline data collection with no active change in skin temperature. Next was one hour of skin-surface cooling at the treatment site with the CTU circulating water with an average temperature of (±SE) 2.4°C ± 0.5 through the pad. At the end of the cooling phase the CTU was turned off while data collection continued for an additional two hours with all instrumentation in place. During this passive rewarming phase heat propagation from the deeper tissue and ambient environment increased the tissue temperature. Table 5.1 shows a detailed description of these experiments.

Durations (min)		Baseline Values			Minimum Achieved		
Baseline	30.1 ± 0.2	Temperature (˚C)		31.4 ± 0.4	Temperature (˚C)		16.6 ± 0.3
Cooling	60.1 ± 0.2	CVC	Absolute	41.9 ± 8.7	CVC	Absolute	8.7 ± 2.0
Rewarming	123.7 ± 4.7		Relative	100%		Relative	26% ± 3.2

Table 5.1. Summary of experiments. General information including baseline, cooling and rewarming durations and the average CVC and skin temperature values during the last 5 minutes of baseline and the minimum achieved after 1 hour of cold exposure. The CVC is presented both relative to baseline and in absolute format. Standard errors of means for all measured values are presented in the table.

Data extraction / Analysis

Hemodynamic and thermal data were collected on a data acquisition system (National Instruments (NI) input modules 9205, and 9213, National Instruments, Austin, TX) which were then subsequently transferred to a laboratory computer via an NI DAQ 9174 (National Instruments, Austin, TX). All perfusion data were collected with a sampling rate of 12 Hz. Temperature data was sampled at the rate of 1 Hz. Three laser Doppler flowmetry perfusion probes were used under the cooling pad in each experiment to measure skin perfusion. VP1T/7 perfusion probes were also used to measure skin temperature at the exact site that perfusion was measured. There was no significant difference between the average perfusions measured by VP1T/7 and VP1-HP probe. Therefore all perfusion and CVC data presented herein is based on the average values of VP1T/7 probes. All reported skin temperatures are the average values of the VP1T/7 probes. In order to account for potential blood pressure changes during the protocol, all blood flow data is reported as cutaneous vascular conductance (CVC) as calculated by CVC = Flux units / mean arterial pressure.

Data from the cooling and rewarming periods were divided into 1-minute segments from the starting point of each phase of a trial. Baseline data was calculated as the median value for perfusion and CVC during the last 5 min of the period. Likewise, median values for perfusion and CVC were determined during each of the 1 min data segments during cooling and rewarming. The same procedure was used to extract temperature data with the exception that the median was replaced with mean to calculate a representative value for each temporal data segment. This data was used to study CVC/skin temperature hysteresis (by visualization and calculation of area, see below). All other application data was downsampled to 1 value/5 min. Data extraction was performed in MATLAB (MATLAB7.10, The MathWorks Inc., Natick, MA, 2010) in a semiautomated fashion with the only input from the researcher being the designation of the starting and ending time points of active cooling.

CVC values were normalized to the baseline period and calculated as percent change from that state. The minimum CVC measured during the cold exposure was calculated and compared to baseline using a one-sample *t*-test in MATLAB.

Persistence of vasoconstriction during the rewarming period

A case-control study using the Dunnett's test was performed to compare CVC and skin temperature from the first five minutes of rewarming with future time points. Additionally, repeated measure ANOVA (rmANOVA) and Freidman tests were used to compare CVC values from the first 5 minute of rewarming to that for all other subsequent time points. Bonferroni correction and false discovery rate (FDR) control were used to adjust the p-value for multiple comparison tests. The modified z-score method was used to identify possible outliers [95]. The Shapiro-Wilk's test was used to assess the assumption of data normality at each time point and the Maulchly's test the assumption

of data sphericity. Mixed model regression (MMR) was used to evaluate the possible increasing trend in CVC during rewarming and its statistical significance. MMR was applied for this purpose rather than linear regression due to the repeated measure nature of the data, which could potentially violate the assumption of independence in linear regression. SPSS (IBM SPSS Version 21.0 for Windows; Armonk, NY: IBM Corp) was used for all statistical analysis with the exception of the one sample *t*-test and the Dunnett's test [96] which were performed in MATLAB.

Hysteresis

MMR was applied to model the change in CVC as a function of skin temperature during both the cooling and passive rewarming periods using SPSS. A quadratic term (temperature^2) was added to the standard linear regression equation (intercept + temperature) to accommodate the nonlinear behavior of the data. The temperature and temperature^2 were used as fixed effects to determine the overall trend and as the random effect to calculate the variation among different subjects. A dummy variable was introduced to differentiate between the cooling and the rewarming portions of the experimental cycle. Finally, two interaction terms (the interactions between the dummy variable and the temperature and the temperature^2) were added to the model to verify the significance of the differential dependence of CVC on skin temperature during cooling and rewarming. The likelihood ratio test for random effects was used to validate the significance of different terms in the regression model. The normal quantile-quantile plot (Q-Q plot) was used to investigate normality of residuals as a diagnostic measure to evaluate the representative accuracy of the MMR model. Significance was accepted at $P \leq 0.05$.

RESULTS

Skin temperature reached an average minimum (± SE) of 16.6˚C ± 0.3 starting from a baseline value of 31.4˚C ± 0.4 at the completion of 1 hr of active cooling. At the end of cooling, the CVC was reduced significantly from its baseline value ($p < 0.001$). Exemplar data presented in Figure 5.2 show changes in CVC and skin temperature during cooling for 60 minutes. The CVC drops by more than 75% of baseline by the end of cooling and remains depressed for the duration of data collection. In contrast, the surface skin temperature drops by about 14˚C during cooling and increases by about 10˚C during the rewarming. This hysteresis between CVC and skin temperature is described in more detail below. CVC measurements at control sites do not show a similar decrease in response to cooling at the treatment site (data not presented here).

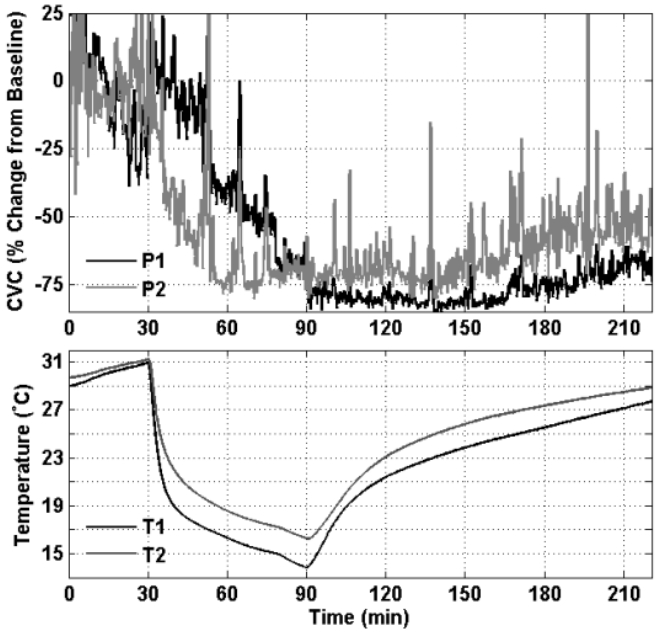

Figure 5.2. Percent change in CVC compared to baseline values (top plots) and skin temperature (bottom plots) from 2 different experiments. Each experiment was composed of 30 minutes of baseline and 60 minute of cooling follow by about 2 hours of passive rewarming.

Persistence of vasoconstriction during the rewarming period

A case-control study applying the Dunnett's test was used to compare the changes in CVC and skin temperature during rewarming. The results show that even though temperature had a significant increase starting at 15 minutes into the rewarming period ($p < 0.0005$), the CVC values showed no significant increase throughout the entirety of rewarming (n.s.), with the exception of the CVC at 120 min which was significantly higher than during the first 5 minutes ($p = 0.035$).

The Shapiro-Wilk's test showed that CVC data at each time point was normally distributed ($p>0.05$), but given our sample size of 6 and the low power of normality tests for low sample sizes [79] we performed both rmANOVA and its nonparametric counterpart, the Friedman test. SPSS was not able to calculate χ^2 statistics and significance for the Mauchly's test but since the estimation of ε was less than 0.75, the Greenhouse-Geisser correction was used to assess the significance of rmANOVA. Since rmANOVA was statistically significant ($p=0.013$), a multiple comparison test was performed. The results of multiple comparison tests with Bonferroni correction and FDR control, and Friedman test are presented in Table 5.2. Multiple comparison tests with Bonferroni correction displayed no significant increase in CVC during the rewarming period. Multiple comparison tests with the FDR control method indicated a significant increase in CVC only at 120 min ($p=0.021$), whereas the Friedman test showed a significant increase after 110min ($p=0.048$ and 0.04, at 110 and 120 min, respectively).

	10 min	20 min	30 min	40 min	50 min	60 min	70 min	80 min	90 min	100 min	110 min	120 min
rmANOVA with Bonferronin adjustment	n.s.	n.s.	n.s.	n.s.	n.s.	n.s.	n.s.	n.s.	n.s.	n.s.	n.s.	n.s.
rmANOVA with adjusted Bonferroni (FDR)	n.s.	n.s.	n.s.	n.s.	n.s.	n.s.	n.s.	n.s.	n.s.	n.s.	n.s.	0.021
Friedman test	n.s.	n.s.	n.s.	n.s.	n.s.	n.s.	n.s.	n.s.	n.s.	n.s.	0.048	0.040

Table 5.2. Results of rmANOVA and Friedman tests**.** Persistence of vasoconstriction resulted from exposure to 15°C for 60 minutes. CVC at different time points during rewarming period are compared to CVC during the first 5 minutes of rewarming. Repeated measure ANOVA with Bonferroni and adjusted-Bonferroni (FDR method) adjustment and Friedman tests were used for this study. The time points are presented in respect to the start of rewarming period. The values presented are the results of pairwise comparison performed in SPSS. All non-significant results are marked as n.s. and the significant p-values are expressed numerically and presented in red.

A mixed model regression study of the CVC rewarming data at first 60, 75, 90, 105 and 120 min showed that the temporal slope of a fitted line was significantly larger than 0 ($p < 0.05$) only at 90 minutes and later and was insignificant earlier (n.s.).

Temperature / CVC hysteresis

The persistence of vasoconstriction results in a hysteresis effect between CVC and skin temperature during the cooling and rewarming cycle. Figure 5.3 shows temperature and CVC as a function of time during the rewarming period as well as their values during baseline and at the end of cooling. Temperature increases immediately upon cessation of cooling, whereas perfusion shows a further drop during the first 10 minutes of rewarming followed by a very slow increase during rewarming. CVC regains only about 30% of vasoconstriction on the 120 min of rewarming while temperature recovers about 70% of the cooling drop. This hysteresis behavior is seen explicitly in Figure 5.4 where CVC is plotted as a function of the skin temperature during cooling (black stars) and rewarming (grey dots). Figure 5.4 shows a CVC / Temperature state space diagram from a single experiment (A) and the average of all 6 experiments (B). Arrows are used to mark the process direction during cooling and rewarming. During baseline period, the skin temperature shows a mild increasing trend due to the insulating effect of covering the treatment area with the ACE bandage and the cooling pad, but in the absence of circulating cold water. Consequently, CVC usually has higher values at the start of cooling compared to its initial baseline state, causing the normalized CVC to begin from a state larger than 100% in Figure 5.4.

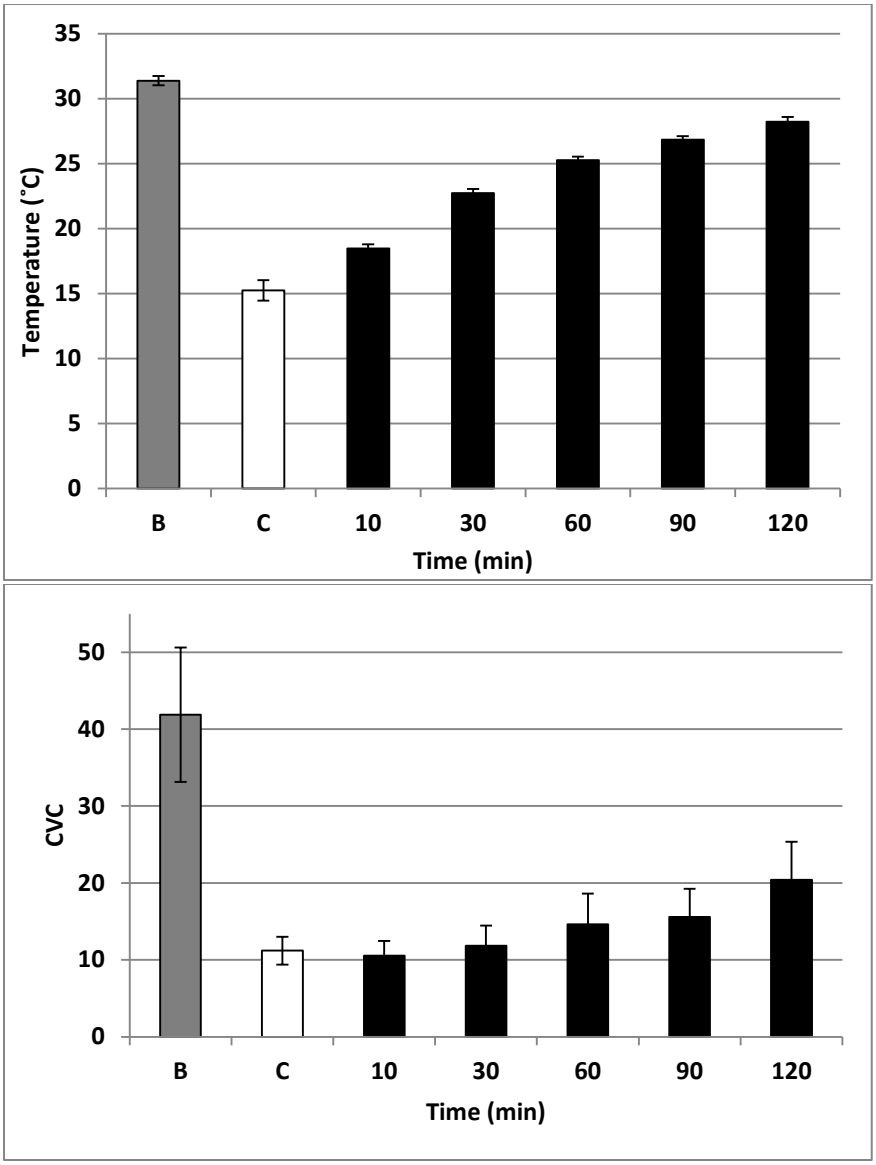

Figure 5.3. Temperature (top panel) and absolute CVC (bottom panel) values during the last 5 minutes of baseline and cooling (marked as B and C, respectively) and at the end of each 10 minute interval during rewarming periods. The represented values are average measurements from 6 different experiments. Error bars show the standard errors of the mean. The cooling phase of experiments lasted for 60 minutes.

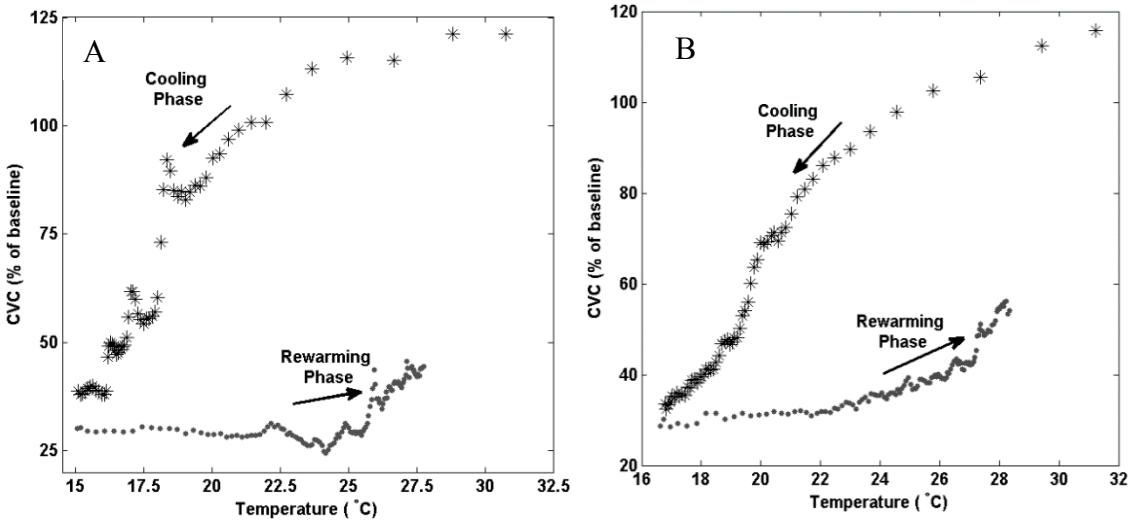

Figure 5.4. Skin perfusion as a function of skin temperature during cooling (stars) and passive rewarming (dots). The arrows show the direction of time progress. Each two subsequent data points are one minute apart from each other. A hysteresis plot from a sample experiment (A). The hysteresis plot based on the average measurements from all the experiments (B).

The area of the space state diagrams was calculated for each experiment, and the average determined to be significantly greater than zero (26.0 ± 4.5 (SE), $p < 0.005$). MMR was used to model the change in CVC as a function of skin temperature during cooling and passive rewarming. A quadratic equation of the form

$$CVC_{ij} = \beta_{0j} + \beta_{1j}T_{ij} + \beta_{2j}T_{ij}^2 + k + k^*T + kT^2 + e_{ij}$$

$$\beta_{0j} = \gamma_{00} + u_{0j}$$

$$\beta_{1j} = \gamma_{10} + u_{1j}$$

$$\beta_{20} = \gamma_{20} + u_{2j}$$

was used for MMR where T stands for temperature; k is a flag that defines if each data point is part of the cooling or rewarming periods; $\gamma_{00}, \gamma_{10}, and\ \gamma_{20}$ are the fixed effects coefficients; $u_{0j}, u_{1j}, and\ u_{2j}$. are the random effects coefficients; k, k^*T and k^*T^2 are the interaction terms; and e_{ij} is the residual error term. The slopes of the regression

lines fitting CVC to skin temperature data are presented in Table 5.3. The interaction terms (between the flag variable and the linear and the quadratic temperature terms) were both significant, implying a significant difference between the two regressions lines. To test the validity of the model, likelihood ratio tests were performed and the Q-Q plot of residuals was created. The likelihood ratio test showed that the current model was significantly better than alternative models with the omission of any or all random effect terms. A visual inspection of the Q-Q plot of residuals of the regression fit meets the requirement for normality.

	Parameter	Estimate (SE)	Significance	Confidence Interval	
Cooling	Intercept	64.05521 (38.31871)	0.144	-28.9535	157.064
	Temperature	-4.77696 (3.133645)	0.176	-12.3662	2.812285
	Temperature^2	0.15019 (0.066007)	0.061	-0.00951	0.30989
Rewarming	Intercept	-216.764 (38.17361)	0.001	-309.747	-123.781
	Temperature	19.31889 (3.140293)	0.001	11.73156	26.90622
	Temperature^2	-0.27249 (0.066417)	0.005	-0.43216	-0.11282

Table 5.3. Mixed Model Regression results. The coefficients for MMR for the slope fitting CVC vs temperature data to a quadratic function are presented for both cooling and rewarming periods.

DISCUSSION

The goal of this study was to investigate the effect of localized cooling with a CTU on skin temperature and CVC at a treatment site. The data show that localized cooling induces a pronounced reduction in CVC which is sustained long into a subsequent passive rewarming phase, in the absence of any external means to stimulate

blood flow. Furthermore, these findings demonstrate that sustained reductions in CVC following cooling persist for an extended period of time despite the recovery of skin temperature, creating a hysteresis effect between CVC and skin temperature during successive active cooling and rewarming. These results extends our prior work that demonstrated with many different CTUs a persistence of vasoconstriction during the passive rewarming period following localized cooling [73].

A significant reduction in tissue perfusion was measured using LDF at multiple sites for 60 minutes of active cooling with an Arctic Ice CTU. The skin blood perfusion showed no significant increase during the first 2 hours of passive rewarming despite a significant increase in skin surface temperature. This coupling (during cooling) followed by decoupling (during rewarming) of skin temperature and blood perfusion results in a hysteresis phenomenon.

Localized cooling is very well known to cause significant vasoconstriction and thus a reduction in tissue perfusion [17,22,86,87,97–100]. The extent of the reduction in tissue perfusion during localized cooling varies among studies. For example, Knoblock, et al. measured an 86% and 70% reduction in skin perfusion at the depth of 2 mm after 7 [17] and 30 [22] minutes of localized cooling, whereas Ho, et al. showed only a 25.8% reduction in soft tissue perfusion after 20 minutes of cold exposure [97]. Part of this discrepancy in results could be related to the measurement methods used or the depth at which blood perfusion was studied. Taber, et al. [101] investigated the effect of cold gel pack application for 20 minutes on tissue perfusion in the ankle region using impedance plethysmography and observed a significant reduction in blood perfusion independent of the applied temperature. However, this study utilized a different methodology to assess tissue perfusion, and it did not isolate the pressure effect of a gel pack from a vasoconstrictive response.

There are only a very limited number of studies that investigate the recovery in tissue perfusion after termination of active cooling. Yanagisawa, et al. used oxyHb as a measure of tissue circulation and showed that perfusion remains significantly depressed during the first 78-90 minutes following cooling [100]. This result is similar to findings presented in this article. Curl, et al. showed no long-term effect on tissue perfusion after cessation of cryotherapy in rat muscle after induction of closed soft tissue injury [86]. We believe the difference in the experimental condition and the tissue site evaluated could be the reason for the dissimilarity with the results.

Vuksanovic, et al. showed a similar hysteresis between skin temperature and blood perfusion during cooling and rewarming in the forearm region in the approximate skin temperature range of 29-38˚C with a cooling rate of 1˚C /min [102]. The current study investigates the hysteresis phenomenon at lower temperatures in the knee region with an average cooling rate of 0.25˚C /min. A quadratic function in MMR was fit the data to accommodate for its conceived concavity and convexity of behavior and to demonstrate the hysteresis effect. In a similar but a much simpler approach, Kozelek, et al. used a linear regression model to show the existence of hysteresis [103].The observed hysteresis between temperature and CVC during cooling and rewarming indicates that the system has a memory and that the state of system is not only dependent on its current condition but also its history and initial condition thus, there is not a one-to-one relationship between tissue temperature and perfusion. Knowing the current value of tissue temperature is not sufficient to determine the perfusion state. A preliminary study (data not presented here) was undertaken with cooling and rewarming rates of 0.1˚C/min to determine whether the hysteresis depends on how rapidly temperature is changing. Data showed the hysteresis to remain present even at this reduced cooling rate but there was a reduction in the area of the CVC/T plot. This finding indicates that there is a true

hysteresis effect that is not simply a product of a delayed response between temperature and CVC. Further investigation is proceeding to more fully define the hysteresis during cryotherapy.

The reason for the persistence of vasoconstriction beyond the termination of active cooling is not yet understood. It could be associated with a biophysical effect of cold exposure or to a humoral agent that is released locally. Further work is needed in this area to understand the process for delayed recovery of tissue perfusion subsequent to active cooling. Some possible mechanistic explanation includes the release of a humoral agent during cooling that prevents vasodilation as skin temperature increases. Localized cooling experiments in the forearm region have been shown to cause vasoconstriction via mechanisms such as activation of the Rho-Rho kinase pathway [41] and inhibition of the nitric oxide system [37]. These experiments are usually performed at higher skin temperatures (24˚C) and at different anatomical locations that commonly practiced in cryotherapy and do not address the vasoactive response beyond the active cooling period. Another possible contributor could be a direct biophysical effect of cold exposure that might last beyond the active cooling period.

There are many examples of hysteresis in biology and physiology [103–105]. Samples of temperature-driven hysteresis are reported in references [106,107]. Extensive review of literature did not identify other thermally-driven hysteresis phenomena in biological systems. However, the consistency with which hysteresis between local temperature and blood perfusion has been observed in the current cryotherapy trials presents a compelling argument for its existence in this system. Given the clinical implications of a prolonged state of vasoconstriction, it would appear to be a feature of cryotherapy of great importance and well worthy of more extensive study.

CONCLUSION

The skin temperature and CVC responses to localized cooling were studied. Data showed a significant decrease in CVC during cooling that persisted well into the rewarming period. Furthermore, a hysteresis effect between CVC and skin temperature was observed during a tissue cooling and rewarming cycle. The persistence of significant reduction in CVC may be a contributing factor in the development of ischemic injury processes associated with localized cooling. Further investigation is needed to understand the mechanism for the persistence of vasoconstriction during rewarming and the hysteresis between CVC and skin temperature.

AUTHOR DISCLOSURE STATEMENT

A patent application has been submitted by Dr. Khoshnevis, Dr. Brothers and Dr. Diller to the United States Patent and Trademark Office under the title Improved Cryotherapy Devices and Methods to Limit Ischemic Injury Side Effects. Ownership rights to this patent reside with The University of Texas System. Dr. Diller has served as an expert witness for both plaintiff and defendant counsel since 2000 in numerous legal cases regarding the safety and design of existing cryotherapy devices.

ACKNOWLEDGEMENTS

This research was sponsored by National Science Foundation Grants CBET 0828131, CBET 096998, and CBET 1250659, National Institutes of Health Grant R01 EB015522, and the Robert and Prudie Leibrock Professorship in Engineering at the University of Texas at Austin. We would also like to thank Dr. Michael Mahometa of the Division of Statistics and Scientific Computation, College of Natural Sciences at the University of Texas at Austin for his help and guidance in statistical analysis of data.

Chapter 6: Conclusion

This research was focused on investigating the effect of localized cryotherapy on skin temperature and perfusion. The first part of the study was performed using commercially available CTUs to examine the dynamics of thermal and vascular response to localized cooling during and beyond the active cooling phase. The second part of this study concentrated on the investigation of the dose-dependent response of tissue perfusion to changing skin temperature where both variations in applied temperature and duration of application were considered. In addition to studying physiological response to skin cooling, the thermal profiles on the cooling pad from multiple CTUs were studied and the thermal uniformity of those pads was compared to each other. Since cold-induced vasoconstriction is considered a contributing factor for developing ischemic complications, methods to stimulate blood flow in tissue was also tested. In addition to reducing the chance of complications, intermittent blood flow stimulation might accelerate and improve the healing process by providing tissue oxygenation and delivery of nutrients and removal of toxic byproducts.

The results show that localized cooling produces a significant reduction in skin perfusion which lasts long after the removal of thermal stimuli independent of the type of CTU in use. A small study comparing the effect of localized cooling on knee and foot/ankle region showed no significant difference in extent of cold-induced vasoconstriction based on the body parts under the investigation. The results of dose-dependent study shows that a minimal drop in skin temperature by only 4˚C results in a significant reduction in skin perfusion and that this reduced skin perfusion further amplifies by additional decline of skin temperature. Similar to the previous study, the reduction in skin perfusion was shown to last long after cessation of active cooling.

Furthermore, a hysteresis response between skin temperature and perfusion was observed and compared among different experimental groups (see Appendix A). The outcome of this study will be prepared for publication at a future time. The study of thermal distribution on the surface of cooling pads associated with multiple CTUs showed a varying degree of nonuniformity which was a function of both cooling pad design as well as the device type. The nonuniformity of pad surface temperature signifies the importance of expressing the pad temperature in a range format as opposed to a single representative temperature.

Blood flow stimulation methods and results are presented in Appendix B. Three different methods to stimulate skin blood flow intermittently were investigated. The thermal stimulation was chosen as the method to reliably and reproducibly increase skin blood flow. Appendix C provides detailed explanation of the downsampling procedure of the raw data and presents data plots from an exemplar experiment.

Another important observation that I made based on the results of cryotherapy experiments was that the skin temperature varied widely in the treatment area and that this temperature variation was not necessarily related to temperature variation on the pad surface. Skin temperature distribution rather seemed to follow a certain anatomical pattern such that skin covering patella always exhibited much colder compared to its surroundings in cryotherapy experiment performed in the knee region with patella coverage (see Appendix D). Similar behavior was observed the foot cryotherapy experiments. This finding suggests that skin temperature measurement at a single point could not be a good representative of thermal conditions in the treatment region.

Appendix A

DOSE-DEPENDENCE OF COLD-INDUCED VASOCONSTRICTION

A set of experiments were designed to study the effect of applied temperature on tissue perfusion. The goal of these experiments was to investigate the dose-dependent response of tissue perfusion while facing different ranges of applied temperature. A Lauda-Brinkmann (LAUDA-Brinkmann, LP, Delran, NJ) water bath in conjunction with an Arctic Ice universal cooling pad (Pain Management Technologies, Akron, OH) were used to deliver water at desired temperature to the treatment site. The detailed description of the controlled skin temperature experiments are presented in Table A.1. These experiments were performed in a repeated measure format on 6 healthy adults (3 males), age (±SE) 22.5 ± 1.4 y and BMI (±SE) 23.4 ± 1.6 kg/m^2. There was at least one week of separation between two consecutive experiments performed on the same subject. The order of experiments remained the same for all subjects. The experiments were performed at 4 nominal cooling (27.5, 25, 20, and 15˚C) and one warming temperatures (37˚C). The cooling duration for experiments performed at 25 and 20˚C was set to either 20 or 60 min. For all other cooling or warming experiments, active thermal manipulation lasted for 60 min. The instrumentation procedures for these set of experiments follow the descriptions provided in Chapter 5. For all experiments, data was collected continuously throughout the baseline (30 min), the active cooling/warming (either 20 or 60 min), and the rewarming periods (120 min).

Experiment	Baseline Duration (min)	Cooling /warming Duration (min)	Recovery Duration (min)	Skin Temperature (°C)
25 °C – 60 min	30.2 ± 0.3	60.4 ± 1.4	121.8 ± 1.9	24.7 ± 0.2
20 °C – 60 min	30.2 ± 0.5	60.4 ± 0.3	122.8 ± 3.3	19.8 ± 0.2
15 °C – 60 min	30.1 ± 0.2	60.1 ± 0.2	123.7 ± 4.7	16.6 ± 1.1
27.5 °C – 60 min	30.1 ± 0.2	60.1 ± 0.2	121.8 ± 1.6	27.3 ± 0.1
37 °C – 60 min	30.4 ± 0.5	60 ± 0.2	123.4 ± 2	37.2 ± 0.1
25 °C – 20 min	30.2 ± 0.3	20.1 ± 0.2	123.4 ± 1.7	23.8 ± 0.8
20 °C – 20 min	29.6 ± 1.1	20.3 ± 0.1	122.2 ± 2.4	21.2 ± 1.1

Table A.1 Skin perfusion caused by change in skin temperature.

Table A.2 contains information regarding the duration of each active thermal manipulation as well as minimum skin temperature and CVC achieved during each of these experiments. The temperature values are based on the average of temperature measured using P1 and P2 perfusion probes. The presented CVC values are either based on the average values measured using P1 and P2 or what was measured using P3. The pick detection depth for P1 and P2 is at 0.5 mm and for P3 at about 2 mm. The numbers presented are the average values and standard deviations.

Duration (± SD) (min)	Temperature (± SD) (°C)	Average CVC Based on P1 and P2 Measurements (± SD) (% of Baseline)	CVC Calculated Based on P3 Measurements (± SD) (% of Baseline)
Baseline	31.2 ± 1.3	100	100
60.4 ± 1.4	24.7 ± 0.2	53.9 ± 10.5	51.6 ± 11.2
60.4 ± 0.3	19.8 ± 0.2	31.4 ± 4.8	29.8 ± 7.2
60.1 ± 0.2	16.6 ± 1.1	26 ± 11.1	24.8 ± 5.2
60.1 ± 0.2	27.3 ± 0.1	59.7 ± 16.1	56.6 ± 18
60 ± 0.2	37.2 ± 0.1	414.8 ± 229.8	266.8 ± 81.2
20.1 ± 0.2	23.8 ± 0.8	46.7 ± 11.4	45.1 ± 21
20.3 ± 0.1	21.2 ± 1.1	39.1 ± 10.2	43.6 ± 14.1

Table A.2 Detail information regarding each experimental group.

The results of a pairwise comparison between minimum CVC achieved as a result of the cooling experiments are presented in Table A.3. The pairwise comparisons were made based on the statistics derived from the Friedman test. The significant pairwise comparisons are marked with X at a significance level of $p \leq 0.05$.

EXP	15 °C – 60 min	20 °C – 60 min	25 °C – 60 min	27.5 °C – 60 min	20 °C – 20 min	25 °C – 20 min
15 °C – 60 min			X	X		
20 °C – 60 min				X		
25 °C – 60 min	X					
27.5 °C – 60 min	X	X				
20 °C – 20 min						
25 °C – 20 min						

Table A.3 Results from pairwise comparison based on Friedman test

A case-control study was performed using the Dunnett's test to investigate the persistence of vasoconstriction during the passive rewarming period by comparing the CVC values from the first 5 min of rewarming to all other time points. The result showed no significant increase in perfusion for all time points and all the experimental groups with the exception of 110, 115, and 120 min for cooling to 20ºC for 60 minutes.

Figure A.1 represents minimum CVC achieved for any given skin temperature with the exception of 37˚C where it denotes the maximum CVC. All presented CVC values are normalized to the baseline measurements. Data bar representing perfusion with skin temperature of 37˚C was excluded from Figure A.1b to improve resolution. The

figure shows an increasing trend in the extent of vasoconstriction by further reduction of skin temperature implying a dose-dependent response between skin perfusion and temperature. Even though a decreasing trend in skin perfusion is observe by lowering applied temperature, not all the differences in skin perfusions are significant. As mentioned earlier, all significant differences are marked in Table 3.

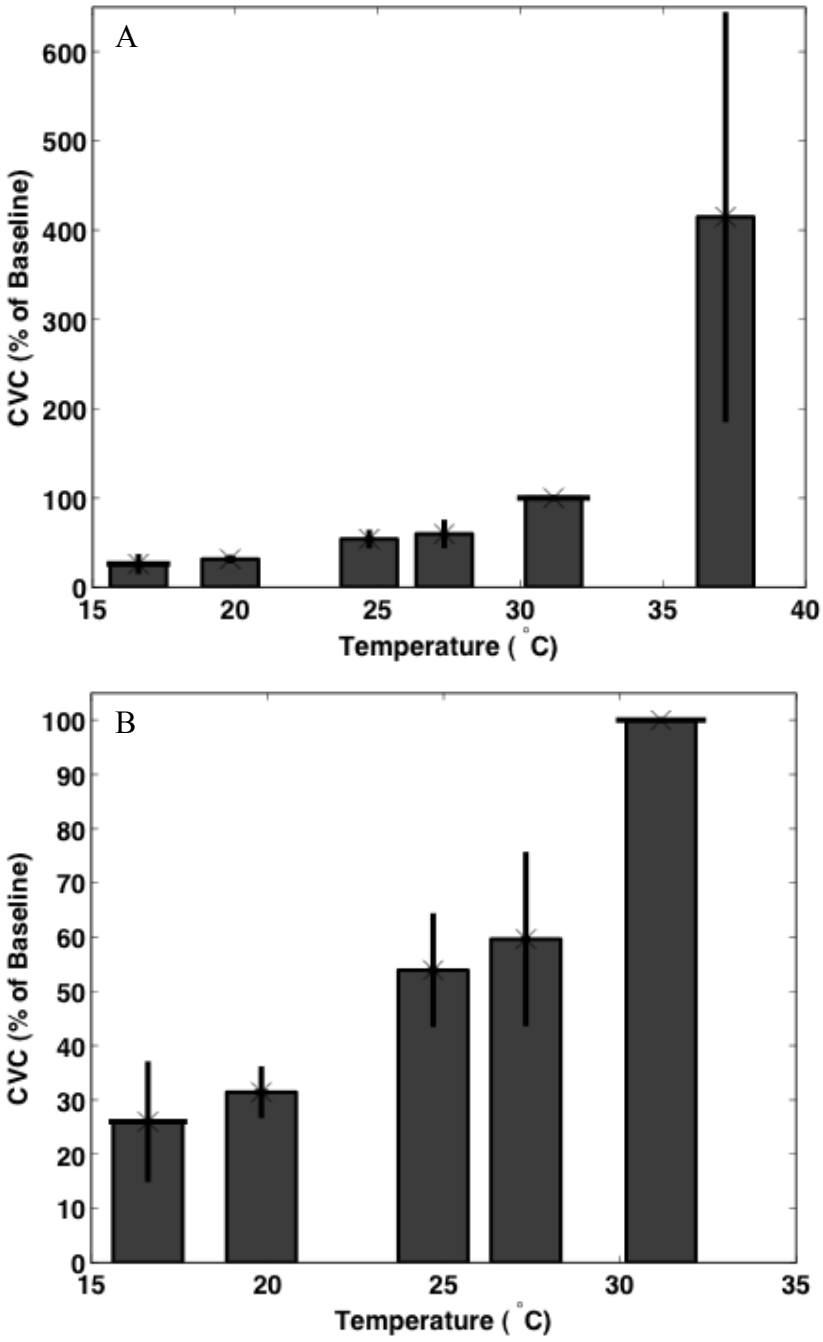

Figure A.1. Minimum CVC as a function of applied temperature for all cooling and heating experiments (A) and cooling only experiments (B). Error bars represent standard error of mean for both temperature and CVC. All CVC values are normalized to the baseline.

Figure A.2 compares the minimum CVCs for cooling skin to nominal values of 20 or 25˚C lasting for either 20 or 60 min. There was no significant difference in minimum CVC at skin temperature of 25ºC when active cooling lasted for either 20 or 60 min. When cooling to 20ºC there was a significant difference between the minimum CVCs given the two possible duration of active temperature manipulations but there was also a significant difference between the applied temperatures therefor no statistical inference could be made.

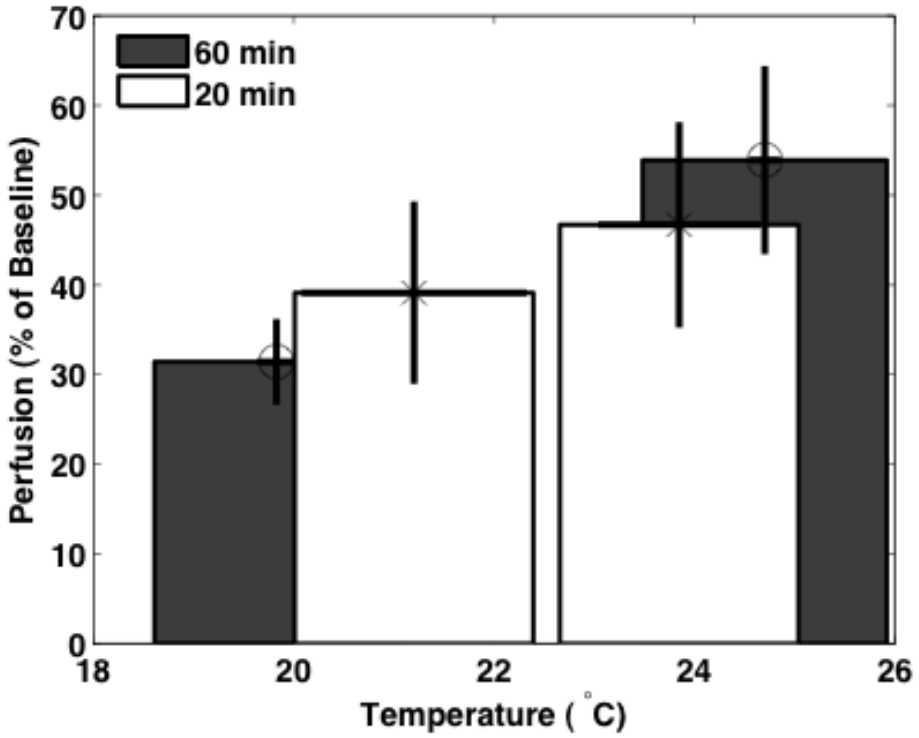

Figure A.1. The effect of cooling duration on minimum CVC based on average measurements made by P1 and P2. Error bars represent standard error of mean for both temperature and CVC.

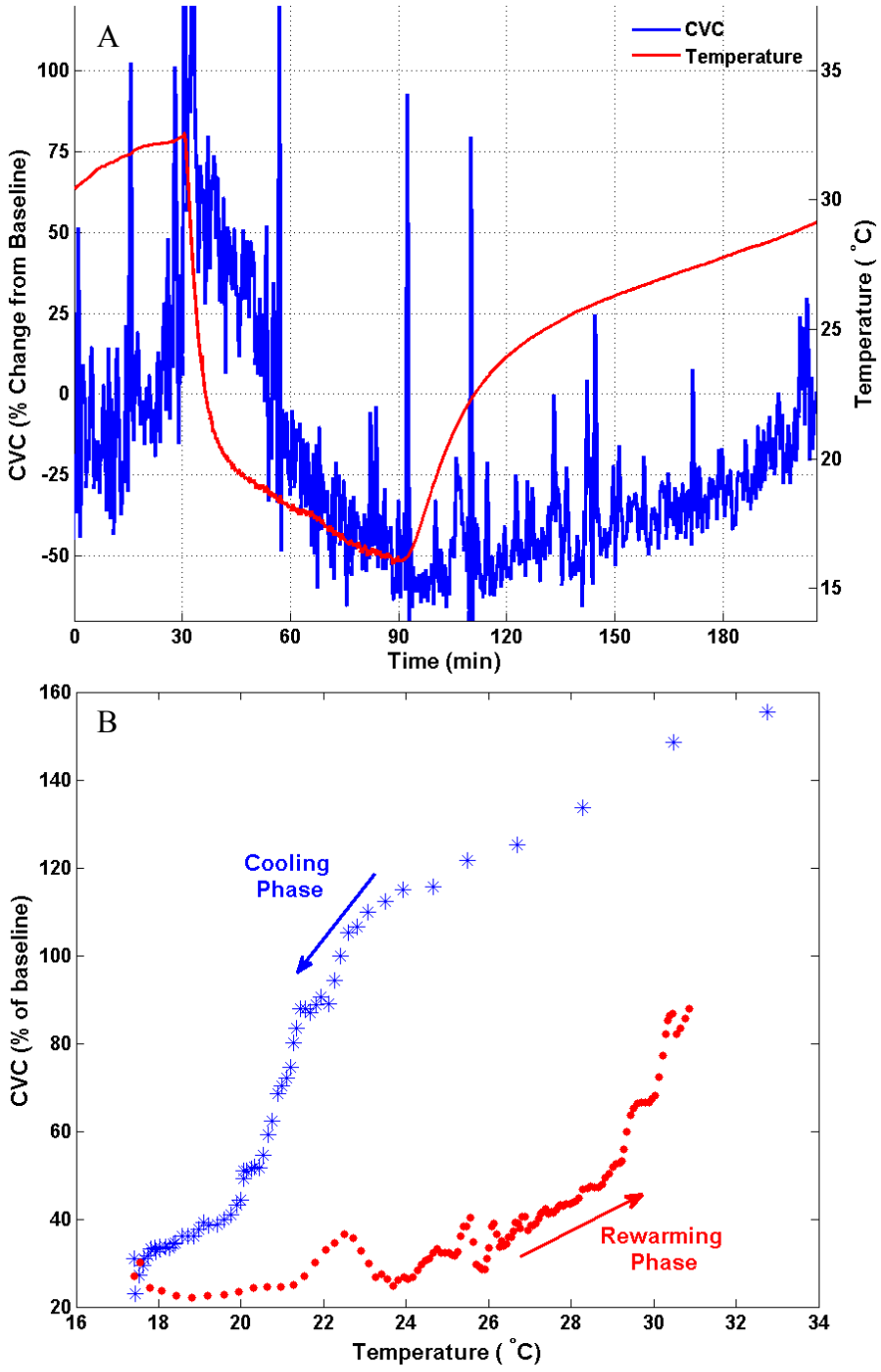

Figure A.2. CVC and skin temperature data from a sample cooling experiment (A) and the temperature/CVC hysteresis plot related to the same experiment (B).

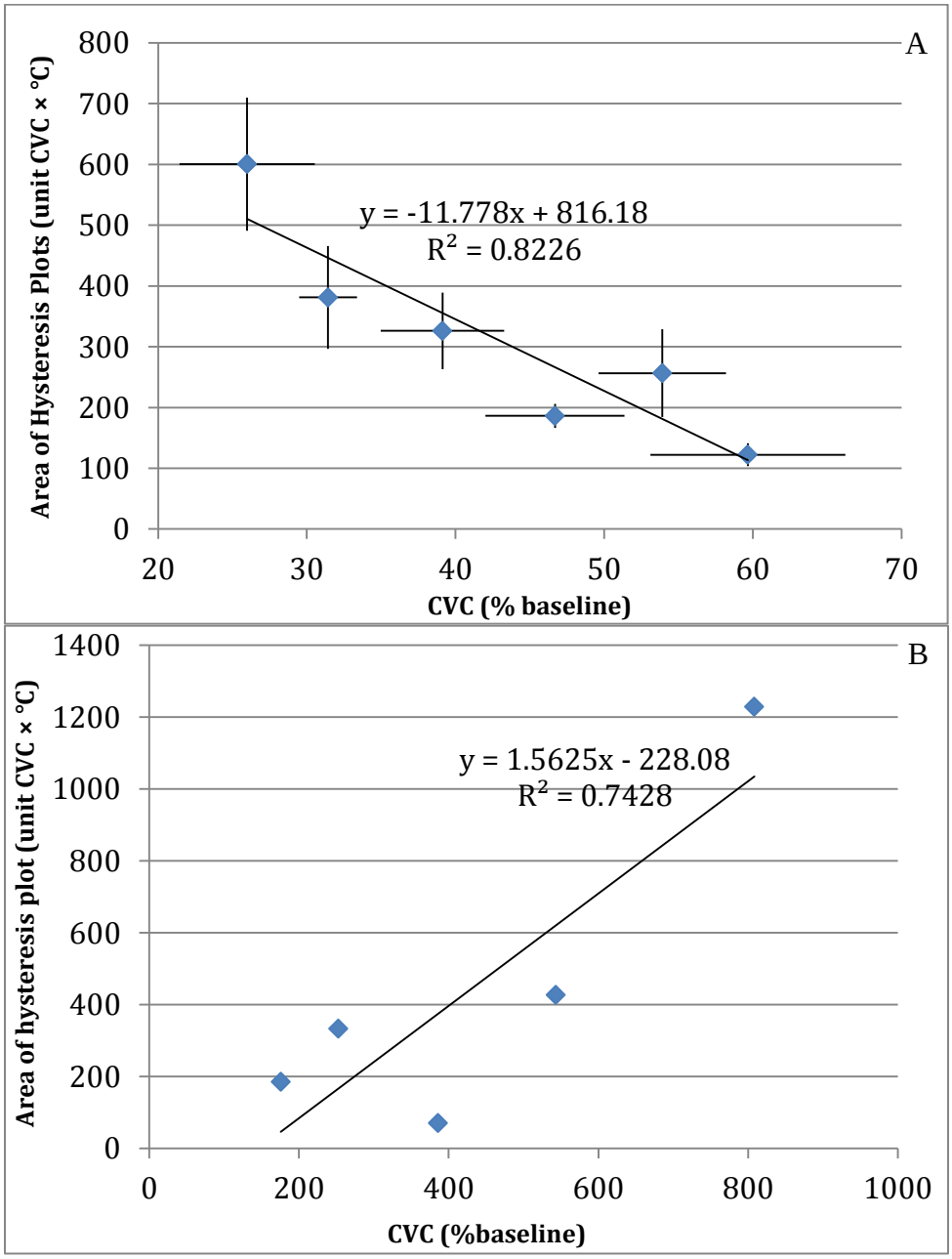

Figure A.3. The area of CVC/Temperature hysteresis plots as a function of minimum CVC for the active cooling (A) and warming (B) experiments.

The data plots presented in Figure A.3a show skin temperature and CVC in response to localized cooling from an exemplar experiment. This experiment was composed of 30 min of baseline, 60 min of cooling, and 120 min of passive rewarming. As it can be seen CVC follows the reduction in skin temperature during cooling much more closely than its increase during the passive rewarming phase. A plot of CVC vs skin temperature during cooling (blue stars) and passive rewarming (red dots) is presented in Figure A.3b. The figure shows an evident hysteresis between CVC and skin temperature. Similarly, hysteresis plots of CVC vs skin temperature were created for each experiment and their areas were calculated. Next the average and standard error for areas of the hysteresis plots for each experimental group were computed. Figure A.4a shows the area of the hysteresis plots versus the minimum CVC achieved for all cooling experiments and Figure A.4b shows the area of the hysteresis plots for the heating experiments across different subjects. The area of the hysteresis plots appears to be linearly related to the minimum CVC achieved. A similar relationship seems to exist between the area of hysteresis plot and the amount of thermal exchange from the skin surface during the cooling (Figure A.5) and the applied skin temperature (Figure A.6). Figure A.6 confirms a dose dependent response for the area of the hysteresis plots to applied skin temperature. The hysteresis between perfusion and skin temperature was also observed at a single experiment with gradual skin cooling and rewarming implying that what we are measuring is a true hysteresis and not a rate-dependent one. Further experiments are needed to evaluate and compare the extent of hysteresis in fast and gradual cooling/rewarming scenarios.

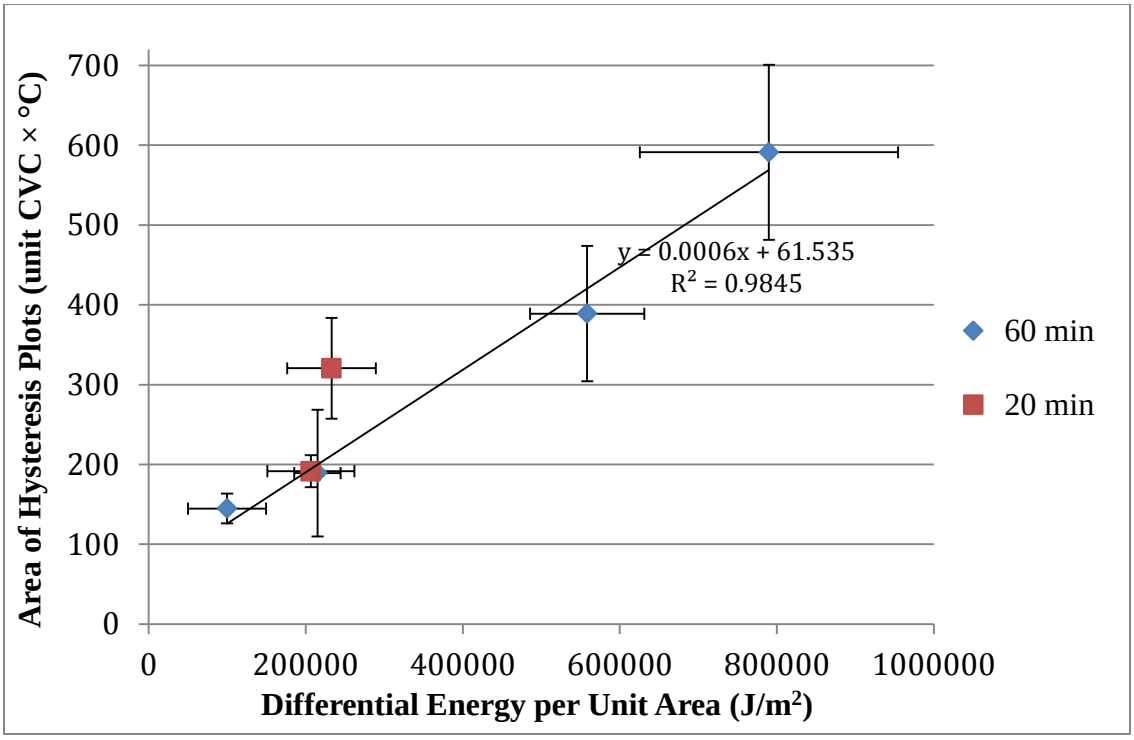

Figure A.4. Area of perfusion/temperature hysteresis plots vs differential energy transfer per unit area during cooling and rewarming periods.

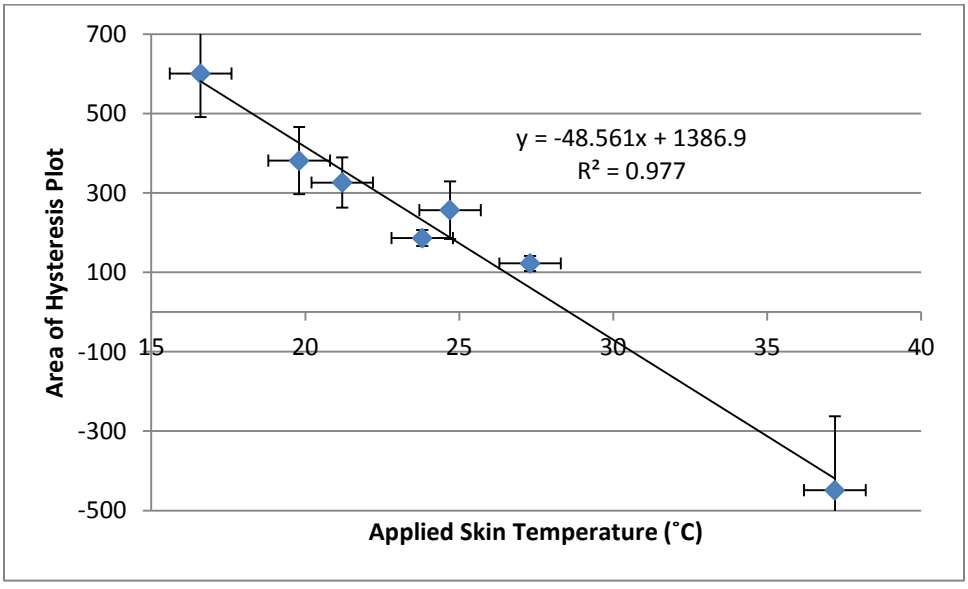

Figure A. 6 The area of perfusion/temperature hysteresis plots as a function of applied temperature.

Appendix B

METHODS TO STIMULATE BLOOD FLOW IN SKIN AT A VASOCONSTRICTED STATE

The goal of this study was to stimulate blood flow in skin following a cooling session and after vasoconstriction has taken place. Different methods were used to achieve this goal including the application of electrical stimulation to skin in the form of TENS or EMS, pneumatic compression (IPC) to ipsilateral foot or leg, or thermal stimulation in the form of increasing skin temperature.

Intermittent pneumatic compression (IPC) devices are commonly prescribed to reduce chances of deep vein thrombosis (DVT) and possible thromboembolism. IPCs are also used in peripheral arterial disease to improve blood flow. The sequential compression of lower extremities improves emptying of veins in the lower extremities and an increase pressure differential between arteries and veins, which causes an increase in arterial blood flow in the region [108]. Abu-Owen and colleagues reported increase in foot skin blood perfusion upon use of IPC in the foot region when subject was in seated position [51]. Morgan, et al. suggest that applied shear stress on vascular endothelial cells due to compression results in release of endothelial-derived relaxing factor (EDRF) which in turn causes relaxation of arterioles and reduced peripheral vascular resistance and increased blood flow [109].

Transcutaneous electrical nerve stimulation (TENS) and electrical muscle stimulation (EMS) function by applying electrical signal to skin surface at or below intensities that cause muscle contraction. When the electrical pulse is applied at high frequency and low intensities it results in nerve stimulation whereas at low frequency and higher intensities causes muscle contraction. TENS is used in management of chronic pain. Electrical stimulations in both regimens are used to improve blood flow to the tissue.

Since the LDF system used for measuring perfusion is laser Doppler based, any movements in the measurement area such as those caused by muscle contractions results in increase in perfusion signal which could mask any true increases in perfusion. TENS at low frequency and high intensity revealed an increase in perfusion signal but it was not possible to distinguish the increase in signal due to true increase in skin perfusion from and increase caused by movement resulted from muscle contraction therefore no conclusion on the effectiveness of using electrical stimulation in increasing tissue perfusion at high intensity and low frequency was achieved. No significant increase in skin perfusion was observed as the result of electrical stimulation of tissue at other frequency/intensity combinations. Similarly, it was impossible to distinguish the source of increase in perfusion signal while using IPC on the foot or leg and as such no conclusion was made regarding its effectiveness in promoting skin perfusion. Moreover, in some occasions no significant increase in perfusion was detected using IPC on either foot or leg. Unlike electrical stimulation of tissue or using pneumatic compression on the foot or leg which were inconclusive in increasing skin perfusion, thermal stimulation of skin successfully resulted in increasing skin perfusion while in a vasoconstrictive state following cold application. Furthermore, subsequent cold application showed that the skin did not lose its vasoconstrictive capabilities.

The details for an experiment involving electrical stimulation of tissue are presented in Table B.1. In this experiment, the electrical stimulations were applied using an LG-TEC combo TENS/EMS unit (LGMedSupply, Cherry Hill, NJ). This experiment was composed of 23 excitation events throughout which the electrical pulse intensity, duration, frequency or mode were varied. The pulse mode is determined by the shape of the pulse and it can be constant over time or applied in bursts (burst mode), have a uniform (normal mode) or crescendo-decrescendo profile (SD1 and SD2 modes), or have

a frequency/pulse-width modulation (modulation mode). A sample perfusion data for this experiment and a picture presenting the waveform of the TENS module are presented in Figure B.1. The events marked with numbers 1-7, 19, 20, and 23 were all associated with some degree of muscle contractions. All other excitation events took place at lower intensities and did not result in a visible change in the perfusion signal. This experiment did not include any active change in skin temperature.

Event	Mode	Frequency (Hz)	Intensity
#1	Normal	4	6
#2	Normal	4	6
#3	Normal	4	6
#4	Normal	4	5
#5	Normal	4	4
#6	Normal	4	4-5
#7	Normal	4	4-5
#8	Normal	30	4
#9	Normal	30	3
#10	Normal	30	3-4
#11	Normal	30/ 30 s on 30 s off	3-4
#12	Normal	150	3-4
#13	Normal	150/ 15 s on 15 s off	3-4
#14	Normal	150	4
#15	Normal	150	4-5
#16	Burst	5	4
#17	Burst	0.5	4
#18	Modulation	150/ 300	4
#19	Modulation	4/ 300	5
#20	SD1	4/ 300	6
#21	SD1	150/ 300	4-5
#22	SD2	150/ 300	4-5
#23	SD2	30/ 300	5-6

Table B.1 Details regarding different episodes of a blood flow stimulation experiment using TENS.

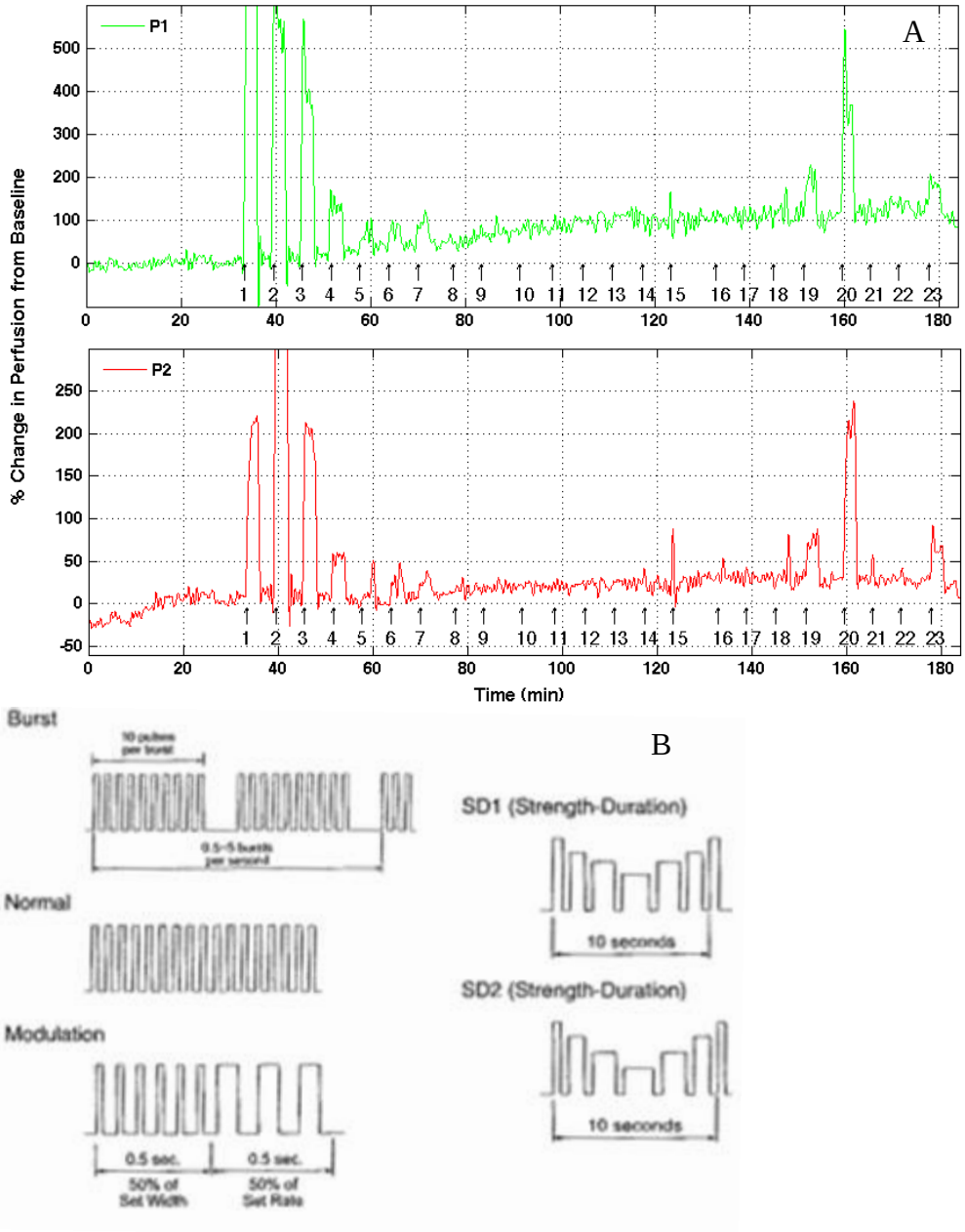

Figure B.1. The effect of electrical stimulation on skin perfusion measured at two different locations (A) and the waveform of TENS module (B). Numbers and arrows on perfusion plots mark the starting point of each stimulation event. The setting of electrical stimulation was changed from one event to the next as is described in Table B.1. Each excitation event lasted for 3 min with 3 min separation between two consecutive episodes.

Figure B.2 shows the instrumentation and the results of the leg compression using an IPC unit (Kendall SCD Sequel 6325 Compression System; Covidien, Dublin, Ireland). Figure B.2 demonstrates the effect of IPC of the leg on skin perfusion in the foot (Figure B.2a) and ankle (Figure B.2b) regions downstream to the location of IPC sleeve (knee length, Kendall SCD Sleeve 5329; Covidien, Dublin, Ireland). Probe A and B were expected to show the differential effect of leg compression on skin blood perfusion in an area actively cooled (the foot; probe A) and a control location (the ankle; probe B) were no active change in temperature was applied. Neither of the two perfusion probes was covered with the IPC sleeve. In Figure B.2 the double arrows delineate the duration of each pneumatic compression cycle. Red and green stars represent perfusion during cooling and passive rewarming periods, respectively, and each star defines the median of perfusion signal for a 5-minute stretch of data straddling the time point it represents. Skin perfusion under the cooling pad showed a significant reduction during the cooling phase. A similar reduction in perfusion in the control location was not observed. As it can be seen perfusion seems to increase while IPC is actively applied but due to aforementioned problem in recognizing the source of increase in perfusion signal we were not able to make further inferences about the skin perfusion from this data.

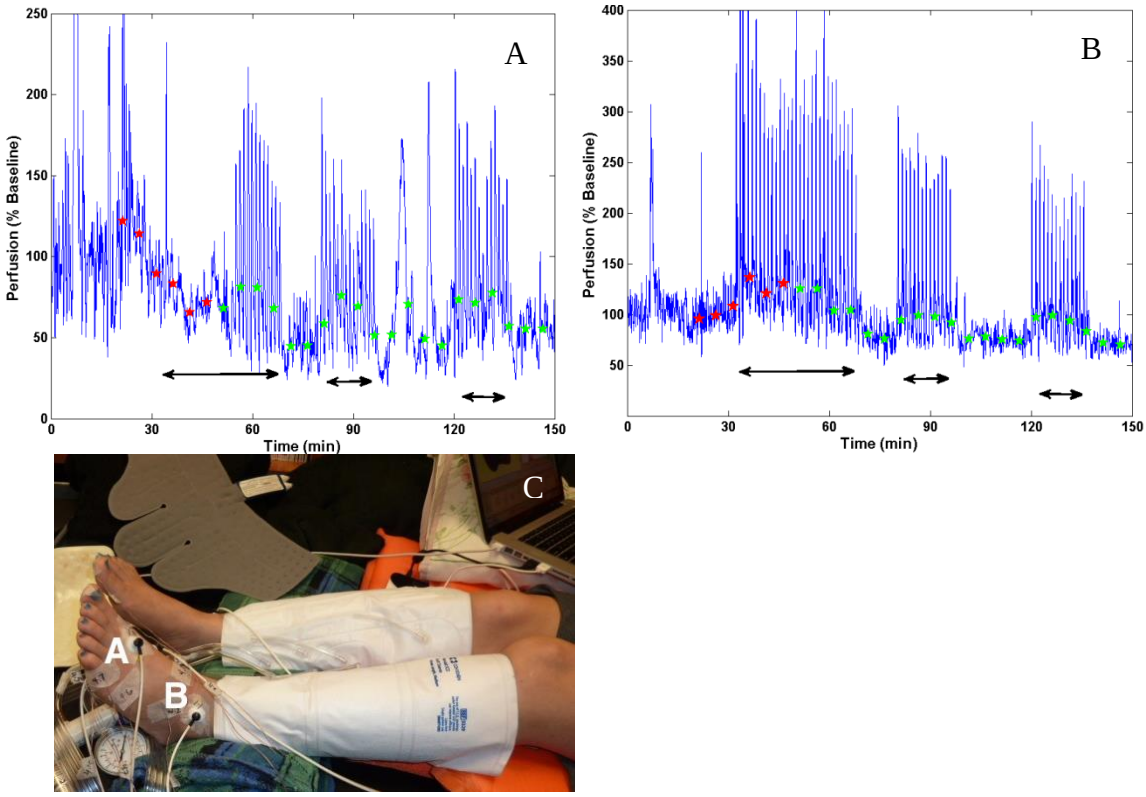

Figure B.2. The effect of IPC application on skin perfusion, under the cooling pad (A), and in a control location (B) where it was affected by the IPC application but not being cooled directly. Instrumentation for the same experiment (C) after the IPC sleeve and the perfusion probes were applied, and before the cooling pad was put on. The foot and all the instrumentation administered to the foot including the probe A were covered with the cooling pad and were actively cooled during the experiment.

As it was mentioned earlier, thermal stimulation of skin resulted in a significant increase in skin perfusion. This increase in skin perfusion was replaced with a reduction upon subsequent cooling. Perfusion (top panel) and temperature (bottom panel) data from a sample experiment with thermal stimulation is presented in Figure B.3. This experiment included three 30-minute long cooling cycles separated by active heating phases lasting for 5, 10 and 15 min, respectively. The 10 and 15 min cycles seemed to result in a substantial increase in perfusion. Skin resumed its vasoconstrictive state during each cold application that follows the active rewarming cycles.

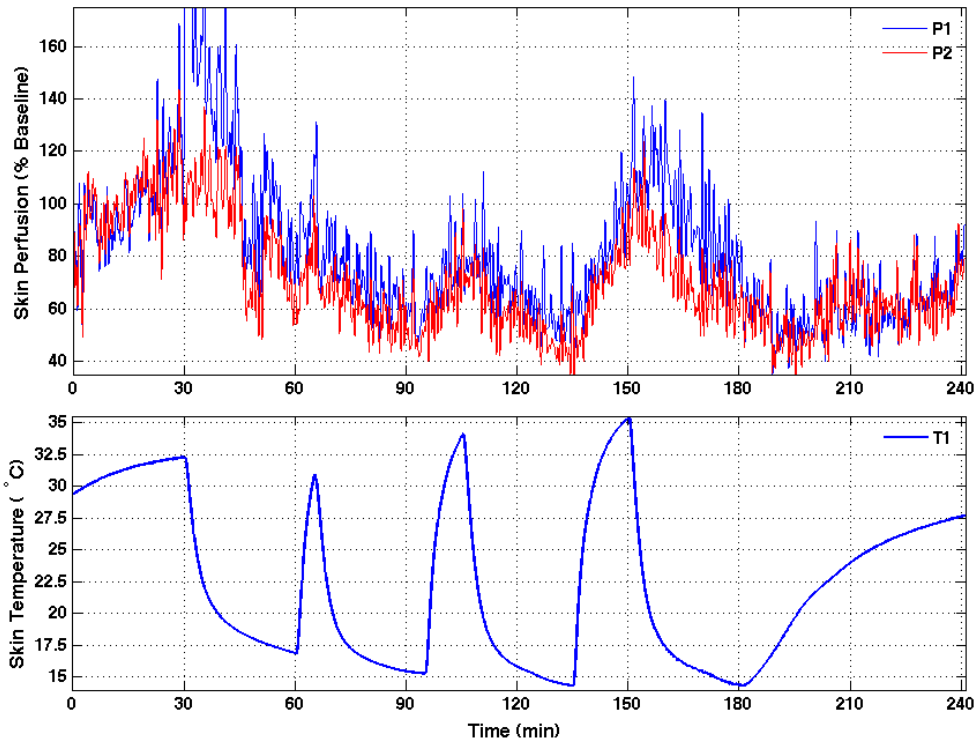

Figure B.3. A sample active cooling/rewarming experiment

The results from other active cooling/warming experiments are presented in Figures B.4-6 where percent change in skin blood perfusion over time is presented in the top panel and the skin temperature in the bottom. The experiment presented in Figure B.4 included three 30-minutes cooling periods separated by 30-min active warming periods. Each of these active warmings resulted in a pronounced increase in skin perfusion such that the following cooling periods were not able to resume the extent of vasoconstriction achieved during the first cooling. Figure B.5 includes only one heating period which lasted for 10 minutes. T1, T2 and T3 represent temperatures measured by P1, P2, and P3 perfusion probes, respectively. In this study, three of the perfusion probes (P2-4) were applied to a region which was exposed to both heating and cooling. P1 perfusion probe was used to measure perfusion in an area that was only cooled. During the active

warming, T1 shows a slight increase in temperature which is due to parasitic heat transfer from the environment and deeper tissue while T2 and T3 show a pronounced increase in temperature. Data presented in Figure B.6 shows a similar result to the other studies. In this experiment each active warming episode lasted for 4-5 minutes with an active cooling of variable duration separating each two consecutive warming. Each warming episode increased the skin temperature to its precooling values and caused a prominent increase in skin blood perfusion. Thermal stimulation data presented here demonstrates the effectiveness of active heating in stimulating skin blood flow. Further study is needed to derive any statistical inferences from the data. Furthermore, the onset of the first active warming episode in respect to the start of cooling as well as the general duration of each episode, the interval and frequency that active warming period should take place, and the applied temperatures need to be defined in order to optimize the therapeutic effect of active warming. Clinical studies need to be designed to evaluate the effect of thermal stimulation in improving the healing process.

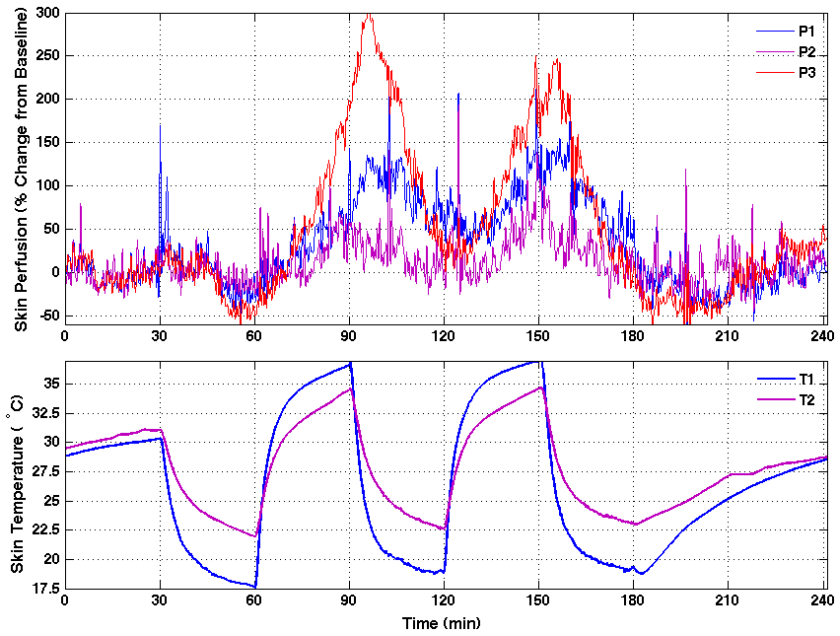

Figure B.4. An active cooling and warming experiment with equal durations of heating and cooling.

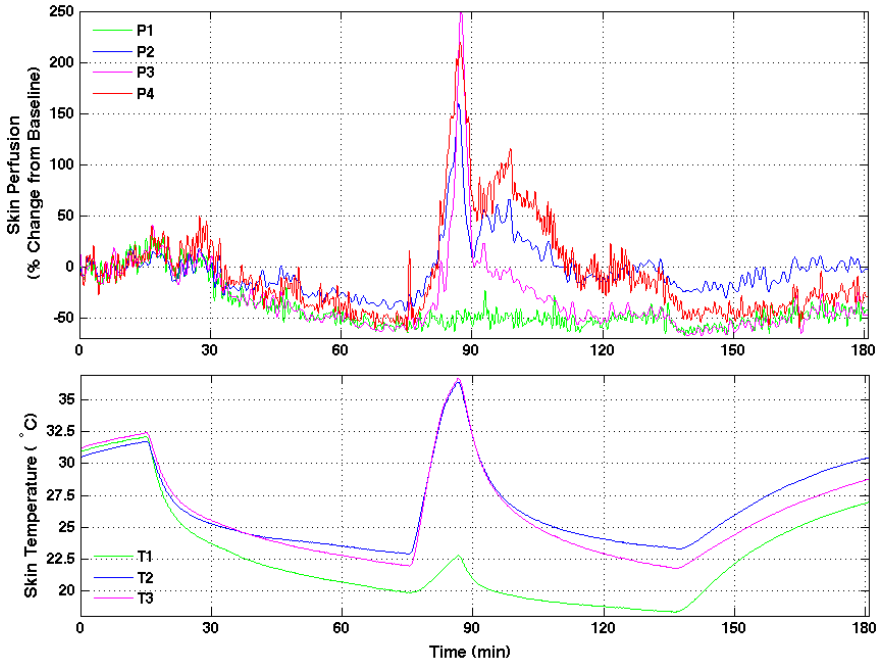

Figure B.5. An active cooling (P1-P4) and warming (P2-P4) experiment. P1 was used as a control to isolate the effect of active warming.

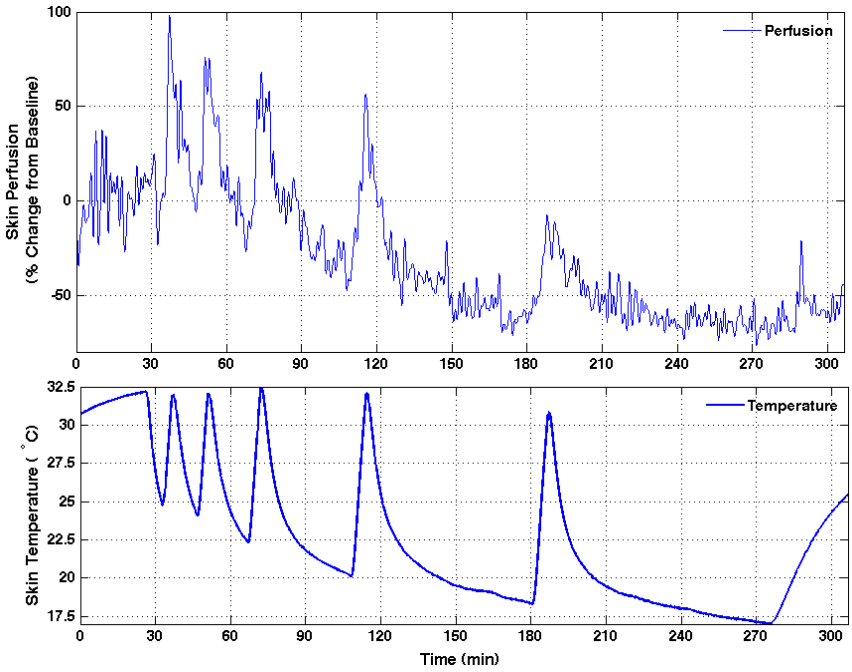

Figure B.6. An active cooling and warming experiment with a saw tooth pattern of heating

Appendix C

DATA EXTRACTION PROCEDURE

The procedure for data extraction was described shortly in Chapters 4 and 5. A detailed explanation of this procedure is presented below. The first step of data extraction is to set the start and end of cooling cycle. This is the only step that a human input is needed. These start and end point are manually recorded during each experiment and inputted into the body of data processing program and are marked automatically on the temperature plot representing the temperature of the cooling pad. An example temperature plot is presented below with the start and end point of cooling marked with magenta stars (Figure C.1). The 3rd star marks the end point of data collection. The person in the charge of data extraction can make corrections by adjusting these points via marking the start and end of cooling phase. These adjusted points are represented by black squares. The numbers next to each square are its corresponding coordinates where x = time (s) and y = temperature (˚C). The second square from the left marks the time point where pad temperature seems to reach a steady state. The beginning and end of each cooling cycle are marked with magenta-colored stars based on these adjusted coordinates on all future data plots. All the future steps are performed by the program automatically. First, the perfusion data during the cooling and rewarming cycles are divided into 5-min segments and the last 5 min of baseline is also defined. Then the median of perfusion for each segment is calculated. The filled circles on all future data plots mark the median of perfusion for each data segment. As it can be seen the median value is a good identifier of trend in data and is blind to noise. A similar procedure was used to extract temperature data with the exception that data segments were each 1-min long and that average temperature was used instead of the median to find the representative value for each segment. The first black circles from the left on each plot

shows the baseline representative value and the other two circles show the global min and max value for each quantity. The red and green circles mark the cooling and passive rewarming periods, respectively. Data plots presented in this segment are from a cryotherapy experiment with 30 min of baseline, 60 min of cooling and 120 min of passive rewarming. The P1, P2 and P3 perfusion probes were used to measure perfusion under the cooling pad. The perfusion and temperature data measured using these probes are presented in Figure C.2-4 and Figure C.7 and C.8. The skin blood perfusion and temperature at two control sites was measured using O1 (the contralateral knee; Figure C.5 and C.9) and O2 (ipsilateral dorsal foot; Figure C.6 and C.10) perfusion probes.

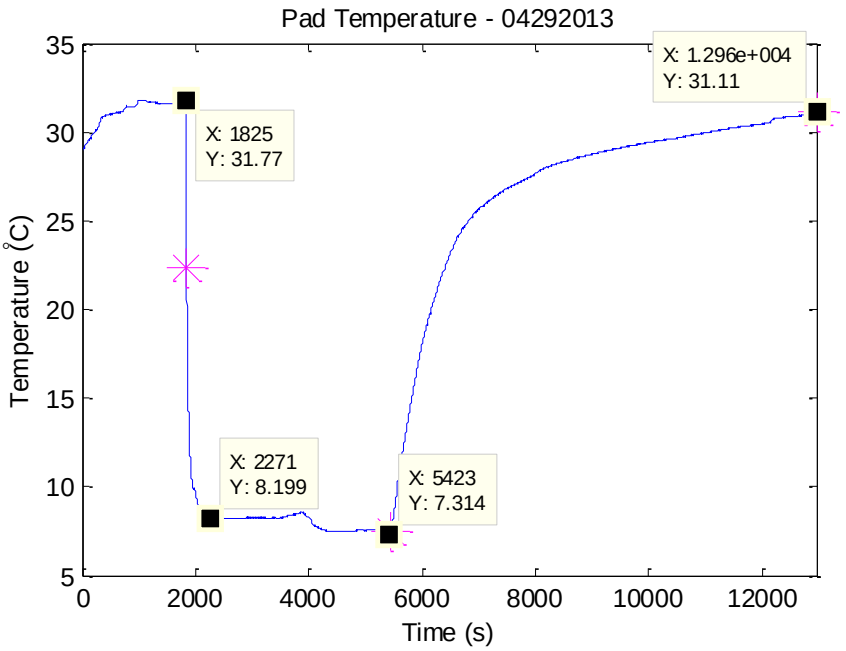

Figure C.1 Cooling pad temperature. The magenta-colored stars from left to right mark the start and the end of the cooling phase and the end of data collection. The locations of the stars are based on times recorded while running the experiment. The black squares from left to right mark the start of cooling, start of steady state for the pad temperature, the end of cooling, and the end of data collection. The numbers next to each square show the time (s) and temperature (ºC) at that point. The locations of the black squares are set by the user.

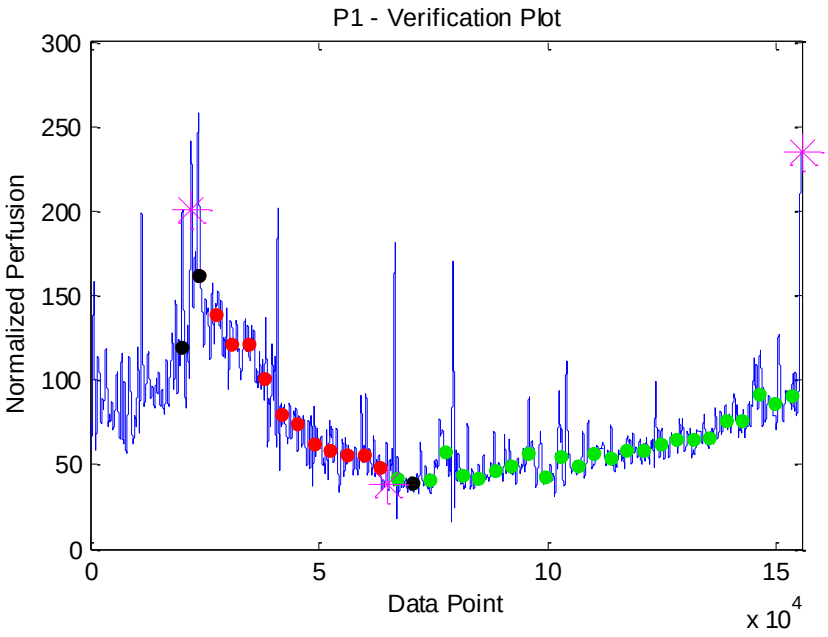

Figure C.2 P1 verification plot. The circles define the perfusion values at each point. The stars, from left to right, mark the beginning, and end of cooling, and end of data collection. Black circles are represent baseline, and the global minima and maxima. Red and green circles are from extracted perfusion values from the cooling and rewarming period. 12data points = 1 s

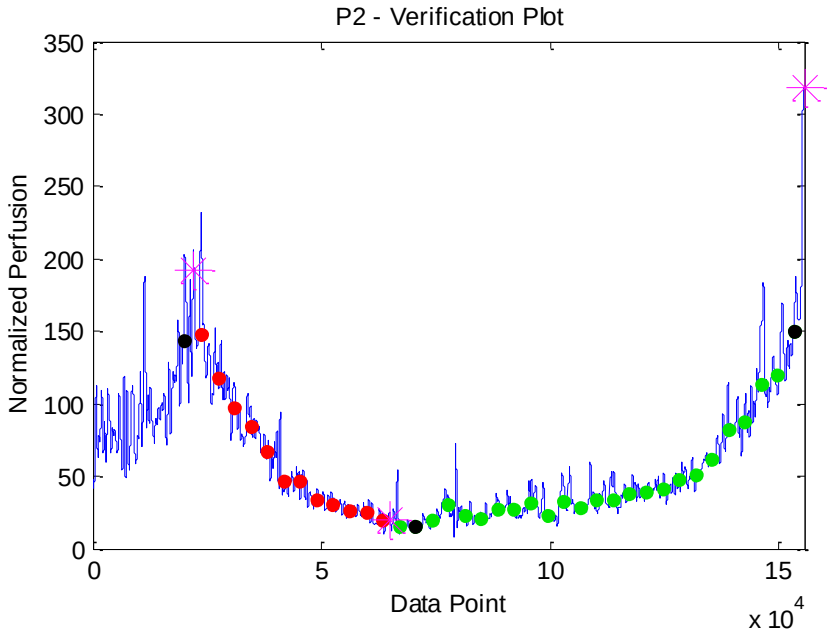

Figure C.3 P2 verification plot. Please refer to caption for Figure C.2 for details.

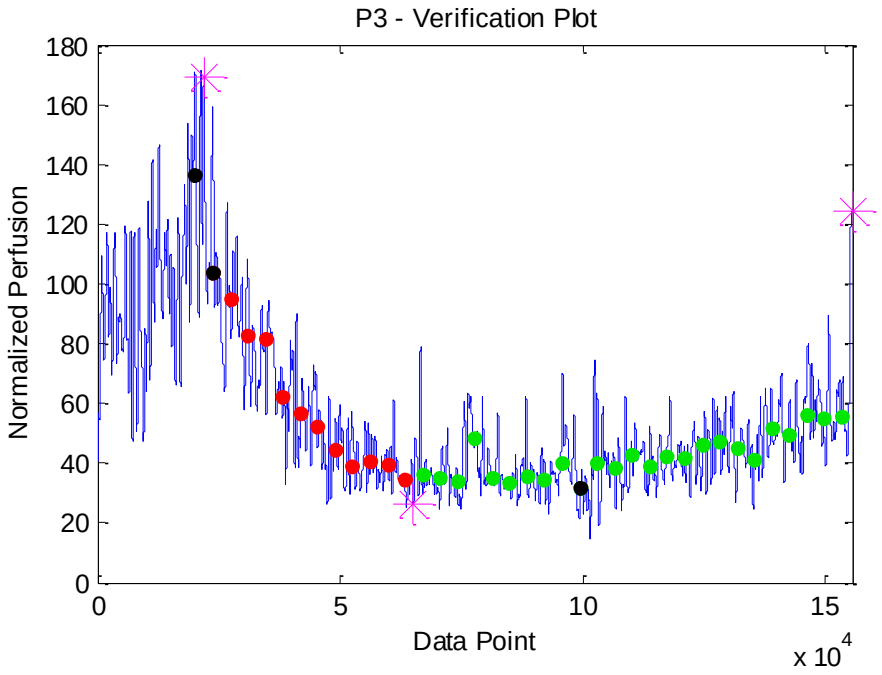

Figure C.4 P3 verification plot. Please refer to caption for Figure C.2 for details.

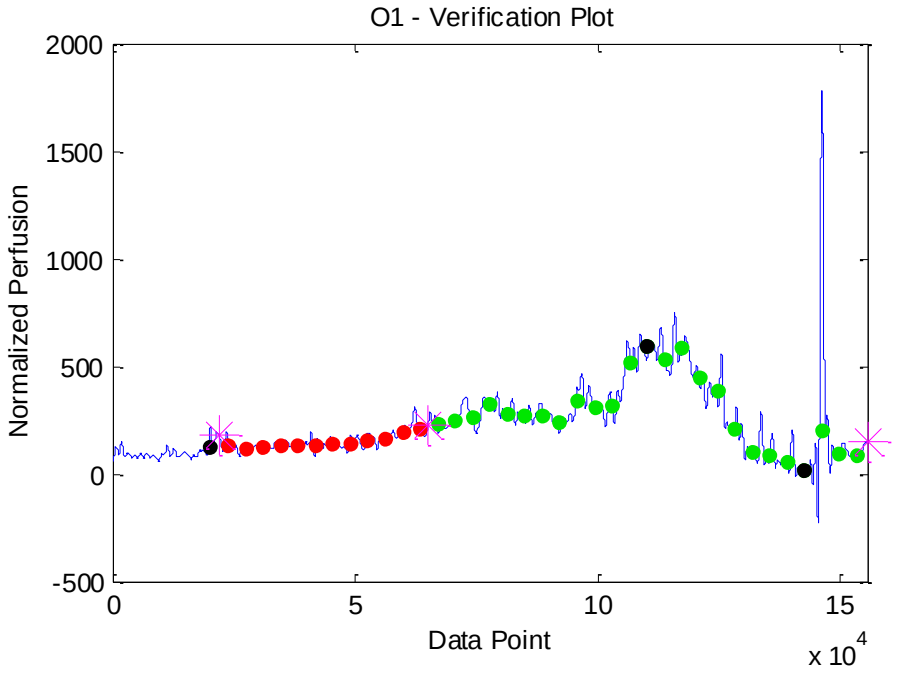

Figure C.5 O1 verification plot. Please refer to caption for Figure C.2 for details.

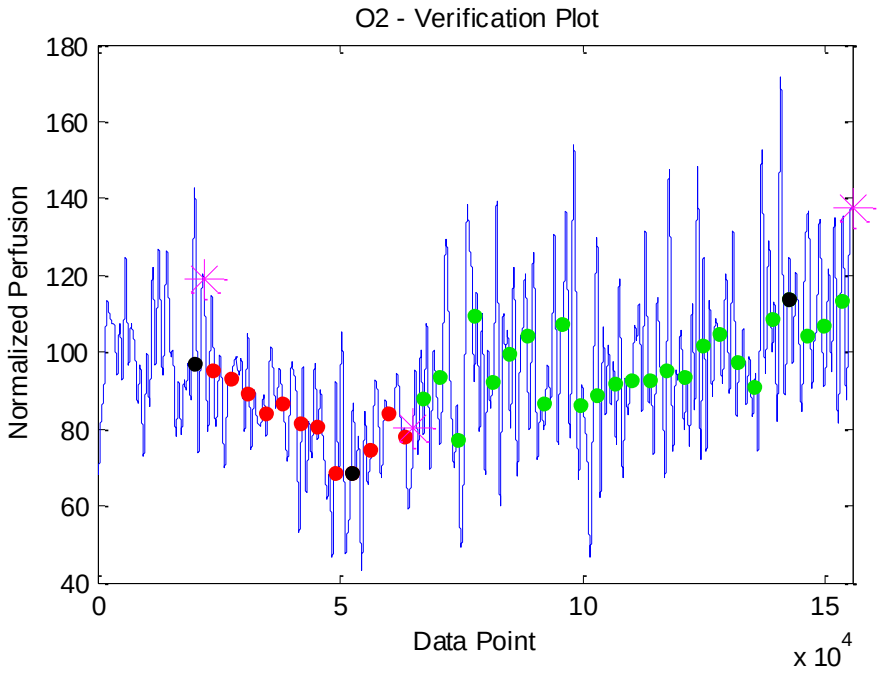

Figure C.6 O2 verification plot. Please refer to caption for Figure C.2 for details.

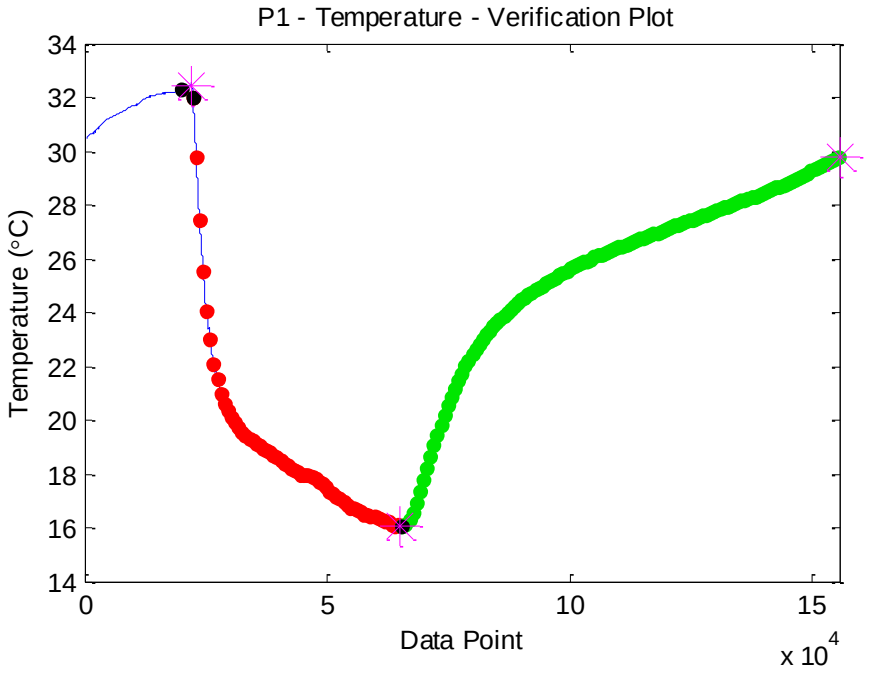

Figure C.7 The verification plot for temperature measured by P1 perfusion probe. Please refer to caption for Figure C.2 for details.

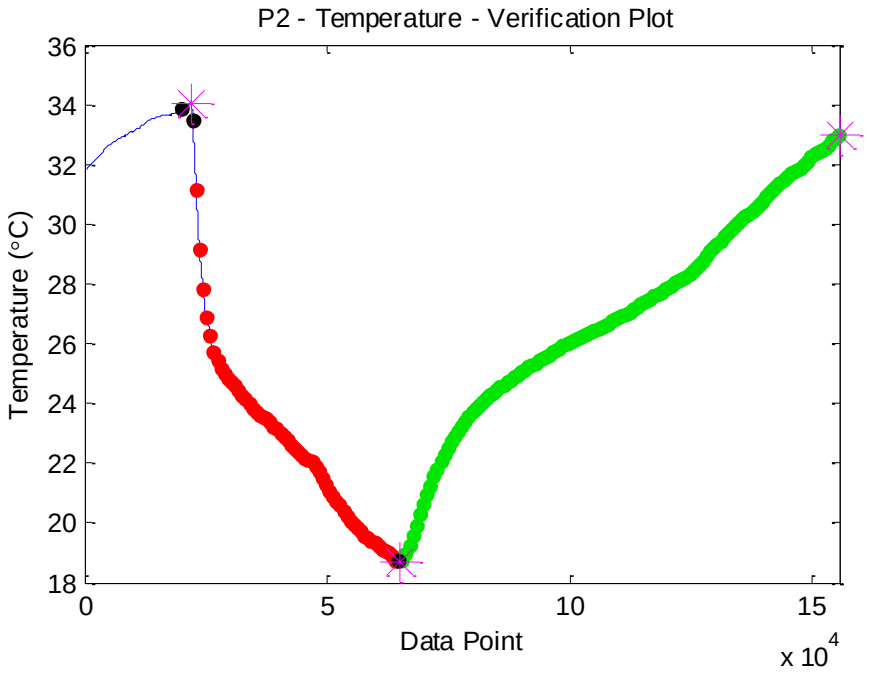

Figure C.8 The verification plot for temperature measured by P2 perfusion probe. Please refer to caption for Figure C.2 for details.

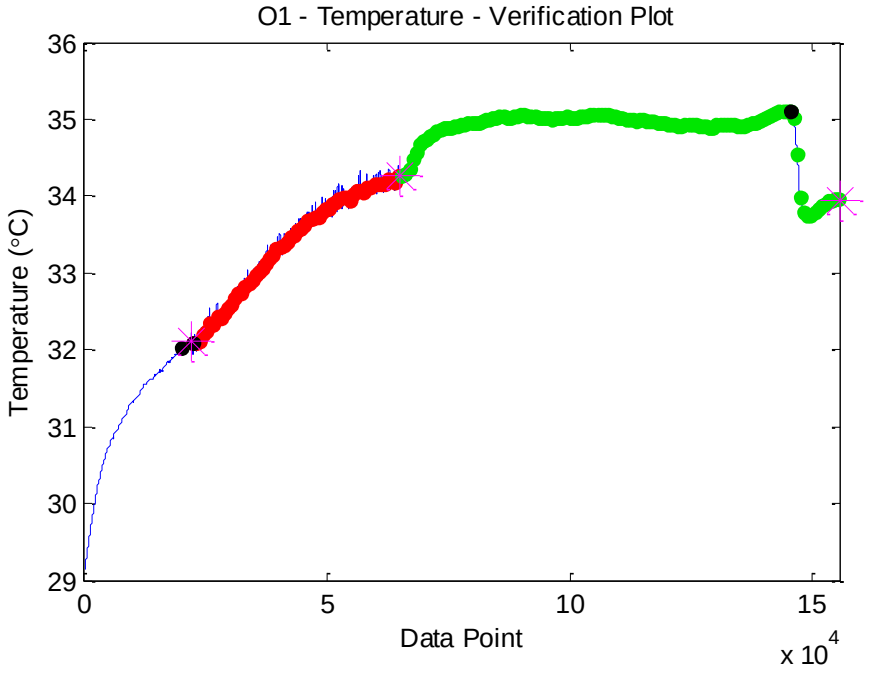

Figure C.9 The verification plot for temperature measured by O1 perfusion probe. Please refer to caption for Figure C.2 for details.

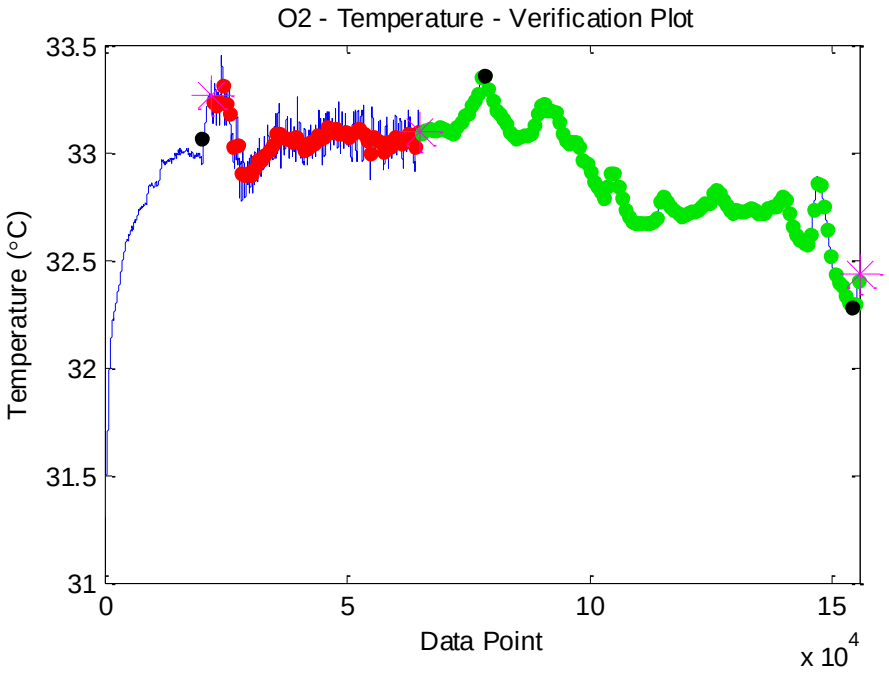

Figure C.10 The verification plot for temperature measured by O2 perfusion probe. Please refer to caption for Figure C.2 for details.

Appendix D

NON-UNIFORMITY OF SKIN TEMPERATURE UNDER THE COOLING PAD

The measurements of skin temperature in response to localized cooling demonstrated a substantial non-uniformity of skin temperature which did not follow the pattern of cooling on the cooling pad such that the coldest area on the skin did not follow the coldest region on the pad. More importantly, the highest and coldest area on the skin were significantly different from each other.

Concurrent measurement of skin temperature using IR imaging and thermocouple readings

Figure D.1-3 present information regarding knee skin following a 60-min long cooling experiment using EBI cryotherapy unit (EBI, LLC., Parsippany, NJ) and square cooling pad. The experimental protocol and instrumentation were similar to those described in Chapter 4 and 5. The skin temperature measurements were made at multiple locations on the patella and around the knee. The skin was covered with an insulation layer underneath the cooling pad. Figure D.1 shows the temporal variation of skin temperature at multiple anatomical locations. Around 80 min into the experiment, cooling pad was removed and shortly after repositioned in the same region resulting in a disturbance in skin temperature pattern. The temperature plot shows roughly 15˚C temperature variation between different sites where temperature was measured.

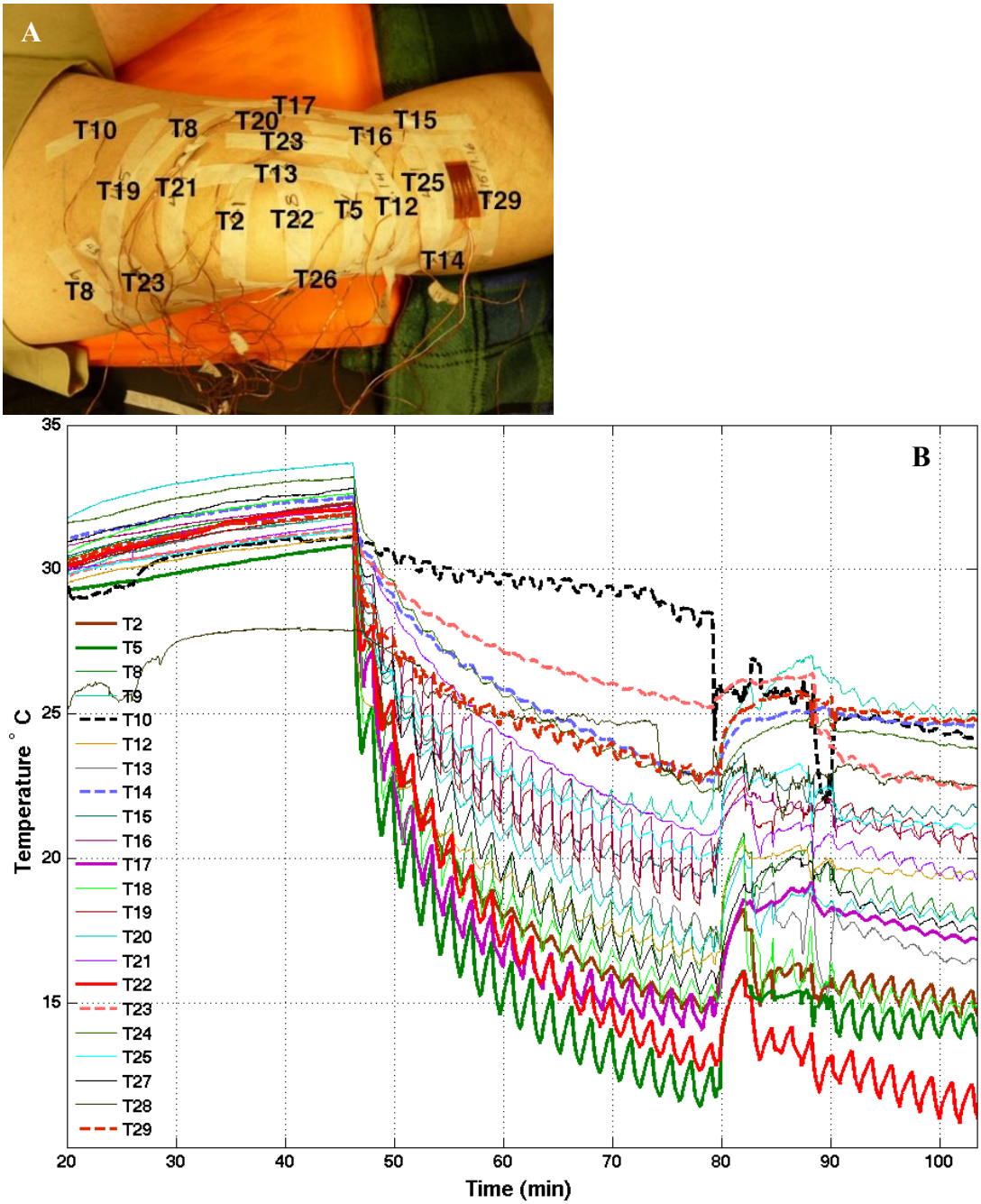

Figure D.1. The localization of thermocouples (a) and temporal profile of skin temperature measured by different thermocouples (b). Data plot related to some of the thermocouples positioned on patella are plotted with higher line thickness for easier identification. For the same reason, some of plots related to the more peripheral thermocouples are marked with dashed line.

At the end of cooling period the cooling pad and the insulation layer were removed to visualize skin and capture IR image. The temperature difference between measurements made by thermocouples (Figure D.1b) and the IR image (Figure D.2A and D.3A) could be due to the time difference between when the measurements were made. Acquiring IR images necessitates removal of the cooling pad and the insulating layer which exposes the treatment area to the ambient temperature. The longer the exposure to the ambient temperature before capturing IR images the higher the difference between the thermocouple readings and IR measurements. Figure D.2b shows minimum skin temperature at different position on the skin measured by thermocouples and Figure D.2a shows an IR image of the same region. Similarly, Figure D.3a and b show the IR image and minimum skin temperature from the lateral aspect of the cooling region. All presented IR images contain a pseudocolor bar showing the range of temperature in the image.

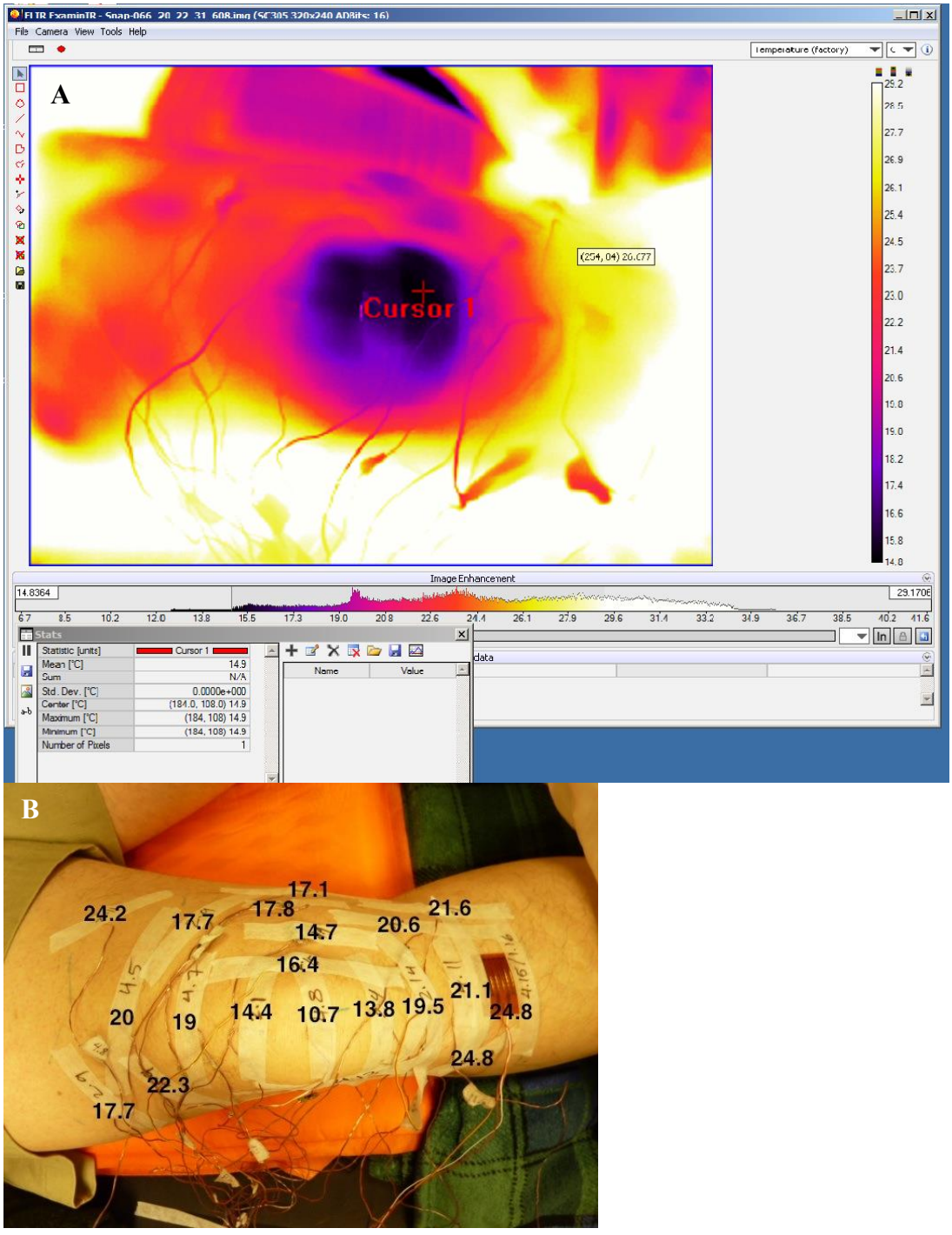

Figure D. 2. The skin temperature in the treatment region at the end of cooling from the frontal aspect using IR imaging (a) and thermocouple readings (b). The thermocouple measurements show minimum temperature measured at each location.

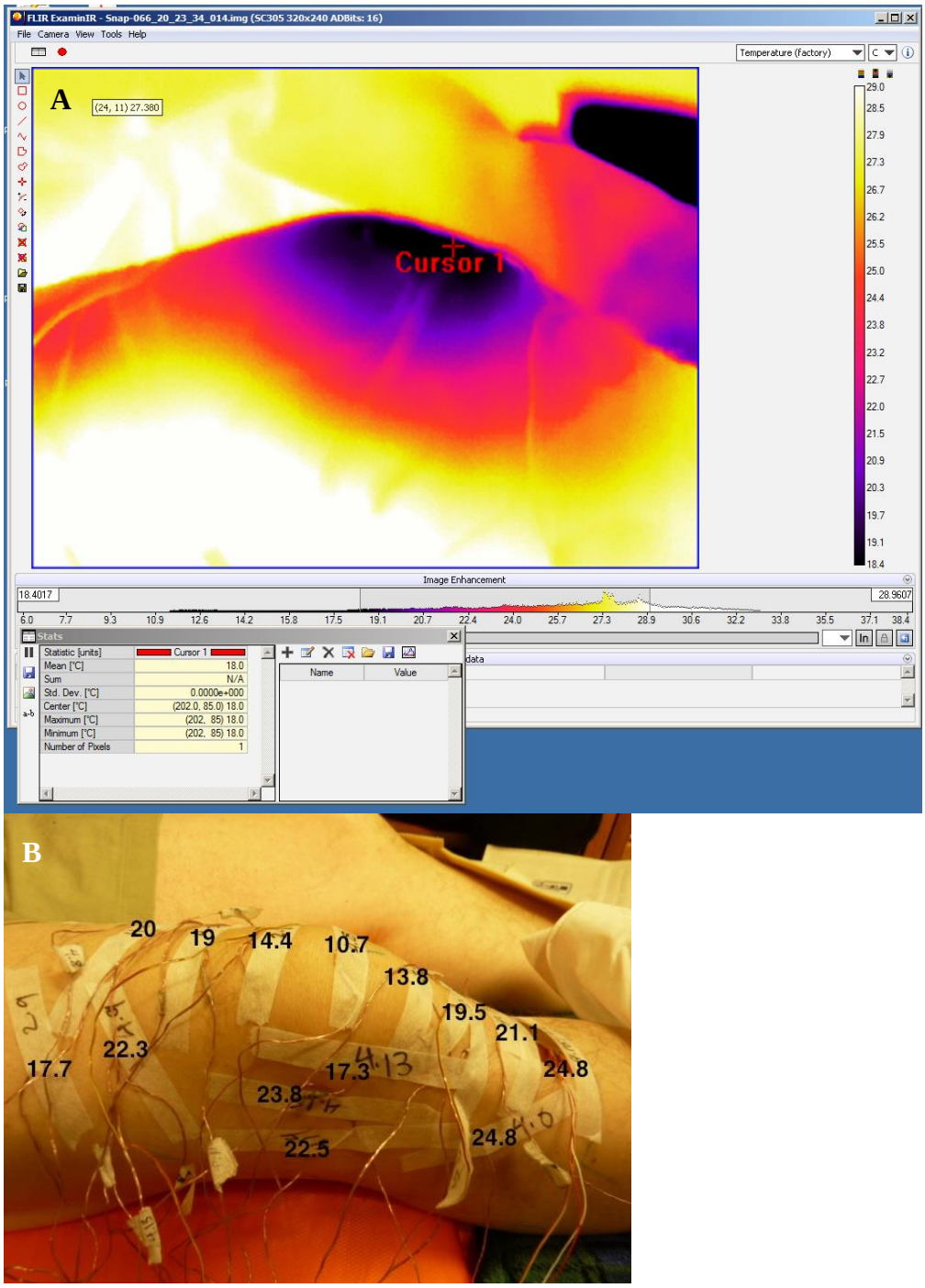

Figure D. 3. The skin temperature in the treatment area from the later aspect using IR imaging (A) and thermocouple measurements (B). The thermocouple readings show minimum temperature measured at each location.

Figure D.4 and D.5 represent temperature data from a 150-min long cryotherapy experiment using EBI cryotherapy unit and U-shaped cooling pad. This pad is designed such that it covers the medial, proximal and lateral regions of the knee without covering patella or the frontal aspect of the shin distal to patella. The disturbance in temperature data about 100 min into the experiment is due to the repositioning of the cooling pad. The temperature data plot (Figure D.4a) is based on measurements using thermocouples and shows more than 10˚C temperature variations between different points in the treatment region. The locations of thermocouples are marked in Figure D.4b. The thermocouples measuring the least amount of drop in temperature (6-9˚C) during cooling are not directly under the cooling pad but are surrounded by it from at least two sides (T14, 9 and 30). T13 was positioned under the edge of the cooling pad and therefore was cooled marginally. Moreover, the temperature measured by these thermocouples have not reached the steady state throughout the cooling cycle and given a longer exposure time in many cryotherapy practices, lower temperature reading in areas surrounded by the cooling pad but not necessarily covered by it should be expected. The skin temperature measured via IR imaging is presented in Figure D.5 where data cursors 1, 2, and 3 mark locations proximal, and medial to the patella and on the center of the patella with the temperature at these locations being presented below the IR image.

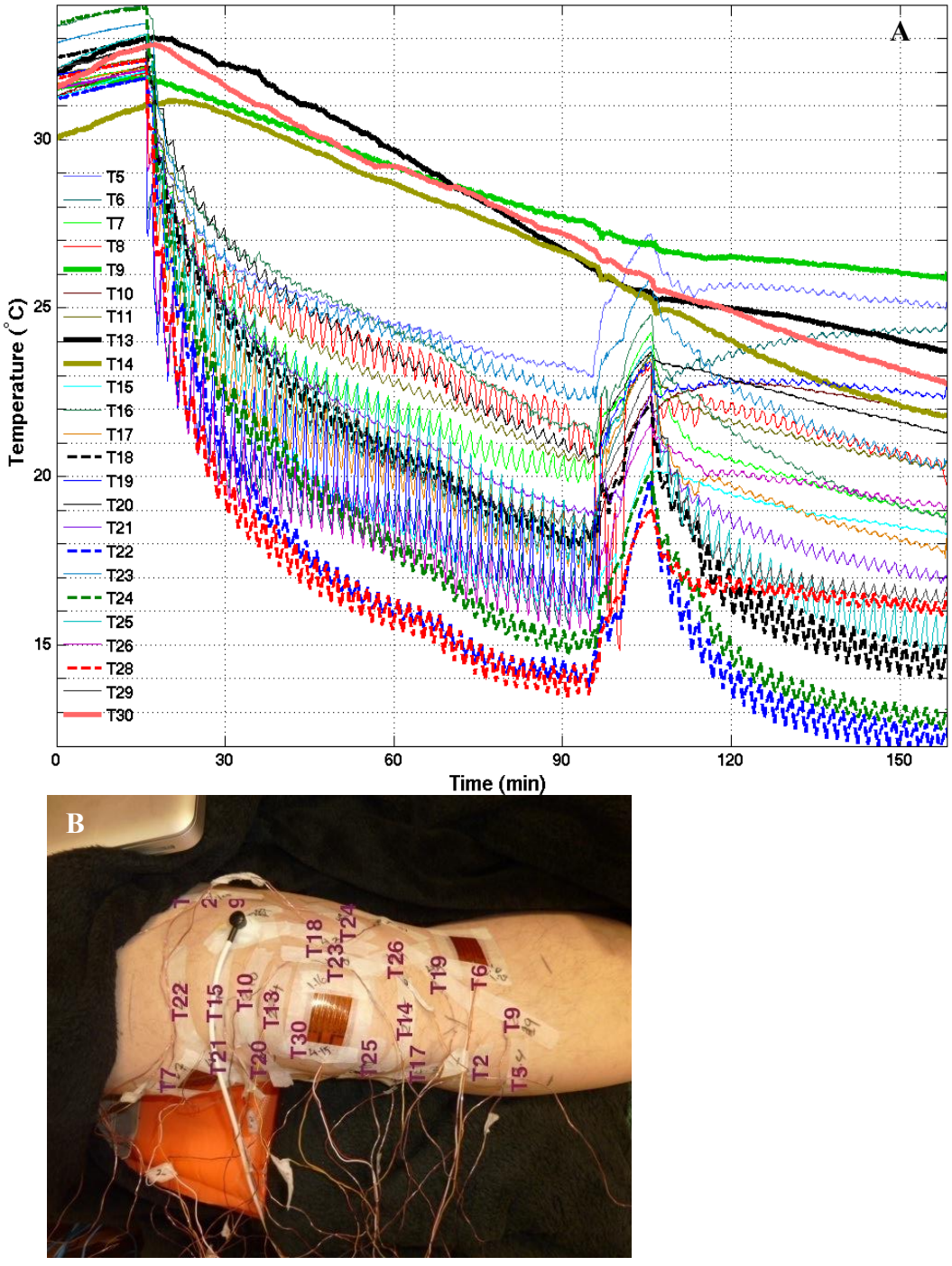

Figure D. 4. The Skin temperature at different locations surrounding the knee during an EBI cryotherapy experiment using the U-shaped pad (a). The disturbance in temperature data is due to repositioning of the cooling pad. The optical image shows the location of thermocouples (b).

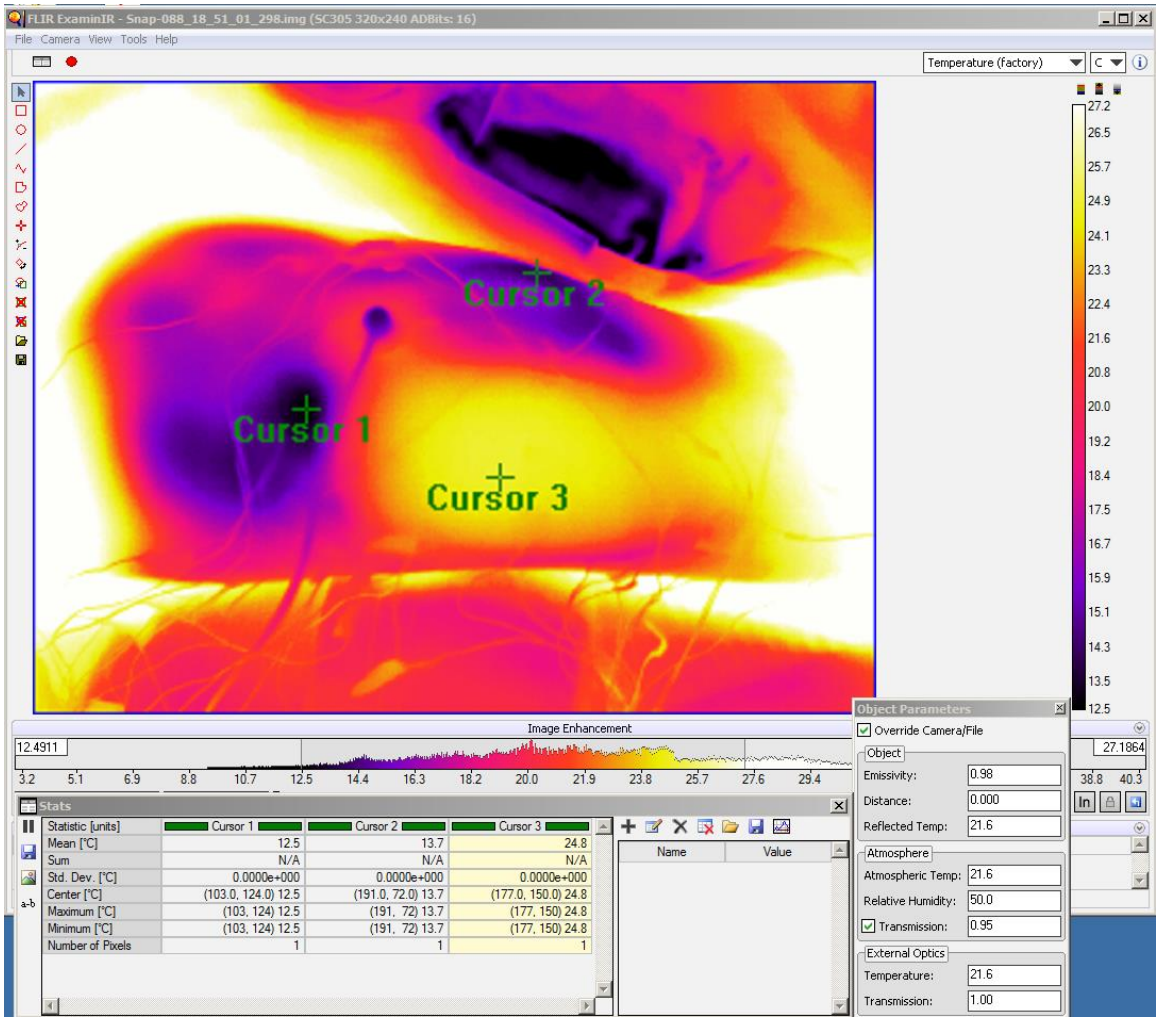

Figure D. 5. IR image of knee undergoing cryotherapy. The image shows the superficial temperature distribution. This images has a similar orientation to the optical one in Figure D.4b. Cursor 3 marks a point on the patella. Cursors 1 and 2 mark regions proximal and medial to patella that undergo direct cooling. Temperature information regarding these three cursors is presented below the IR image.

Evaluating variation in skin temperature following cryotherapy

In experiments presented in the Appendix A skin temperature was measured continuously at multiple anatomical locations, five on the patella and four on the four quadrants surrounding the knee, using multiple type T bead thermocouples. To investigate the statistical significance of temperature variability in the knee region during

a cryotherapy experiments, the minimum temperature during the cooling cycle was extracted at each of these positions and the minimum temperature on patella was compared to the temperature from the regions surrounding the knee using the Dunnett's test. The p-value for each of the tests is presented in the Table D.1. In this table, region 1-4 each designate one of the quadrants surrounding the knee. The statistically significant test results are marked in red for easier identification. In the case of cooling to 25 or 15˚C for 60 min, one of the thermocouples was not in use for at least one of the subjects and therefore was eliminated from the study. Hence no p-value is presented in the table for that specific thermocouple. As the results of the Dunnett's test show, the temperature on patella is significantly lower than that of regions farther away from patella. This temperature difference is independent of temperature profile on the cooling pad.

Experiment	Region 1	Region 2	Region 3	Region 4
2560	0.0187	0.0547	0.0019	
2060	0.0081	0.00003	0.0002	0.0159
1560	0.0491	0.0124	0.0203	
2760	0.0004	0.0022	0.0016	0.00004
2520	0.0220	0.0002	0.0044	0.0012
2020	0.0162	0.0161	0.0182	0.0764
3760	0.0430	0.0169	0.1022	0.0272

Table D. 1. The p-values resulted from the case control study comparing the minimum patellar temperature compared to the surrounding knee area. Case-control study was performed using the Dunnett's test. The statistically significant differences are marked in red.

The minimum representative patellar temperature (circle) and the average (square) and the maximum (star) temperature in regions 1-4 at the end of cooling for each experimental group are presented in Figure D.6. As it can be seen the patella temperature is always lower than that of surrounding regions and the difference in temperature between patella and the other regions are higher when skin is cooled to lower temperatures.

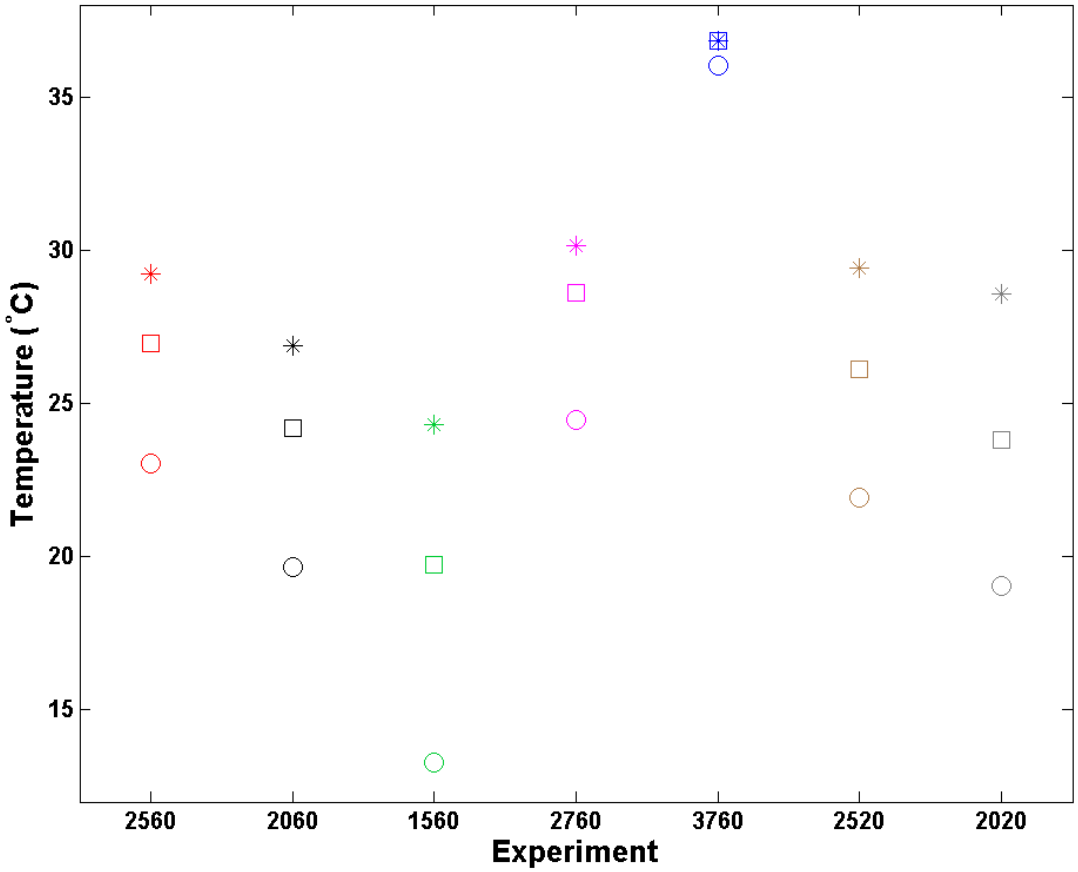

Figure D. 6. The difference between minimum patellar temperatures and the maximum temperatures in surrounding regions of the knee for each of the experimental groups. The first 2 digits for X-axis tics are the nominal skin temperature at the end of cooling and the last 2 are the duration of active cooling/ warming. Circle = minimum patellar temperature, Square = average surrounding temperatures, Star = maximum surrounding temperature.

Bibliography

[1] BSc, N. B., and Freiman, A. C., 2005, "History of cryotherapy," Dermatol. Online J., **11**(2).

[2] Yiu, W., Basco, M. T., Aruny, J. E., Cheng, S. W., and Sumpio, B. E., 2007, "Cryosurgery: a review," Int. J. Angiol. Off. Publ. Int. Coll. Angiol. Inc, **16**(1), p. 1.

[3] Knight, K. L., 1995, Cryotherapy in sport injury management, Human Kinetics, Champaign, IL.

[4] Todnem, K., Knudsen, G., Riise, T., Nyland, H., and Aarli, J. A., 1989, "The non-linear relationship between nerve conduction velocity and skin temperature.," J. Neurol. Neurosurg. Psychiatry, **52**(4), pp. 497–501.

[5] Algafly, A. A., and George, K. P., 2007, "The effect of cryotherapy on nerve conduction velocity, pain threshold and pain tolerance," Br. J. Sports Med., **41**(6), pp. 365 –369.

[6] Swenson, C., Swärd, L., and Karlsson, J., 1996, "Cryotherapy in sports medicine," Scand. J. Med. Sci. Sports, **6**(4), pp. 193–200.

[7] Bleakley, C. M., McDonough, S. M., and MacAuley, D. C., 2006, "Cryotherapy for acute ankle sprains: a randomised controlled study of two different icing protocols," Br. J. Sports Med., **40**(8), pp. 700 –705.

[8] Meeusen, R., and Lievens, P., 1986, "The use of cryotherapy in sports injuries," Sports Med., **3**(6), pp. 398–414.

[9] Barber, F. A., McGuire, D. A., and Click, S., 1998, "Continuous-flow cold therapy for outpatient anterior cruciate ligament reconstruction," Arthrosc. J. Arthrosc. Relat. Surg. Off. Publ. Arthrosc. Assoc. N. Am. Int. Arthrosc. Assoc., **14**(2), pp. 130–135.

[10] Babwah, T., 2011, "Common peroneal neuropathy related to cryotherapy and compression in a footballer," Res. Sports Med. Print, **19**(1), pp. 66–71.

[11] Collins, K., Storey, M., and Peterson, K., 1986, "Peroneal Nerve Palsy AfterCryotherapy," Physician Sportsmed, **14**(5), pp. 105–108.

[12] Drez, D., Faust, D. C., and Evans, J. P., 1981, "Cryotherapy and nerve palsy," Am. J. Sports Med., **9**(4), pp. 256 –257.

[13] Brown, W., and Hahn, D., 2009, "Frostbite of the Feet After Cryotherapy: A Report of Two Cases," J. FOOT ANKLE Surg., **48**(5), pp. 577–580.

[14] Lee, C. K., Pardun, J., Buntic, R., Kiehn, M., Brooks, D., and Buncke, H. J., 2007, "Severe frostbite of the knees after cryotherapy," Orthopedics, **30**(1), pp. 63–64.

[15] Barber, F. A., 2000, "A comparison of crushed ice and continuous flow cold therapy.," Am. J. Knee Surg., **13**(2), p. 97.

[16] Airaksinen, O. V., Kyrklund, N., Latvala, K., Kouri, J. P., Grönblad, M., and Kolari, P., 2003, "Efficacy of cold gel for soft tissue injuries a prospective randomized double-blinded trial," Am. J. Sports Med., **31**(5), pp. 680–684.

[17] Knobloch, K., Grasemann, R., Spies, M., and Vogt, P. M., 2008, "Midportion achilles tendon microcirculation after intermittent combined cryotherapy and

compression compared with cryotherapy alone: a randomized trial," Am. J. Sports Med., **36**(11), pp. 2128–2138.
[18] McGuire, D. A., and Hendricks, S. D., 2006, "Incidences of frostbite in arthroscopic knee surgery postoperative cryotherapy rehabilitation," Arthrosc. J. Arthrosc. Relat. Surg., **22**(10), pp. 1141–e1.
[19] Singh, H., Osbahr, D., Holovacs, T., Cawley, P., and Speer, K., 2001, "The efficacy of continuous cryotherapy on the postoperative shoulder: A prospective, randomized investigation," J. Shoulder Elbow Surg., **10**(6), pp. 522–525.
[20] Warren, T. A., 2004, "Intra-articular knee temperature changes: ice versus cryotherapy device," Am. J. Sports Med., **32**(2), pp. 441–445.
[21] Woolf, S. K., Barfield, W. R., Merrill, K. D., and McBryde, A. M. J., 2008, "Comparison of a continuous temperature-controlled cryotherapy device to a simple icing regimen following outpatient knee arthroscopy," J. Knee Surg. January 2008, **21**(1), pp. 15–19.
[22] Knobloch, K., Kraemer, R., Lichtenberg, A., Jagodzinski, M., Gosling, T., Richter, M., and Krettek, C., 2006, "Microcirculation of the ankle after Cryo/Cuff application in healthy volunteers," Int. J. Sports Med., **27**(3), p. 250.
[23] Bleakley, C., McDonough, S., and MacAuley, D., 2004, "The Use of Ice in the Treatment of Acute Soft-Tissue Injury," Am. J. Sports Med., **32**(1), pp. 251 –261.
[24] MacAuley, D., 2001, "Do textbooks agree on their advice on ice?," Clin. J. SPORT Med., **11**(2), pp. 67–72.
[25] Cohn, B., Draeger, R., and Jackson, D., 1989, "The effects of cold therapy in the postoperative management of pain in patients undergoing anterior cruciate ligament reconstruction," Am. J. Sports Med., **17**(3), pp. 344–349.
[26] Chesterton, L. S., Foster, N. E., and Ross, L., 2002, "Skin temperature response to cryotherapy," Arch. Phys. Med. Rehabil., **83**(4), pp. 543–549.
[27] Anson, J. A., McCormick, J., and Zambramski, J. M., 1992, "Oxygen dissociation characteristics of hemoglobin and blood substitute in relation to temperature," BNI Q., **8**, pp. 35–42.
[28] Lawson, W. H., Holland, R. a. B., and Forster, R. E., 1965, "Effect of temperature on deoxygenation rate of human red cells," J. Appl. Physiol., **20**(5), pp. 912–918.
[29] "DeRoyal® Hot/Cold Therapy Unit" [Online]. Available: http://www.deroyal.com/medicalproducts/orthopedics/product.aspx?id=pc-temptherapy-hotcoldtherunit. [Accessed: 25-Oct-2013].
[30] "USER GUIDE T505 COLD THERAPY UNIT" [Online]. Available: http://www.deroyal.com/filedisplay.aspx?id=571. [Accessed: 24-Oct-2013].
[31] "GrPro 2.1 Control unit user's Manual" [Online]. Available: http://www.gameready.com/wp-content/uploads/2012/10/GR21-CU-UM-703758-F-WEB-English-050713.pdf. [Accessed: 24-Oct-2013].
[32] "Bledsoe Cold Control" [Online]. Available: http://www.bledsoebrace.com/products/cold-control/. [Accessed: 24-Oct-2013].

[33] "Bledsoe bMini/bPRO" [Online]. Available: http://www.bledsoebrace.com/wp-content/uploads/2012/11/bMinibPRO_AIs_CP020246_RevB.pdf. [Accessed: 24-Oct-2013].
[34] "Donjoy Printed Instructions."
[35] "Cold Therapy Protocol" [Online]. Available: http://www.breg.com/sites/default/files/downloads/prod-files/Kodiak-Cube-Glacier-IFU-1_00372B.pdf. [Accessed: 10-Nov-2013].
[36] "EBI Instruction Sheet."
[37] Hodges, G. J., Zhao, K., Kosiba, W. A., and Johnson, J. M., 2006, "The involvement of nitric oxide in the cutaneous vasoconstrictor response to local cooling in humans," J. Physiol., **574**(3), pp. 849–857.
[38] Johnson, J. M., and Kellogg, D. L., 2010, "Local thermal control of the human cutaneous circulation," J. Appl. Physiol., **109**(4), pp. 1229–1238.
[39] Johnson, J. M., 2006, "Mechanisms of vasoconstriction with direct skin cooling in humans," AJP Heart Circ. Physiol., **292**(4), pp. H1690–H1691.
[40] Minson, C. T., 2010, "Thermal provocation to evaluate microvascular reactivity in human skin," J. Appl. Physiol., **109**(4), pp. 1239–1246.
[41] Thompson-Torgerson, C. S., Holowatz, L. A., Flavahan, N. A., and Kenney, W. L., 2006, "Cold-induced cutaneous vasoconstriction is mediated by Rho kinase in vivo in human skin," AJP Heart Circ. Physiol., **292**(4), pp. H1700–H1705.
[42] Francis, T. J., 1984, "Non freezing cold injury: a historical review," J. R. Nav. Med. Serv., **70**(3), pp. 134–139.
[43] Hamlet, M. P., 2001, "Nonfreezing cold injury," Wilderness Medicine, Mosby, St. Louis, Missouri, pp. 129–134.
[44] Irwin, M. S., 1996, "Nature and mechanism of peripheral nerve damage in an experimental model of non-freezing cold injury," Ann. R. Coll. Surg. Engl., **78**(4), pp. 372–379.
[45] Francis, T. J., and Golden, F. S., 1985, "Non-freezing cold injury: the pathogenesis.," J. R. Nav. Med. Serv., **71**(1), pp. 3–8.
[46] Thomas, J. R., and E. H. N. Oakley, 2002, Nonfreezing cold injury. In: Textbooks of Military Medicine: Medical Aspects of Harsh Environments, Office of the Surgeon General, U. S. Army, Falls Church, VA.
[47] Jia, J., and Pollock, M., 1999, "Cold nerve injury is enhanced by intermittent cooling," Muscle Nerve, **22**(12), pp. 1644–1652.
[48] Jia, J., Pollock, M., and Jia, J., 1998, "Cold injury to nerves is not due to ischaemia alone," Brain J. Neurol., **121 (Pt 5)**, pp. 989–1001.
[49] Indergand, H. J., and Morgan, B. J., 1994, "Effects of high-frequency transcutaneous electrical nerve stimulation on limb blood flow in healthy humans," Phys. Ther., **74**(4), pp. 361–367.
[50] Labropoulos, N., Watson, W. C., Mansour, M. A., Kang, S. S., Littooy, F. N., and Baker, W. H., 1998, "Acute effects of intermittent pneumatic compression on popliteal artery blood flow," Arch. Surg., **133**(10), p. 1072.

[51] Abu-Own, A., Cheatle, T., Scurr, J. H., and Coleridge Smith, P. D., 1993, "Effects of intermittent pneumatic compression of the foot on the microcirculatory function in arterial disease," Eur. J. Vasc. Surg., **7**(5), pp. 488–492.
[52] Khoshnevis, S., Craik, N., and Diller, K., "Experimental characterization of the domains of coupling and uncoupling between surface temperature and skin blood flow," Int. J. Transp. Phenom., **In Review**.
[53] Konrath, G., Lock, T., Goitz, H., and Scheidler, J., 1996, "The use of cold therapy after anterior cruciate ligament reconstruction - A prospective, randomized study and literature review," Am. J. SPORTS Med., **24**(5), pp. 629–633.
[54] Levy, A. S., and Marmar, E., 1993, "The role of cold compression dressings in the postoperative treatment of total knee arthroplasty," Clin. Orthop., (297), pp. 174–178.
[55] Leutz, D., and Harris, H., 1994, "Continuous cold therapy in total knee arthroplasty.," Am. J. Knee Surg., **8**(4), pp. 121–123.
[56] Large, A., and Heinbecker, P., 1944, "Nerve Degeneration Following Prolonged Cooling of an Extremity," Ann. Surg., **120**(5), pp. 742–749.
[57] Schaumburg, H., Byck, R., Herman, R., and Rosengart, C., 1967, "Peripheral nerve damage by cold," Arch. Neurol., **16**(1), p. 103.
[58] Jia, J., and Pollock, M., 1997, "The pathogenesis of non-freezing cold nerve injury. Observations in the rat," Brain J. Neurol., **120 (Pt 4)**, pp. 631–646.
[59] Clough, G., Chipperfield, A., Byrne, C., de Mul, F., and Gush, R., 2009, "Evaluation of a new high power, wide separation laser Doppler probe: potential measurement of deeper tissue blood flow," Microvasc. Res., **78**(2), pp. 155–161.
[60] Rowell, L., 1986, Human circulation regulation during physical stress, Oxford University Press, New York.
[61] Diller, K. R., 1992, "Modeling of bioheat transfer processes at high and low temperatures," Adv. Heat Transf., **22**, pp. 157–357.
[62] Diller, K. R., 2006, "Stress Protein Expression Kinetics," Annu. Rev. Biomed. Eng., **8**(1), pp. 403–424.
[63] Alvarez, G. E., 2006, "Relative roles of local and reflex components in cutaneous vasoconstriction during skin cooling in humans," J. Appl. Physiol., **100**(6), pp. 2083–2088.
[64] Johnson, J. M., Yen, T. C., Zhao, K., and Kosiba, W. A., 2005, "Sympathetic, sensory, and nonneuronal contributions to the cutaneous vasoconstrictor response to local cooling," Am. J. Physiol. - Heart Circ. Physiol., **288**(4), pp. H1573 – H1579.
[65] Thompson, C. S., Holowatz, L. A., and Kenney, W. L., 2005, "Attenuated noradrenergic sensitivity during local cooling in aged human skin," J. Physiol., **564**(1), pp. 313–319.
[66] Roustit, M., Maggi, F., Isnard, S., Hellmann, M., Bakken, B., and Cracowski, J.-L., 2010, "Reproducibility of a local cooling test to assess microvascular function in human skin," Microvasc. Res., **79**(1), pp. 34–39.

[67] Crandall, C. G., Etzel, R. A., and Johnson, J. M., 1997, "Evidence of functional beta-adrenoceptors in the cutaneous vasculature," Am. J. Physiol.-Heart Circ. Physiol., **273**(2), pp. H1038–H1043.
[68] Kellogg, D. L., Liu, Y., Kosiba, I. F., and O'Donnell, D., 1999, "Role of nitric oxide in the vascular effects of local warming of the skin in humans," J. Appl. Physiol., **86**(4), pp. 1185–1190.
[69] Minson, C. T., Berry, L. T., and Joyner, M. J., 2001, "Nitric oxide and neurally mediated regulation of skin blood flow during local heating," J. Appl. Physiol., **91**(4), pp. 1619–1626.
[70] Clough, G. F., Avery, M. R., Voegeli, D., Byrne, C. D., and Simpson, D. M., 2010, "Cutaneous vascular response to local warming: a response to letter from Cracowski and Roustit," Microcirculation, **17**(2), pp. 81–82.
[71] Roselli, R. J., and Diller, K. R., 2011, Biotransport: Principles and Applications, Springer.
[72] Khoshnevis, S., Nordhauser, J., Craik, N., and Diller, K. R., 2014, "Quantitative Evaluation of the Thermal Heterogeneity on the Surface of Cryotherapy Cooling Pads," J. Biomech. Eng.
[73] Khoshnevis, S., Craik, N., K., and Diller, K. R., In publication, "Cold-Induced Vasoconstriction May Persist Long After Cooling Ends: an Evaluation of Multiple Cryotherapy Units," Knee Surg. Sports Traumatol. Arthrosc.
[74] Khoshnevis, S., Craik, N. K., Brothers, R. M., and Diller, K. R., "Persistent vasoconstriction after cutaneous cooling: hysteresis between skin temperature and blood perfusion," J. Appl. Physiol., **In Review**.
[75] Rheinecker, S., 1998, "Using ice therapy to alleviate pain and edema," J. Am. Acad. Physician Assist., **11**, pp. 73–4, 77–81.
[76] 2013, "MoorVMS-LDF Specifications," Moor Instrum. [Online]. Available: http://gb.moor.co.uk/product/moorvms-ldf-laser-doppler-monitor/1/o/14/specifications. [Accessed: 09-Apr-2013].
[77] Moor Instruments, "Tissue blood flow and temperature monitoring with moorVMS-LDF."
[78] Royston, P., 1995, "A Remark on Algorithm AS 181: The W-test for Normality," J. R. Stat. Soc., **44**(4), pp. 547–551.
[79] Razali, N. M., and Wah, Y. B., 2011, "Power comparisons of Shapiro-Wilk, Kolmogorov-Smirnov, Lilliefors and Anderson-Darling tests," J Stat Model Analytics, **2**(1), pp. 21–33.
[80] Faul, F., Erdfelder, E., Buchner, A., and Lang, A.-G., 2009, "Statistical power analyses using G* Power 3.1: Tests for correlation and regression analyses," Behav. Res. Methods, **41**(4), pp. 1149–1160.
[81] Faul, F., Erdfelder, E., Lang, A.-G., and Buchner, A., 2007, "G* Power 3: a flexible statistical power analysis program for the social, behavioral, and biomedical sciences," Behav. Res. Methods, **39**(2), pp. 175–191.
[82] Fleiss, J. L., 1986, Design and analysis of clinical experiments, John Wiley and Sons, New York.

[83] Flack, V. F., Afifi, A. A., Lachenbruch, P. A., and Schouten, H. J. A., 1988, "Sample size determinations for the two rater kappa statistic," Psychometrika, **53**(3), pp. 321–325.
[84] VanNess, P. H., Towle, V. R., and Juthani-Mehta, M., 2008, "Testing measurement reliability in older populations: methods for informed discrimination in instrument selection and application," J. Aging Health, **20**(2), pp. 183–197.
[85] Walter, S. D., Eliasziw, M., and Donner, A., 1998, "Sample size and optimal designs for reliability studies," Stat. Med., **17**(1), pp. 101–110.
[86] Curl, W. W., Smith, B. P., Marr, A., Rosencrance, E., Holden, M., and Smith, T. L., 1997, "The effect of contusion and cryotherapy on skeletal muscle microcirculation.," J. Sports Med. Phys. Fitness, **37**(4), p. 279.
[87] Schaser, K.-D., Disch, A. C., Stover, J. F., Lauffer, A., Bail, H. J., and Mittlmeier, T., 2007, "Prolonged Superficial Local Cryotherapy Attenuates Microcirculatory Impairment, Regional Inflammation, and Muscle Necrosis After Closed Soft Tissue Injury in Rats," Am. J. Sports Med., **35**(1), pp. 93–102.
[88] Selfe, J., Hardaker, N., Whitaker, J., and Hayes, C., 2007, "Thermal imaging of an ice burn over the patella following clinically relevant cryotherapy application during a clinical research study," Phys. Ther. Sport, **8**(3), pp. 153–158.
[89] Bassett, F. H., 3rd, Kirkpatrick, J. S., Engelhardt, D. L., and Malone, T. R., 1992, "Cryotherapy-induced nerve injury," Am. J. Sports Med., **20**(5), pp. 516–518.
[90] Moeller, J. L., Monroe, J., and McKeag, D. B., 1997, "Cryotherapy-induced common peroneal nerve palsy," Clin. J. Sport Med. Off. J. Can. Acad. Sport Med., **7**(3), pp. 212–216.
[91] Ramanathan, N. L., 1964, "A new weighting system for mean surface temperature of the human body," J. Appl. Physiol., **19**, pp. 531–533.
[92] Bissonnette, B., Sessler, D. I., and LaFlamme, P., 1989, "Intraoperative temperature monitoring sites in infants and children and the effect of inspired gas warming on esophageal temperature," Anesth. Analg., **69**(2), pp. 192–196.
[93] Brinnel, H., and Cabanac, M., 1989, "Tympanic temperature is a core temperature in humans," J. Therm. Biol., **14**(1), pp. 47–53.
[94] Gagnon, D., Lemire, B. B., Jay, O., and Kenny, G. P., 2010, "Aural canal, esophageal, and rectal temperatures during exertional heat stress and the subsequent recovery period," J. Athl. Train., **45**(2), p. 157.
[95] 2014, "NIST/SEMATECH e-Handbook of Statistical Methods" [Online]. Available: http://www.itl.nist.gov/div898/handbook/. [Accessed: 04-Apr-2014].
[96] Pokala, N., 2012, "Dunnett test for multiple comparisons," MATLAB Cent. File Exch. [Online]. Available: http://www.mathworks.com/matlabcentral/fileexchange/file_infos/38157-dunnett-m. [Accessed: 26-Oct-2013].
[97] Ho, S. S. W., Illgen, R. L., Meyer, R. W., Torok, P. J., Cooper, M. D., and Reider, B., 1995, "Comparison of Various Icing Times in Decreasing Bone Metabolism and Blood Flow in the Knee," Am. J. Sports Med., **23**(1), pp. 74 –76.

[98] Karunakara, R. G., Lephart, S. M., and Pincivero, D. M., 1999, "Changes in Forearm Blood Flow During Single and Intermittent Cold Application," J. Orthop. Sports Phys. Ther., **29**(3), pp. 177–180.
[99] Sendowski, I., Savourey, G., Besnard, Y., and Bittel, J., 1997, "Cold induced vasodilatation and cardiovascular responses in humans during cold water immersion of various upper limb areas," Eur. J. Appl. Physiol., **75**(6), pp. 471–477.
[100] Yanagisawa, O., Homma, T., Okuwaki, T., Shimao, D., and Takahashi, H., 2007, "Effects of cooling on human skin and skeletal muscle," Eur. J. Appl. Physiol., **100**(6), pp. 737–745.
[101] Taber, C., Contryman, K., Fahrenbruch, J., LaCount, K., and Cornwall, M. W., 1992, "Measurement of reactive vasodilation during cold gel pack application to nontraumatized ankles," Phys. Ther., **72**(4), pp. 294–299.
[102] Vuksanović, V., Sheppard, L. W., and Stefanovska, A., 2008, "Nonlinear Relationship between Level of Blood Flow and Skin Temperature for Different Dynamics of Temperature Change," Biophys. J., **94**(10), pp. L78–L80.
[103] Kozelek, P., Holcik, J., and Sedlinska, M., 2007, "Statistical Analysis of QT/RR Hysteresis in Healthy Horses," Engineering in Medicine and Biology Society, 2007. EMBS 2007. 29th Annual International Conference of the IEEE, IEEE, pp. 5319–5322.
[104] Goudkamp, J. E., Seebacher, F., Ahern, M., and Franklin, C. E., 2004, "Physiological thermoregulation in a crustacean? Heart rate hysteresis in the freshwater crayfish Cherax destructor," Comp. Biochem. Physiol. A. Mol. Integr. Physiol., **138**(3), pp. 399–403.
[105] Zachariassen, K. E., 1985, "Physiology of cold tolerance in insects," Physiol. Rev., **65**(4), pp. 799–832.
[106] George, N. T., Irving, T. C., Williams, C. D., and Daniel, T. L., 2013, "The Cross-Bridge Spring: Can Cool Muscles Store Elastic Energy?," Science, **340**(6137), pp. 1217–1220.
[107] Inoue, I., Kobatake, Y., and Tasaki, I., 1973, "Excitability, instability and phase transitions in squid axon membrane under internal perfusion with dilute salt solutions," Biochim. Biophys. Acta BBA-Biomembr., **307**(3), pp. 471–477.
[108] Chen, A. H., Frangos, S. G., Kilaru, S., and Sumpio, B. E., 2001, "Intermittent Pneumatic Compression Devices – Physiological Mechanisms of Action," Eur. J. Vasc. Endovasc. Surg., **21**(5), pp. 383–392.
[109] Morgan, R. H., Carolan, G., Psaila, J. V., Gardner, A. M. N., Fox, R. H., and Woodcock, J. P., 1991, "Arterial Flow Enhancement by Impulse Compression," Vasc. Endovascular Surg., **25**(1), pp. 8–16.